

# Suspended Sediment Modelling in the Port of Rotterdam

by

**Sjoerd de Groot**

in partial fulfillment of the requirements for the degree of

**Master of Science**

in Hydraulic Engineering

Section Environmental Fluid Mechanics

Delft University of Technology,

Faculty of Civil Engineering and Geosciences

To be defended publicly on November 8, 2018 13:30

Thesis committee:	Prof. dr. J. D. Pietrzak,	TU Delft
	Dr. C. Chassagne,	TU Delft
	Dr. A. Kirichek,	TU Delft
	Ir. S. Rijnsburger,	TU Delft
	Ir. L. Hulsen,	Port of Rotterdam



**Port of  
Rotterdam**





# Abstract

This Master thesis presents an improved model for the transport of fine suspended sediment (SPM) in the Rhine region of fresh water influence (ROFI) and in the Port of Rotterdam. It is known that the transport of SPM in the Rotterdam harbor depends on marine as well as fluvial processes. SPM transport inside the harbor has been modelled in the past, but these studies did not take into account the dynamic nature of SPM concentrations at sea because they employed constant sediment boundary conditions and did not resolve wind waves. At the same time, numerous model studies of SPM transport in the Southern North Sea have been carried out, but none included the Rotterdam harbor as more than a discharge point. This MSc thesis is the first study to combine a North Sea SPM model with a detailed model of the Port of Rotterdam. By doing so, it incorporates the dynamic nature of sediment concentrations in the North Sea, and its effect on sediment transport in the Rotterdam harbor.

A new suspended sediment model of the Rotterdam harbor was set up with the Delft3D-WAQ software package and the NSC-Course model grid already in use by Port of Rotterdam. A validated hydrodynamic model was available for this grid schematization, and has been used as model forcing. At the open sea boundaries, the validated ZUNO-DD model for SPM transport on the North Sea was used to compute suspended sediment concentrations, which were then applied as boundary conditions. In addition, a wave buoy assimilation technique was used to include the effect of wind waves on the resuspension of sediment. A set of initial conditions was created by repeating a single spring-neap cycle with calm, virtually waveless conditions until sediment concentrations reached a dynamic equilibrium. A byproduct of this method was that it created a large sediment availability in the bed, which lead to higher than expected resuspension during storms. To investigate the response of the system to variable forcing conditions, three 14 day periods have been selected from measured environmental conditions of the year 2007, containing different combinations of storms and river discharges.

The model shows positive results, but does need improvement. Principally, the episodic nature of siltation in the harbor basins lining the mouth of the Rotterdam Waterway was reproduced. In line with observations, storms at sea correspond to high SPM concentrations at sea, large influxes through the harbor mouth, and increased siltation rates in the harbor basins. Furthermore, differential advection of the salinity structure and the trapping of SPM in the Rotterdam Waterway was observed. However, erosion was also observed, and harbor basins lining the Rotterdam Waterway showed a strong response to events at sea which contradicts observations. This is attributed to the wave stress assimilation performed on NSC-Coarse grid which generates large wave stresses inside the harbor and causes unwanted resuspension. Three different forcing scenarios were chosen to highlight the differences between marine and fluvial processes, but a clear distinction could not be made. This is expected to be caused by the erroneous wave shear stresses which obfuscate the effects of different siltation mechanisms. It is recommended that this aspect of the model is improved and that the model is reassessed using measurements.



# Acknowledgements

This thesis marks the completion of my MSc degree in Hydraulic Engineering at Delft University of Technology, specializing in Environmental Fluid Mechanics. It has been funded by Port of Rotterdam, and was carried out there as well. I was supervised by Prof. dr. Julie D. Pietrzak, dr. Claire Chassagne, dr. Alex Kirichek, ir. Sabine Rijnsburger, and ir. Lambèr Hulsen. I would like to thank them for their supervision and advise. In particular, I would like to thank Lambèr Hulsen for his at times intensive support during the challenges that arose while conducting this research.

Throughout the course of this thesis, I received valuable support from Deltares. I would like to thank Thijs van Kessel and Katherine Kronin for their help. Finally, I would like to thank Port of Rotterdam for giving me the opportunity to complete this work.

---

# Contents

<b>Abstract</b>	<b>iii</b>
<b>Acknowledgements</b>	<b>v</b>
<b>1 Introduction</b>	<b>1</b>
1.1 Physical environment . . . . .	2
1.2 Current model practices . . . . .	3
1.3 Research objective . . . . .	4
1.4 Chapter Outline . . . . .	5
<b>2 Theoretical background</b>	<b>7</b>
2.1 Sediment characteristics . . . . .	7
2.2 Large scale dynamics of the North Sea . . . . .	8
2.3 Dynamics of the coastal zone . . . . .	10
2.4 Advection in the Rotterdam Waterway . . . . .	12
2.5 Harbour siltation . . . . .	13
<b>3 Model Setup</b>	<b>15</b>
3.1 Introduction . . . . .	15
3.2 Overview of the models used . . . . .	15
3.3 Grid and bathymetry . . . . .	16
3.4 Substances, bed layers, and important model parameters . . . . .	17
3.5 Forcing conditions . . . . .	18
3.5.1 Treatment of wind waves . . . . .	18
3.6 Boundary conditions . . . . .	19
3.7 Initial conditions and spin-up of NSC-Coarse (WAQ) model . . . . .	21
3.8 Model Scenarios . . . . .	23
<b>4 Analysis of model results</b>	<b>25</b>
4.1 ZUNO-DD: Salinity and SPM structure at Sea . . . . .	25
4.1.1 Frictional and Ekman response of salinity field to wind forcing . . . . .	25
4.1.2 Relationship SPM and the salinity structure and bottom shear stresses . . . . .	27
4.2 Comparison with NSC-Coarse model . . . . .	29
4.3 Interactions at the mouth . . . . .	29
4.4 Assessment of sedimentation and dredging loads within the Port area . . . . .	32
4.4.1 Role of settling velocity . . . . .	35
4.4.2 Time development of sedimentation . . . . .	38
4.5 Bottom shear stresses . . . . .	38
4.6 Advection in the Rotterdam Waterway . . . . .	39
4.6.1 Salinity . . . . .	39
4.6.2 Along channel velocity . . . . .	40
4.6.3 Suspended sediment and the ETM . . . . .	40
<b>5 Discussion</b>	<b>45</b>
5.1 Modelling SPM variability . . . . .	45
5.2 Marine processes . . . . .	45
5.3 Inside the port . . . . .	46

<b>6</b>	<b>Conclusions and recommendations</b>	<b>49</b>
6.1	Conclusions . . . . .	49
6.2	Recommendations . . . . .	51
	<b>Appendices</b>	<b>53</b>
<b>A</b>	<b>Supporting figures: Model Forcing Conditions and spin-up of NSC model</b>	<b>55</b>
A.1	Forcing conditions . . . . .	55
A.2	Tables showing the spin-up of the NSC-Coarse (WAQ) model . . . . .	61
<b>B</b>	<b>Supporting figures: Surface and cross-sectional plots from the ZUNO-DD and NSC-Coarse models</b>	<b>67</b>
<b>C</b>	<b>Supporting figures: Plots and charts relating to harbour sedimentation</b>	<b>83</b>
<b>D</b>	<b>Mathematical model description</b>	<b>105</b>
D.1	Hydrodynamic equations . . . . .	105
D.2	Sediment transport equations . . . . .	107
D.2.1	Suspended transport . . . . .	107
D.2.2	Deposition and erosion . . . . .	108
D.2.3	Calculation of bottom shear stresses . . . . .	110
D.3	Model parameters . . . . .	111

# List of Figures

1.1	Annually dredged quantities . . . . .	2
1.2	Areas of marine and fluvial sedimentation . . . . .	3
1.3	Overview of model improvements . . . . .	4
2.1	Sediment processes . . . . .	8
2.2	Residual currents in the North Sea . . . . .	8
2.3	Large scale surface SPM . . . . .	9
2.4	Baroclinic flow . . . . .	11
2.5	Tidal straining . . . . .	11
2.6	Estuarine Turbidity Maximum . . . . .	12
2.7	Relation wave orbital velocity and Maasmond siltation . . . . .	13
2.8	Fluvial siltation mechanism . . . . .	14
3.1	Model interactions . . . . .	16
3.2	Computational domain . . . . .	17
3.3	Schematization of bed layers . . . . .	18
3.4	Wave buoy locations of data assimilation . . . . .	18
3.5	Seaside boundaries of the NSC-Coarse (WAQ) model . . . . .	20
3.6	spin-up forcing conditions . . . . .	22
3.7	spin-up of NSC-Coarse (WAQ) model. . . . .	22
4.1	Rhine ROFI response to strong wind forcing . . . . .	26
4.2	Rhine ROFI response under calm conditions . . . . .	28
4.3	Overview of observation areas . . . . .	30
4.4	SPM fluxes through Maasmond . . . . .	31
4.5	Total deposition in bed layer S1 . . . . .	33
4.6	Total deposition in bed layer S2 . . . . .	34
4.7	Contribution of sediment fractions in harbour deposition . . . . .	35
4.8	Difference map over period 1 of IM1 concentration in layer S2 . . . . .	36
4.9	Difference map over period 1 of IM2 concentration in layer S2 . . . . .	37
4.10	Map overview of wave bottom shear stresses . . . . .	39
4.11	Location of the observation points of Figure 4.12 to Figure 4.14 . . . . .	40
4.12	Rotterdam Waterway, observation point 1 . . . . .	41
4.13	Rotterdam Waterway, observation point 2 . . . . .	42
4.14	Rotterdam Waterway, observation point 3 . . . . .	43
A.1	Bottom shear stresses, river discharge, and wind for forcing Period 1 . . . . .	56
A.2	Bottom shear stresses, river discharge, and wind for forcing Period2 . . . . .	57
A.3	Bottom shear stresses, river discharge, and wind for forcing Period 3 . . . . .	58
A.4	Bottom shear stresses, river discharge, and wind for forcing Period 4 . . . . .	59
A.5	Water levels for all forcing periods . . . . .	60
A.6	Location of observation points used for model spin-up assessment . . . . .	62
B.1	Cross section location of Figure B.13 and Figure B.14 . . . . .	68
B.2	Surface salinity and SPM plots . . . . .	69
B.3	ZUNO-DD cross-section of Northern boundary on 24/01/2007 . . . . .	70
B.4	ZUNO-DD cross-section of Southern boundary on 24/01/2007 . . . . .	71

LIST OF FIGURES

---

B.5	ZUNO-DD surface plots of tidal cycle on 17/01/2007 . . . . .	72
B.6	ZUNO-DD cross-section of Northern boundary on 17/01/2007 . . . . .	73
B.7	ZUNO-DD cross-section of Southern boundary on 17/01/2007 . . . . .	74
B.8	ZUNO-DD surface plots of tidal cycle on 10/11/2007 . . . . .	75
B.9	ZUNO-DD cross-section of Northern boundary on 10/11/2007 . . . . .	76
B.10	ZUNO-DD cross-section of Southern boundary on 10/11/2007 . . . . .	77
B.11	NSC-Coarse surface plot of corresponding to Figure B.2 . . . . .	78
B.12	NSC-Coarse surface plot corresponding to Figure B.5. . . . .	79
B.13	Salinity cross-section of the Rotterdam Waterway on 17/01/2007 . . . . .	80
B.14	SPM cross-section of the Rotterdam Waterway on 17/01/2007 . . . . .	81
B.15	Surface salinity and surface SPM on 10/11/2007 . . . . .	82
C.1	Total deposition of IM1 in layer S2 after Period 1 . . . . .	84
C.2	Total deposition of IM1 in layer S2 after Period 1 . . . . .	85
C.3	Total deposition of IM1 in layer S2 after Period 1 . . . . .	86
C.4	Total deposition of IM1 in layer S2 after Period 1 . . . . .	87
C.5	Total deposition of IM2 in layer S2 after Period 1 . . . . .	88
C.6	Total deposition of IM2 in layer S1 after Period 2 . . . . .	89
C.7	Total deposition of IM1 in layer S2 after Period 2 . . . . .	90
C.8	Total deposition of IM2 in layer S2 after Period 2 . . . . .	91
C.9	Total deposition of IM1 in layer S2 after Period 1 . . . . .	92
C.10	Total deposition of IM1 in layer S2 after Period 1 . . . . .	93
C.11	Total deposition of IM1 in layer S2 after Period 4 . . . . .	94
C.12	Total deposition of IM2 in layer S2 after Period 4 . . . . .	95
C.13	Decomposition of total deposition into sediment fractions per observation area . .	96
C.14	SPM import through mouth of Rotterdam Waterway for Period 1 . . . . .	97
C.15	SPM import through mouth of Rotterdam Waterway for Period 2 . . . . .	98
C.16	Time development of sedimentation in layer S1 per observation area for Period 1 .	99
C.17	Time development of sedimentation per observation area in layer S2 for Period 1 .	100
C.18	Time development of sedimentation per observation area in layer S1 for Period 2 .	101
C.19	Time development of sedimentation per observation area in layer S2 for Period 2 .	102
C.20	Time development of sedimentation per observation area in layer S1 for Period 4 .	103
C.21	Time development of sedimentation per observation in area layer S2 for Period 4 .	104
D.1	Schematization of sediment bed . . . . .	109

# List of Tables

3.1	Vertical layer thickness distribution of the ZUNO-DD and NSC-Coarse models. . .	16
3.2	Sediment fractions included in the WAQ models . . . . .	18
3.3	Overview of model scenarios . . . . .	23
A.1	spin-up at different observation points for substance IM1S1 . . . . .	63
A.2	spin-up at different observation points for substance IM1S2 . . . . .	63
A.3	spin-up at different observation points for substance IM2S1 . . . . .	64
A.4	spin-up at different observation points for substance IM2S2 . . . . .	64
A.5	spin-up at different observation points for substance Total Inorganic Matter . . . .	65
D.1	User defined model paramters . . . . .	111



# Chapter 1

## Introduction

In this thesis, a fine sediment transport model is set up for the Port of Rotterdam. The Port of Rotterdam is the largest port of Europe, receiving about 30,000 sea going vessels and 110,000 inland waterway vessels annually, and is host to the largest ships of the world. This places stringent demands on the nautical depths of the various harbour basins. Like many harbours around the world, the Rotterdam harbour does not naturally meet the nautical depths required by the ships it receives, and is therefore artificially maintained through dredging. As a result, the port area is subject to a continuous process of sedimentation and dredging. Between 1982 and 2013, the Port of Rotterdam annually dredged between four to six million cubic meters of sediment from the various harbour basins. After the completion of Maasvlakte 2, this figure has risen to between eight million and 12 million cubic meters. This figure excludes dredged material from the main waterways, which are maintained by the Dutch Ministry of Infrastructure (Rijkswaterstaat). In practice, almost exclusively fine sediment (silt, clay, organic matter) is dredged from the harbour basins, while more sandy material is found in the main waterways. These fine sediments are predominantly advected by the water flow as suspended particulate matter (SPM), and bed load transport is negligible.

Port of Rotterdam partakes in numerous research projects aimed at understanding, predicting, and managing sediment processes inside the harbour. A notable example is the PRISMA project, which studies the properties and effects of mud processes with measurement and modelling techniques with the aim of optimizing sediment management in harbours. One of the pillars of the program is the numerical modelling of sediment dynamics, and that is where this master thesis contributes. The goal of this thesis is to create a model that can be used as a tool to investigate the impact of varying environmental conditions as well as changes in harbour infrastructure or dredging strategies on sediment dynamics in the Rhine-Meuse estuary.

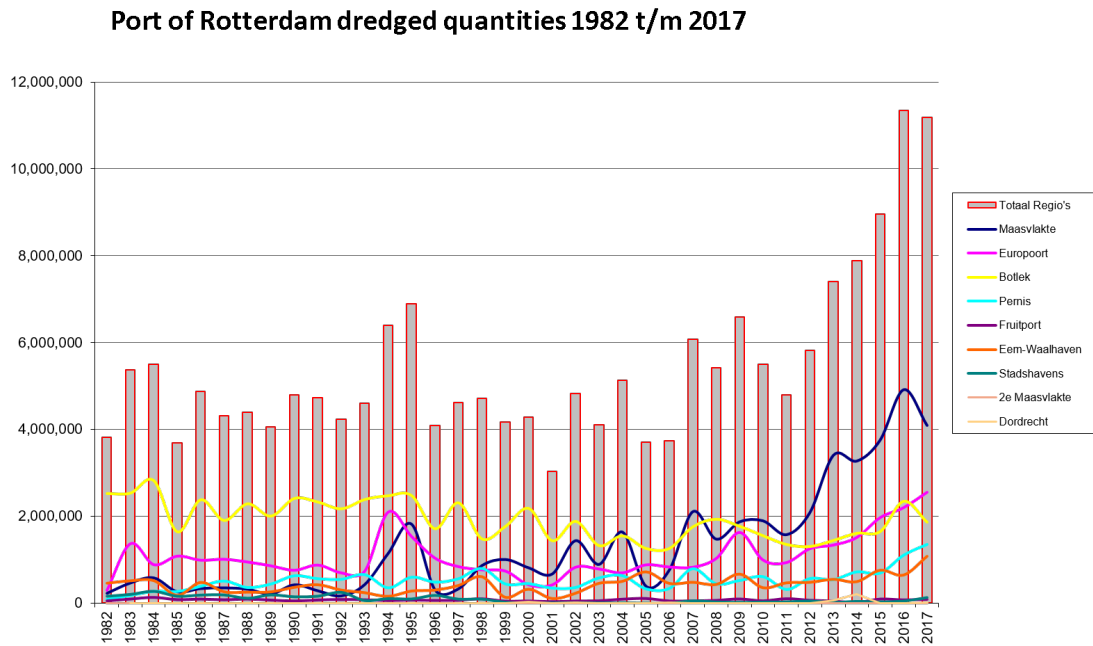


Figure 1.1: Time development of the quantities of dredged material by Port of Rotterdam. Since the completion of Maasvlakte 2 in 2013, the annual dredging loads in the Maasvlakte and Europoort areas has increased significantly.

## 1.1 Physical environment

Being positioned in an estuarine environment, the Rotterdam harbour forms the area of interaction between the freshwater outflow of the rivers Rhine and Meuse and the periodic tidal in and outflow of salty water from the North Sea. It is well known that the Rhine-Meuse outflow creates a buoyant plume of fresh water in the North Sea, forming a vertically stratified area known as a region of fresh water influence (ROFI) (Simpson et al., 1993; de Boer, 2009; Pietrzak et al., 2011; Souza et al., 1996; van Leeuwen et al., 2015; Eleveld et al., 2008; van der Giessen et al., 1990). Conversely, the tide advects dense sea water into the Rotterdam Waterway, driving a salt wedge that oscillates approximately between Botlek Harbor and the harbour mouth (de Nijs et al., 2010). The result is a complex interplay of wind, waves, tides, and density, which governs the transport, erosion, and deposition of fine sediment in this region (Joordens et al., 2001; Suijlen et al., 2002; Pietrzak et al., 2011; van Alphen, 1990; M. Visser et al., 1991; de Nijs et al., 2011).

Figure 1.1 shows that sedimentation is dominated by the Maasvlakte, Europoort, and Botlek areas. These three areas are all known to have a strong marine influence, though the exact sedimentation mechanisms vary. On the harbour basins lining the Maasmond (Maasvlakte, Europoort), sediment that is suspended at sea is advected into the basins by the tidal and baroclinic currents and through fluid mud processes (Verlaan et al., 2000; Winterwerp et al., 2003). Its siltation rates are found to correlate strongly to significant wave heights at sea, and are characterized by episodic events. SPM concentrations at sea are controlled by sediment availability, bottom shear stresses, and turbulent kinetic energy in the water column and these processes are in turn governed by highly variable environmental forcing conditions (wind, waves, stratification, tides) (Suijlen et al., 2002; Pietrzak et al., 2011; Eleveld et al., 2008; Flores et al., 2017). Due to turbulence damping at the pycnocline, SPM tends to concentrate into the (salty) lower layer of the water column when stratification is present (Geyer, 1993; Pietrzak et al., 2011; Joordens et al., 2001). The SPM concentrations are then advected into the port area by the ambient currents.

However, not much marine SPM is found in the Rotterdam Waterway, and marine concentrations dwindle fast in the upstream direction. In the harbour basins lining the Rotterdam waterway (Botlek harbour being the most prominent), almost exclusively fluvial SPM is found (Verlaan et al., 2000; de Nijs et al., 2011). Here, the vertically stratified density structure in the Rotterdam Waterway is known to reduce turbulence levels near the pycnocline (de Nijs et al., 2010; de Nijs et al., 2012). SPM is kept in suspension by turbulent kinetic energy, and a reduction will cause

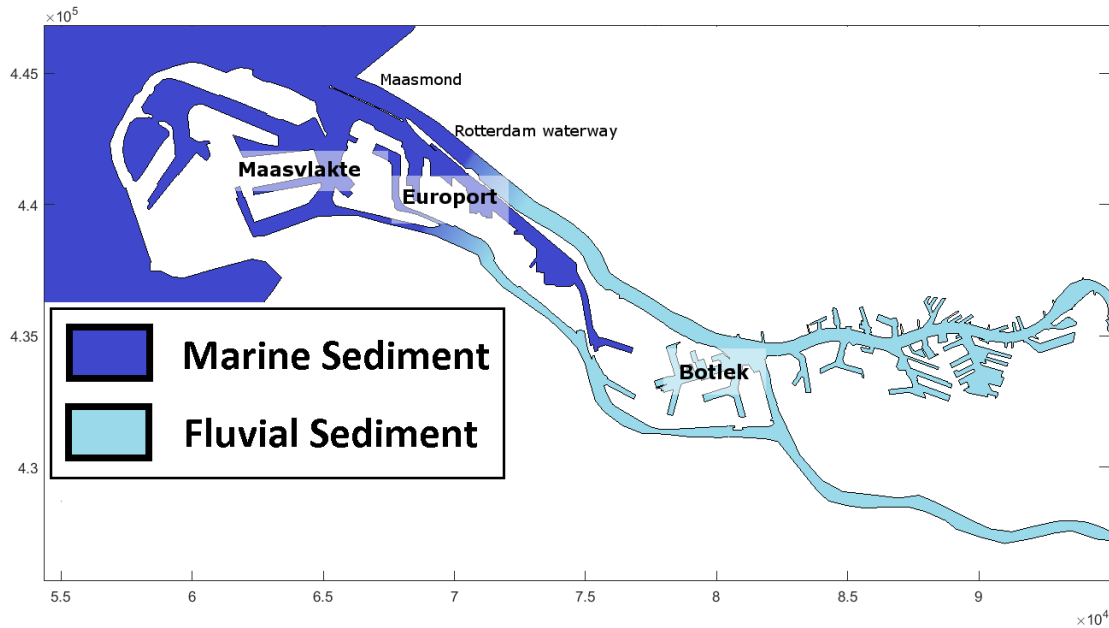


Figure 1.2: Sediment is imported into the harbour through the combined effects of tides, baroclinic flow (sea) and through river discharge (river). The interface of the two mechanisms lies inside the harbour, with tidal inflow being the dominant sedimentation mechanism on the sea side of the harbour, and fluvial inflow on the river side of the harbour. The strength of the tides and discharge fluctuates, but on average the limit of salt water intrusion is at Botlek Harbor.

fluvial SPM to settle through the pycnocline and accumulate in the tip of the salt wedge in an estuarine turbidity maximum (ETM) (de Nijs et al., 2011; Geyer, 1993). The positioning of Botlek harbour at the limit of salt water intrusion allows for large SPM exchange fluxes between the ETM and Botlek harbour, giving this basin a very large sediment trapping efficiency (de Nijs et al., 2009). This separates the Rotterdam harbour into a region of marine siltation and a region of fluvial siltation, shown in Figure 1.2. However, by controlling the advection of the salt wedge, marine conditions still impact fluvial sedimentation.

## 1.2 Current model practices

Currently, the simulation of hydrodynamics by Port of Rotterdam is standard practice, and is implemented as a predictive model that produces reliable forecasts of water levels, flow velocities and salt concentrations in the harbour based on predicted environmental conditions. It is known as the OSR (Operationeel Stromingsmodel Rotterdam), and is based on the NSC-Fine model schematization. The NSC-Coarse grid is a 3x3 aggregation of the NSC-Fine grid, and has been used in the past for sediment modelling. The NSC-Fine and to a lesser extent the NSC-Coarse hydrodynamic models have been validated for water levels, velocities, and salinity (Rotsaert, 2010). So far, these sediment models always employed sediment boundary conditions that were constant in the vertical and time dimensions, due to a lack of better information. Furthermore, these models did not include any information on wind waves.

Others have modelled SPM transport in the Rotterdam harbour as well. (de Nijs et al., 2012) created a model to simulate SPM entrapment in the Rotterdam waterway, while (Winterwerp et al., 2003) developed a sediment model for the harbour mouth which included sediment-flow interactions. (de Kok, 2001) created an SPM model to assess the impact of the river discharge distribution on the advection of SPM into the harbour. However, these models too assumed constant SPM boundary conditions, and omitted the effect of wind waves on the resuspension of sediment. This does not capture the high variability of SPM concentrations that is known to exist on the North Sea.

	Previous SPM simulations by Port of Rotterdam	Improved model setup
Model components	<ol style="list-style-type: none"> <li>1. Constant SPM boundary conditions in time and depth</li> <li>2. Repetition of single day hydrodynamic conditions</li> <li>3. No inclusion of wave shear stresses</li> <li>4. Single particle settling velocity</li> <li>5. One sediment bed layer</li> </ol>	<ol style="list-style-type: none"> <li>1. Time and depth varying SPM boundary conditions</li> <li>2. Full spring-neap cycle modelled (14 days)</li> <li>3. Wave shear stresses included in sediment resuspension</li> <li>4. Three distinct sediment fractions</li> <li>5. Two sediment bed layers</li> </ol>
Consequences for model application	<ol style="list-style-type: none"> <li>1. Constant boundary inflow of SPM throughout simulation period</li> <li>2. No forcing variations over more than 1 day included</li> <li>3. No additional suspension of sediment during storms</li> <li>4. No effect of different particle/floc sizes included</li> <li>5. Only one deposition/erosion timescale possible</li> </ol>	<ol style="list-style-type: none"> <li>1. Boundary inflow of SPM varies with environmental conditions at sea</li> <li>2. Spring-neap and storm variability can be included in model forcing</li> <li>3. Effect of storms on SPM concentrations included</li> <li>4. Some differential settling of sediment included</li> <li>5. Short term events (storms) as well as long term events (spring-neap, seasons) can be represented with different bed residence times</li> </ol>

Figure 1.3: Overview of the differences between the sediment model previously used by Port of Rotterdam and the model that is set up in this thesis. By generating the model boundaries with the ZUNO-DD model and by including wave shear stresses on sediment resuspension in combination with a longer simulation time, the time varying effect of the environmental conditions (weather) can be simulated. This is important, as siltation is known to have a time varying character.

### 1.3 Research objective

This thesis aims to create an improvement of the previous sediment model used by Port of Rotterdam by setting up a new model that incorporates the dynamic nature of SPM concentrations at sea. This is done by adding the effect of wind waves on resuspension at sea and by including temporally and spatially varying SPM boundary conditions. Besides this, the model is expanded with an improved schematization of the sediment bed allowing for different residence times, three SPM fractions characteristic of different particle or floc sizes instead of one, and a model period of 14 days instead of one to allow for variable forcing conditions. This will increase the applicability of the model by incorporating the effects of variable environmental conditions. A summary of the differences in model setup and their effects on model applicability is given in Figure 1.3.

To accomplish this, the sediment boundary conditions will be generated with a larger model known as the ZUNO-DD model. This model spans the entire Southern North Sea, and has been developed, calibrated, and validated for the Port of Rotterdam by Deltares (van der Kaaij et al., 2017). It has previously been used for impact studies for the construction of Maasvlakte 2 (Winterwerp, 2006; van Kessel et al., 2006), the calculation of return flows from sediment dumping locations (Hendriks et al., 2017), and to assess the impact of sand mining in the North Sea. It is therefore a natural candidate for this task. With this in mind, the following research objective has been formulated:

#### Research objective:

Investigate the sediment dynamics of the Rhine ROFI and the Port of Rotterdam and its impact on siltation in the Port of Rotterdam with a numerical sediment model.

This objective is supported by the following research questions:

#### Research questions:

1. Which physical processes govern suspended sediment transport at sea and in the Port of Rotterdam?
2. How well can the physical behaviour be reproduced by improving the NSC-Coarse model with the inclusion of dynamic boundary conditions and wave resuspension?
3. To what extent can the deposition of marine sediment in the Port of Rotterdam be modelled

more accurately by improving the NSC-Coarse model with the inclusion of dynamic boundary conditions and wave resuspension?

## 1.4 Chapter Outline

Chapter 2 contains an overview of the physical system by reviewing the existing literature. Theory is presented regarding sediment processes, hydrodynamic processes in the Dutch coastal zone, hydrodynamic processes inside the harbour, and its impact on SPM transport and harbour siltation. This forms the basis on which the model behaviour will be examined. This section also answers research question 1.

Chapter 3 gives an overview of the models that are used, and their interactions. It describes the model setup, including the model schematization, boundary conditions, spin-up procedure, and three model scenarios that have been run to assess the model behaviour. A mathematical description of the model as well as the exact settings used are found in Appendix D.

In chapter 4, the results of the three model simulations described in chapter 3 are analyzed. This is done by considering the large scale sedimentation behaviour resulting from each scenario and by assessing the time dependent behaviour. The effect of wind waves and stratification on SPM concentrations at sea is considered, and this is linked to sedimentation events inside the harbour. In addition, the effect of the wind wave generation procedure inside the harbour is investigated. To assist in the visualization of the model behaviour, three tidal cycles with different wind directions have been selected. Three hourly snapshots over these cycles have been made for the ZUNO-DD and NSC-Coarse models to be able to draw comparisons between the two. Surface plots and cross-sectional plots at the NSC-Coarse boundary have been made for the ZUNO-DD model, and surface plots and cross-sectional plots through the Rotterdam Waterway have been made for the NSC-Coarse model. For brevity, these have been included in appendix B.

Chapter 5 reflects on the applicability and limitations of the model with respect to the known physics that have been discussed in chapter 2. Together with chapter 6, this chapter provides an answer to research questions 2 and 3.

Finally, conclusions drawn from the analysis of chapter 4 are summed up in chapter 6. The strengths and shortcomings of the current model performance are addressed, and recommendations are given for future model improvement. Together with chapter 5, this chapter answers research questions 2 and 3.



## Chapter 2

# Theoretical background

*This chapter provides an overview of the existing literature regarding the hydro dynamics and cohesive sediment dynamics of the Rhine-Meuse estuary. It is used to provide insight in the physical behaviour of the system, and provides a detailed answer to research question 1. This knowledge is used in chapter 5 and chapter 6 to judge the the behaviour of the model results presented in chapter 4.*

### 2.1 Sediment characteristics

The material dredged from the harbour basins consists of fine (particle size  $< 63\mu\text{m}$ ), cohesive sediment, often referred to as mud. This is usually composed of a mixture of different clay types, silts, fine sand, organic matter, and a lot of water. Particles are characterized by very low settling velocities, and as a result they are predominantly transported as suspended load. Particles are suspended from the bed by bottom shear stresses and are kept in suspension by turbulent mixing within the water column. They are advected by the main flow, and when an area of sufficiently low turbulent mixing is reached, they settle due to gravity<sup>1</sup>. While in suspension these particles are often referred to as suspended particulate matter (SPM).

As a result of their cohesive behavior and the presence of organic material, particles may interact with one another in complex ways, which in turn may alter their sedimentary properties. While in suspension, particles collide due to velocity differences induced by turbulent diffusion. Upon collision, particles may stick to each other, and form highly porous structures known as flocs. These flocs may in turn be broken up into smaller flocs by turbulent shear stresses, which results in a balance between the floc forming processes and the floc breaking shear stresses (Winterwerp, 2002). The potential of floc formation is largely determined by the electrical charge of the particles, which in turn depends on the salinity, acidity, and the presence of organic polymers in the ambient water (Mietta et al., 2009). Usually, particles coalesce into basic floc structures known as primary particles that cannot be broken up by the local hydrodynamics, and undergo processes of growth and break up from there. This process is referred to as flocculation. Floc growth may enhance the settling velocity, and therefore sedimentation is influenced by flocculation.

An important parameter for the deposition is the particle settling velocity. However, this is a much more difficult concept for cohesive sediments than for granular material, as the settling of flocs is outside the stokes regime. In practice, the particle settling velocity in models is usually regarded as a calibration parameter (Winterwerp, 2011).

Once an area with sufficiently low turbulent kinetic energy is reached, particles settle to the bed. As they settle, near bed concentrations can become very high, and the return flow of water leads to hindered settling. Through this process, SPM settles into a highly porous, easily erodible 'fluff layer'. If calm conditions persist long enough, water is slowly squeezed out of the pores by the weight of the particles, and the particles consolidate into the bed. From there, material may be eroded again if sufficiently high bottom shear stresses occur.

---

<sup>1</sup>A notable exception is the formation of fluid mud, where high sediment concentrations may actually drive density driven currents by themselves.

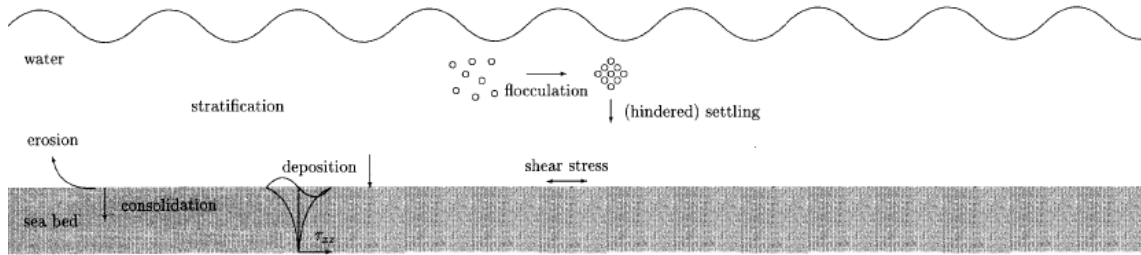


Figure 2.1: Overview of the relevant processes for the erosion, deposition, and transport of cohesive sediments. Sediment is eroded by bottom shear stresses. In the water column, particles interact and flocculate, and at some point settle to the bed. At the bed, they form a transitional fluff layer from which they may quickly be eroded, or consolidate into the bed. Obtained from (van Kessel, 1997).

## 2.2 Large scale dynamics of the North Sea

On large time scales (seasonal averages), dominant flow patterns in the North Sea are controlled by residual currents generated by winds, tides, and the density structure of the water. In a broad sense, these mechanisms all contribute to a cyclonic circulation of water and Suspended Particulate Matter (SPM) in the North Sea, and a Northeast directed current along the Dutch coast specifically. An impression of the residual current patterns is given in figure 2.2.

The Southern Bight of the North Sea is characterized by a dominant southwesterly wind field. These winds push water through the Dover straits, resulting in a Northward directed residual current along the Dutch coast (van der Giessen et al., 1990; Pingree et al., 1980). Tides enhance this current by generating higher harmonics upon interacting with the local topography, causing a flood dominant tidal asymmetry (Nihoul et al., 1975). Finally, river outflows and seasonal heating may vertically stratify regions of the North Sea, creating frontal zones which drive baroclinic currents that become stronger as the degree of stratification increases (Simpson et al., 1974; M. Visser et al., 1991). Fresh water outflow of the continental rivers turns right under the influence of earth's rotation and forms a band of relatively fresh water that, upon hitting the coast, flows North under a thermal wind balance (de Boer, 2009). The combination of these three residual flows is a cyclonic circulation of water through the North Sea basin, where Fresh water outflows are largely confined in a cyclonic flow along the coast<sup>2</sup>.

On shorter timescales, this time averaged current signal is modified by variations in the forcing conditions. (van der Giessen et al., 1990) showed wind variations may increase the residual transport through the Dover strait, but that prolonged easterly winds may also weaken or even temporarily reverse the residual circulation. Increased river discharges lead to a stronger density gradient, which can strengthen on-shore near-bottom current velocities and off-shore surface velocities (M. Visser et al., 1991). Changes in tidal energy also induce variations. On timescales of hours, the ebb/flood cycle is dominant, but also the fortnightly spring/neap cycle is important, as it alters the amplitude of the tidal signal (Simpson, 1997).

These processes form the driving force behind the large scale transport of SPM in the North Sea.

<sup>2</sup>A notable exception is the Thames discharge, which turns in a cyclonic direction and crosses the North Sea basin to join the continental coastal rivers. However this confluence occurs North of the Dutch coastal zone, and does not impact the Dutch coastal sediment budget. For that reason, it will not be further discussed.

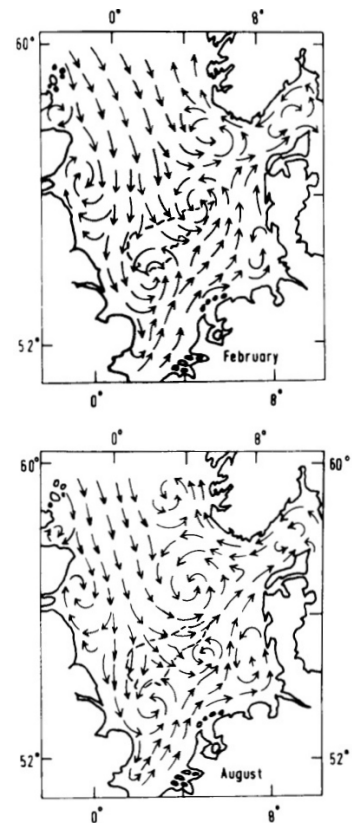


Figure 2.2: Residual current patterns in the North Sea. Taken from (Böhnecke, 1922), as cited in (Otto et al., 1990).



Figure 2.3: Satellite image (MODIS Terra) taken on March 27<sup>th</sup> 2007 of the Southern North Sea, showing surface SPM. Along the main continent, SPM is concentrated in a narrow band along the continental coast due the Coriolis force. The stochastic nature of wind wave action causes period deposition and resuspension of SPM, while the residual currents transport it North along the coast. Concentrations in winter are significantly higher than during summer. Obtained from (el Serafy et al., 2007)

There is a residual Northern transport of SPM along the Dutch coastal zone and as a result the dominant sediment sources are found to the South. SPM in the Dutch coastal zone originates mainly from an influx through the English channel, erosion of the French coast lining the channel, and the discharge of the Rhine-Meuse estuary (Suijlen et al., 2002; van Alphen, 1990; M. Visser et al., 1991). A strengthening or weakening of the residual circulation will increase or decrease the amount of sediment transported along the Dutch coast. Estimations of the total SPM transport along the Dutch coast vary widely, but are generally between  $7 * 10^7$  and  $10 * 10^7$  tonne/year, with variations up to 17% (van Alphen, 1990; Suijlen et al., 2002).

Transport of SPM is governed by the flow and by the amount of sediment in suspension. The latter is governed by the periodic deposition and resuspension of SPM due to the environmental forcing conditions. The Southern Bight is shallow enough for waves with wave periods of more than 10s to exert shear stresses on the bottom. Hence, waves are an important resuspension mechanism and wave height strongly relates to the amount of SPM in the water column. As a result seasonal averages of SPM concentrations show much higher concentrations during winter than during summer (Eleveld et al., 2008; Pietrzak et al., 2011). Moreover, SPM concentrations shortly after storm events show SPM concentrations three to four times higher than winter averages (Suijlen et al., 2002). Significant wave height is strongly connected to wind fetch, and the highest waves are associated with Northwesterly winds (Baeye et al., 2011). (Otto et al., 1990) notes that a large part of the tidal energy is dissipated through bottom friction and becomes available for the mobilization of sediment. Both the tidal period and the spring/neap cycle are therefore important

controls on the suspension of sediment by tides.

Vertical stratification of the water column affects SPM concentrations through turbulence damping and through baroclinic flows. In a stratified water column, turbulence is inhibited at the pycnocline because vertical fluctuations are dampened by the density gradient, thereby limiting the turbulent mixing length. This causes sediment to settle through the pycnocline while SPM in the bottom layer cannot cross to the top layer (Simpson, 1997; Pietrzak et al., 2011; Geyer, 1993). The result is a strong vertical gradient in the sediment concentration, with very high concentrations near the bottom, and virtually no SPM in the top layer (Eleveld et al., 2004; Pietrzak et al., 2011). Second, vertical stratification drives baroclinic flows with an on-shore near-bottom velocity. These on-shore velocities concentrate SPM into a thin band along the shore (van Alphen, 1990). All else equal, an increased river discharge will increase these buoyancy induced fluxes.

## 2.3 Dynamics of the coastal zone

In the Dutch coastal zone, and near the mouth of the Rotterdam Waterway specifically, local effects are superposed on the large scale residual circulation. This region is highly influenced by the freshwater outflow of the Rhine-Meuse estuary through the Rotterdam Waterway and the Haringvliet, which has a combined average discharge of  $2400m^3/y$  but can vary between  $600m^3/y$  and  $19500m^3/y$ . The outflowing river water is of lower density than the seawater into which it discharges, and forms a large vertically stratified water body with variable size and shape, known as a region of fresh water influence (ROFI) (Simpson et al., 1993). Under the influence of earth's rotation, the low density outflow turns to the right (cyclonically) until it is confined by the coast, and then forms a band of low salinity water that flows North under the thermal wind balance like coastal river (de Boer, 2009). The lateral buoyancy input of the Rhine and Meuse discharge causes a lock exchange type mechanism, which drives a baroclinic flow with an off-shore traveling freshwater front and on-shore near bottom currents in the saline lower part of the water column. This is schematized in Figure 2.4, which shows the distinct two layer velocity profile that is characteristic of baroclinic flow.

This density structure exists under constant competition between the stratifying and mixing forces that arise from the complex interplay of variable river discharge, wind velocity, tidal currents and waves (Simpson, 1997; Souza et al., 1995).

Stratification is important because induces significant cross-shore and vertical exchange flows as well as damping turbulence at the pycnocline, which in turn influences the distribution of SPM concentrations. The tide propagates along the shoreline as a Kelvin wave, and imposes a periodic strengthening and weakening on the stratification, a phenomenon known as tidal straining (Simpson et al., 1990). Due to bottom friction surface waters are advected further than bottom waters, and are deflected by the Coriolis force. As a result, surface waters are advected off-shore over during ebb flow (enhancing stratification), and on-shore during flood flow (weakening stratification). Because water cannot cross the coastline, this induces periodic upwelling (ebb flow) and downwelling (flood flow) along the coast, and on-shore (ebb) and off-shore (flood) near bottom currents (de Boer et al., 2006). This phenomenon is illustrated in Figure 2.5. This means that surface water moves in anticyclonic tidal ellipses, while near bottom water moves in cyclonic tidal ellipses (Souza et al., 1995). Stratification strengthens this effect by decoupling the surface and bottom ellipses from each other (A. Visser et al., 1994).

Stratification is counteracted by tidal stirring, which results from the shear stresses in the water column induced by tidal velocities (see Figure 2.4). The amplitude of the tidal velocities (and thereby the amount tidal stirring) is modulated by the spring-neap cycle. During spring tide, larger tidal amplitudes cause larger velocity gradients (due to bottom friction), which in turn cause larger shear stresses in the water column, mixing the vertical density structure. During neap tide, tidal velocities are lower, and this process diminishes. The result is a fortnightly cycle in which stratification stability is enhanced during neap tide and reduced during spring tide.

Finally, the wind stresses may either weaken or enhance stratification. Surface wind stresses drive an Ekman transport in the water column to the right of the wind direction, much like tidal straining. Hence, alongshore Northerly winds advect fresh surface water over the dense lower water, enhancing stratification and coastal upwelling, while alongshore Southerly winds drive an

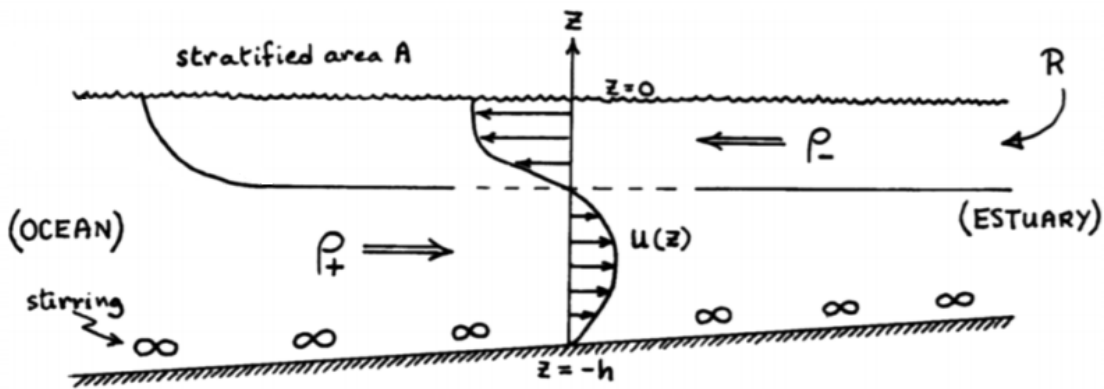


Figure 2.4: Overview of the baroclinic exchange current that results from the freshwater buoyancy input of an estuary outflow. The low-density river outflow (marked by 'R') floats on top of the denser sea water and generates a near surface off-shore current marked by a distinct front with a strong kink known as a pycnocline (or halocline if caused by salinity differences). Meanwhile the denser sea water dives under the freshwater lens and drives an on-shore near bed current. Bed friction induces shear stresses in the water column, which leads to mixing of the vertical density structure. If the mixing influences dominate over the buoyancy input, the vertical density gradient is broken up and the water column becomes well mixed. Image obtained from (Simpson et al., 1990).

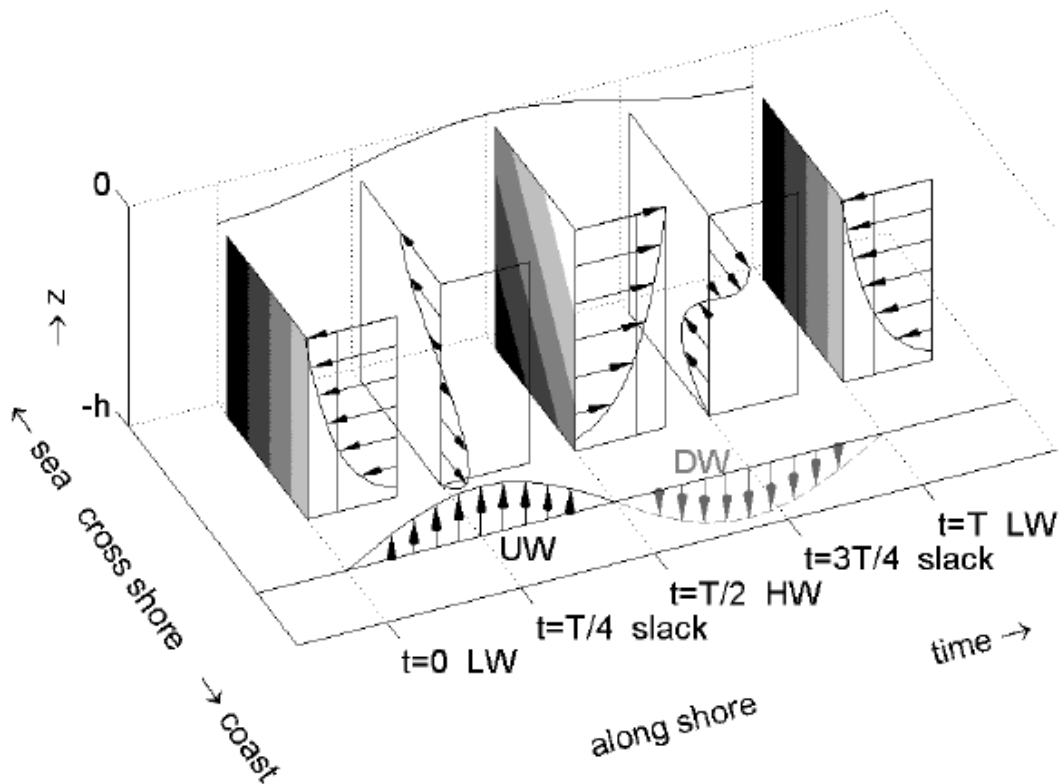


Figure 2.5: Schematization of the interaction between a Kelvin wave type tidal current and horizontally stratified water body in a rotating reference frame over one tidal cycle. During ebb flow, the surface water is deflected off-shore by the Coriolis force. Differential advection pushes the surface water over the bottom water, which causes vertical stratification. This process is known as tidal straining. Continuity requires the off-shore flowing water to be replaced, which leads to upwelling (UW) along the coast and a near bottom on-shore current. During flood, this process reverses. Surface currents are deflected on-shore, weakening vertical stratification and causing downwelling (DW), while near bottom currents are directed off-shore. Image obtained from (de Boer, 2009).

on-shore Ekman transport, weakening stratification and enhancing downwelling.

This periodic stratification is important for the distribution of SPM in the water column. Stratified water bodies are known to have significantly reduced turbulent kinetic energy (TKE) near the pycnocline, as the density gradient imposes a limit on the turbulent mixing length. As a result, SPM in the lower layer is no longer advected to the upper layer, and SPM present in the upper layer settles through the pycnocline into the lower layer, leaving a surface layer largely devoid of SPM and high concentrations in the bottom layers (Pietrzak et al., 2011; Eleveld et al., 2008). Furthermore, stratification imposes near bed on-shore currents, which resuspend deposited sediment and transfer it on-shore. In some instances, baroclinic forcing can also transport SPM off-shore. (Horner-Devine et al., 2017) observed that SPM is transported from the surf zone to the near shore by on-shore propagating freshwater fronts that induce near bottom off-shore return flows.

Storms and spring tides resuspend sediment sediment and mix up stratification, allowing for large sediment concentrations throughout the water column (Joordens et al., 2001; Souza et al., 1996). Conversely, low wave energy, neap tides, and high discharge enhance stratification and reduce surface SPM, but SPM can still be present in the bottom layer.

## 2.4 Advection in the Rotterdam Waterway

With the tide, the vertically stratified density structure is advected back and forth into the Rotterdam Waterway in the form of a salt wedge. (de Nijs et al., 2010) performed measurements along the Rotterdam Waterway to assess the development of the salinity and current structure over a tidal cycle. They found that the barotropic tidal forcing advects the salt wedge up and down the estuary between an area just inland of the Maasmond and slightly beyond the juncture between the Old and New Meuse, and found it to remain stable throughout the entire tidal cycle. Furthermore, they observed a much longer ebb than flood period, and attributed this to the combination of the barotropic and baroclinic forcing.

Stratification induces the damping of turbulence, and this is often associated with the accumulation of SPM in the tip of a salt wedge, known as an Estuarine Turbidity Maximum (ETM) (Geyer, 1993). (de Nijs et al., 2011) showed that an ETM is maintained in the Rotterdam Waterway as well. Specifically, they found fluvial SPM to be transported over the salt wedge during ebb. As a result of turbulence damping at the pycnocline, the SPM settles through the interface and into the salty bottom layer. There it is resuspended upon flood, and the transport path finally converges in the head of the salt wedge thereby forming and maintaining an ETM. The ETM loses mass through exchanges with various harbour basins lining the Rotterdam Waterway. Especially Botlek harbour stands out because it is located roughly at the limit of saltwater intrusion, leading to large exchange rates between the ETM in the Rotterdam Waterway and Botlek harbour. The large dredging requirements of Botlek harbour have been ascribed to this phenomenon.

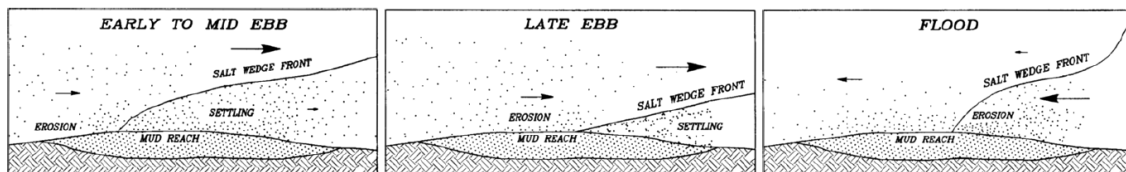


Figure 2.6: Formation of an Estuarine Turbidity Maximum (ETM) as described by (Geyer, 1993). Stratification inhibits the size of turbulent eddies, and causes a reduction of turbulent kinetic energy near the pycnocline. This causes SPM to settle through the pycnocline and accumulate in the lower water layer. Flood currents resuspend sediments, generating a region of high SPM concentrations in the tip of the salt wedge.

## 2.5 Harbour siltation

As a result of the estuarine nature of the Rotterdam harbour, both fluvial and marine sediments play a role in harbour siltation. Depending on the positioning of the harbour, different siltation mechanisms are dominant.

(de Nijs et al., 2011) constructed a sediment balance from literature and dredging records, and concluded that there is virtually no marine sedimentation in the harbour basins lining the Rotterdam Waterway because the Maasmond area is much deeper than the Rotterdam Waterway, and acts as a marine sediment trap. (Verlaan et al., 2000) showed the importance of wave have height to siltation in the Maasmond by relating the near bottom orbital wave velocity at sea to measurements of bed elevation obtained from echo soundings of the Maasmond area (see Figure 2.7). During storms, they observed two transport mechanisms produce this phenomenon. First, storms stir up large amounts of sediment into the water column, which are advected into the harbour by the ambient current. Second, they note that during storms a wave induced boundary layer of approximately 0.1m forms near the bed, marked by high wave induced shear stresses. This boundary layer is able to hold a much larger amount of sediment in suspension than the rest of the water column, forming a layer of high near bottom SPM concentrations marked by a lutocline at the height of the wave boundary layer (where shear stresses decrease). This highly concentrated SPM layer is kept fluid by the waves, is transported into the Maasmond by friction with the above currents, and settles in the deeper Maasmond area. Upon settling, it forms a fluid mud layer that spreads to adjoining harbour basins through density driven currents. This process causes the siltation in the Maasmond, Maasvlakte, and Europoort to have a strong episodic nature.

Inside the Rotterdam Waterway, fluvial SPM is trapped and deposited through the mechanism described in 2.4. (de Nijs et al., 2009) concluded that the siltation in the harbor basins lining the Rotterdam Waterway is largely controlled by the limit of salt water intrusion and the positioning of the ETM associated therewith. (de Nijs et al., 2011) concluded that the Rotterdam Waterway and the adjoining harbour basins have a silt trapping efficiency of between 65% and 82% and the remaining percentage is trapped in the Maasmond.

The result is that the siltation rates of the harbour basins lining the Rotterdam Waterway are largely detached from the siltation rates in the Maasmond, Calandkanaal, and Maasvlakte areas, allowing for the construction of Figure 1.2. This causes siltation rates in the harbour basins lining the Maasmond to have a much stronger episodic character than siltation rates in basins lining the Rotterdam Waterway.

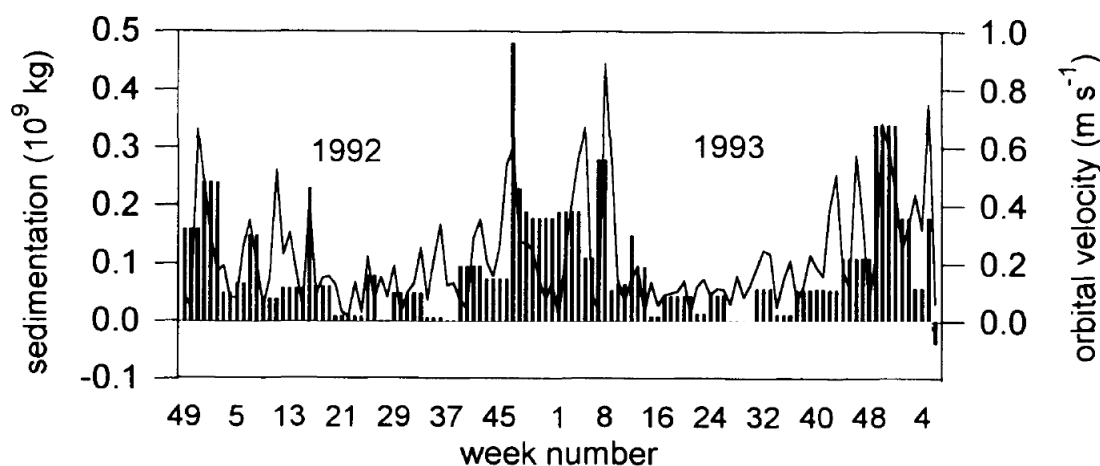


Figure 2.7: Relation between siltation in the Maasmond region and wave orbital velocities at sea. Storms at sea correlate with large siltation events. Image obtained from (Verlaan et al., 2000).

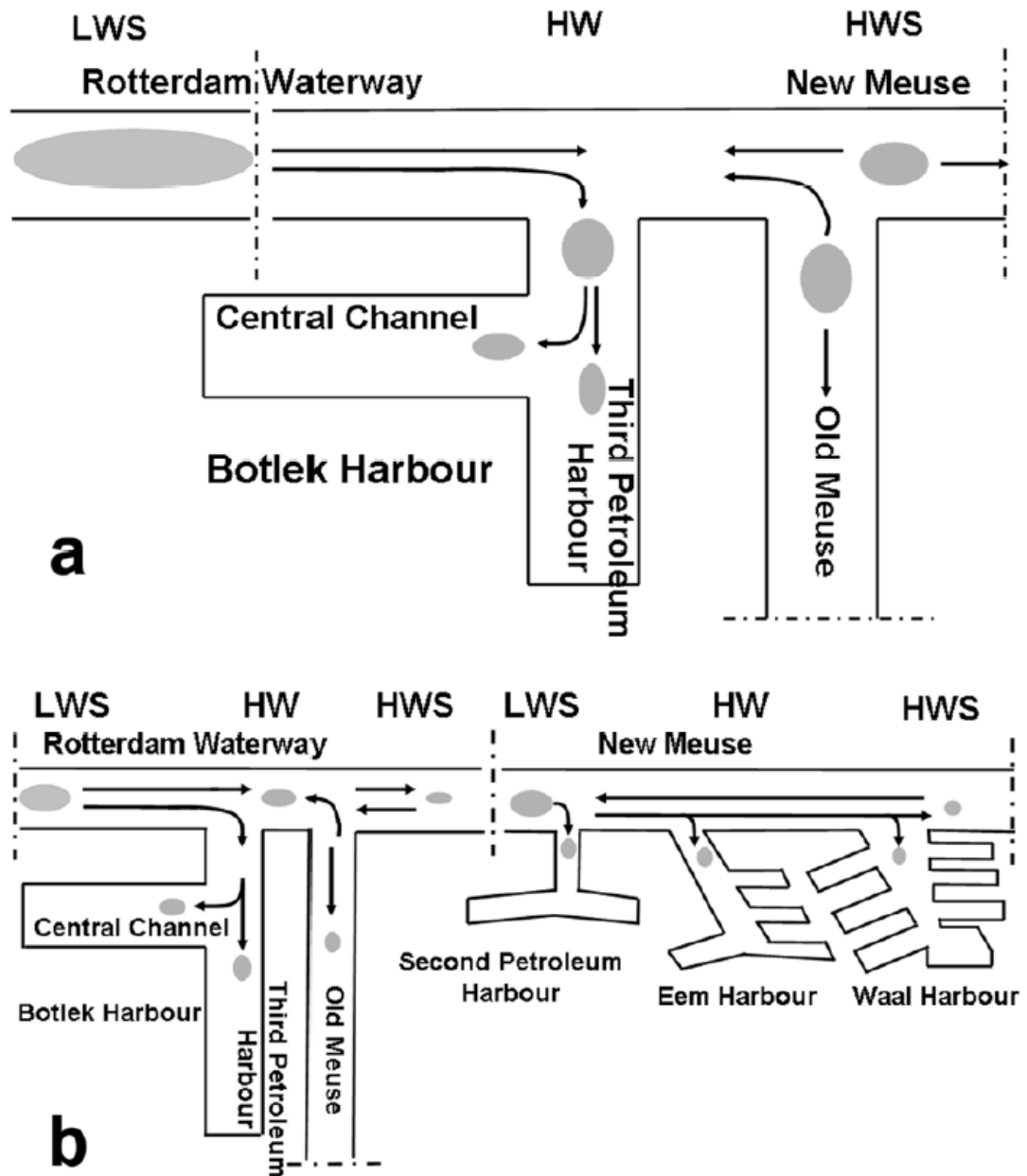


Figure 2.8: Overview of the mechanism through which fluvial SPM deposits in the harbour basins lining the Rotterdam Waterway. Stratification in the Rotterdam Waterway causes the formation of an ETM, which exchanges sediment with the Harbor Basins lining the Rotterdam Waterway. The top panel (A) shows typical conditions, when the limit of salt water intrusion lies approximately at Botlek Harbor. This causes high siltation rates in Botlek harbor, and explains the large dredging loads in this basin. The bottom panel (b) shows a case in which the salt wedge is advected further upstream. This causes the ETM to split at the junction of the Old and New Meuse, and exchange with basins further upstream. Image obtained from (de Nijs et al., 2009).

# Chapter 3

## Model Setup

*This chapter describes the model setup employed in this thesis. Five five model have been used, which are described in section 3.2. After that, an overview of the computational domain and some relevant model parameters are presented. An important concept is the inclusion of the sediment boundary conditions on the open sea boundary. This is covered in section 3.6. The model spin-up is discussed in section 3.7. A detailed description of the model is presented in appendix A.*

### 3.1 Introduction

To study the effects of SPM concentrations in the North Sea on siltation in the Port of Rotterdam, a model is needed that covers the entire physical domain of interest and has sufficient resolution. In other words, the model area must sufficiently capture the SPM processes of advection, erosion, and deposition on the North Sea, while also having enough resolution inside the harbour basin to model where the SPM is advected within the complex harbour geometry.

At the time of writing this thesis, no such model exists. However, there are different models that cover different domains with sufficient resolution and have overlap. In this thesis, these models will be combined by using one model to generate the boundary conditions for the other. The result is a high resolution model of the Rotterdam harbour that also includes the variability of SPM concentrations at sea. In total, five models will be used. They are introduced in this chapter, including the required initial and boundary conditions.

### 3.2 Overview of the models used

Five models are used to sufficiently cover both the processes at sea and in the harbour:

- **ZUNO-DD (FLOW)**: A 3D Delft3D-Flow model that is used to model the hydrodynamic processes in the Southern North sea. Its name stands for ZUidelijke NOordzee-DomeinDecompositie (Southern North Sea-Domain Decomposition). It has been validated together with the ZUNO-DD (WAQ) model.
- **ZUNO-DD (WAQ)**: A 3D Delft3D-WAQ model that is used to model the advection, resuspension, and deposition of SPM as a result of the aforementioned hydrodynamic simulation. This model was validated for SPM concentrations in the North Sea by (van der Kaaij et al., 2017).
- **Harbor model**: A 2DH SIMONA model that is used as an intermediate step to generate the hydrodynamic boundary conditions for the NSC-Coarse model. This model was is part of the NSC-Coarse model train, and has been validated in that context.
- **NSC-Coarse (FLOW)**: A 3D SIMONA model that is used to simulate the hydrodynamic processes inside the Port of Rotterdam. This model has been validated by (Rotsaert, 2010; Kranenburg et al., 2015a; Kranenburg et al., 2015b).

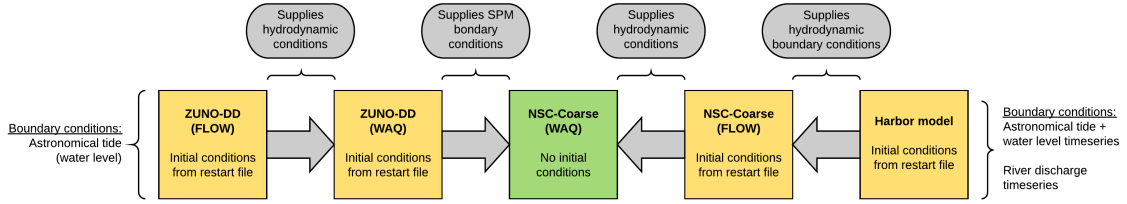


Figure 3.1: Overview of the interactions between the 5 models that are used in this thesis. Each model is run independently, but most of them use the results of other models as input.

- NSC-Coarse (WAQ):** The model that is set up in this thesis. A 3D Delft3D-WAQ model that uses the NSC-Coarse computational domain and Hydrodynamics to simulate suspended matter processes inside the port of Rotterdam.

All of these models run independently. The harbour model and ZUNO-DD (FLOW) models can be seen as the starting point of a computation, as they do not rely on any of the other models. The harbour model is larger than the NSC-Coarse model in surface area, but has a far lower resolution and is two dimensional. It generates water levels and (depth averaged) velocities, which are used by the NSC-Coarse (FLOW) model as boundary conditions.

Consequently, the NSC-Coarse model (FLOW) and the ZUNO-DD (FLOW) model are used to generate the hydrodynamic conditions that are used by the NSC-Coarse (WAQ) model and the ZUNO-DD (WAQ) model, respectively. Finally, the ZUNO-DD (WAQ) model is used to generate the sediment boundary conditions at sea for the the NSC-Coarse (WAQ) model, implicitly linking the ZUNO-DD (FLOW) and Harbor models. An overview of the models and their interactions is given in Figure 3.1.

The ZUNO-DD model uses a computational grid that spans the southern part of the North Sea from the Dover strait to the North of Denmark. The model uses domain decomposition to achieve the highest grid resolution near the Dutch coast (approximately 1x1km), while having much larger grid cells further off-shore (approximately 20x30km). To save computational resources, the ZUNO-DD (WAQ) grid has the finest grid cells aggregated to the size of the intermediate grid (approximately 3x1.5km). Consequently, there are only two different grid resolutions in the computational domain of the ZUNO-DD (WAQ) model, while the ZUNO-DD (FLOW) model uses three different resolutions (see Figure 3.2). In vertical direction, the ZUNO-DD model has 12 sigma layers, with each layer thickness a fixed percentage of the water depth. Their distribution over the water column is shown in Table 3.1. All grids are shown in Figure 3.2.

### 3.3 Grid and bathymetry

The Harbor model (or Zeedelta model) has a much higher resolution, with grid cells ranging from approximately 200x200m at sea down to 40x40m in some areas of the harbour. However, the model is two-dimensional so it has fewer cells. Its computational domain stretches between 25km and 35km off-shore and runs from the coast of Schouwen-Duivenland South to Zandvoort in the North. Upstream, its domain reaches to measuring stations at Hagestein (Lek), Tiel (Waal), and Lith (Maas) which mark the upstream end of the Rhine-Meuse estuary.

The NSC-Coarse (WAQ and FLOW) grid has the same resolution as the Harbor model, but is three dimensional. For this thesis, its vertical layers have been increased from 10 to 12 and the layer distribution has been adapted to match the ZUNO-DD model exactly. The resolution near the bed and surface has been increased to sufficiently capture boundary effects. Its layer distribution is given in Table 3.1. Horizontally, the computational domain extends about 17km off-shore from

$\sigma$ -layer	Layer thickness
1	4%
2	5.6%
3	7.8%
4	10.8%
5	10.9%
6	10.9%
7	10.9%
8	10.9%
9	10.8%
10	7.8%
11	5.6%
12	4%

Table 3.1: Vertical layer thickness distribution of the ZUNO-DD and NSC-Coarse models.

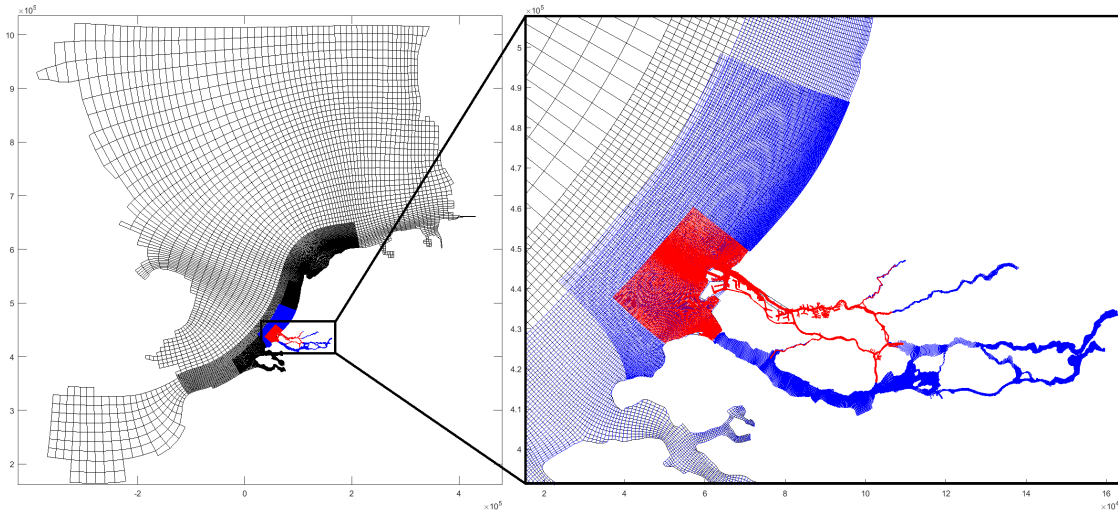


Figure 3.2: Overview of the computational domains used by the various models. The ZUNO-DD grid is shown in black, the Harbor model grid is shown in blue, and the NSC-Coarse grid is shown in red. The ZUNO-DD (FLOW) model uses domain decomposition to combine three different grid resolutions on the North Sea. In the WAQ model, the finest grid is aggregated to the size of the intermediate grid. The right panel shows the decomposition of the ZUNO-DD grid into a coarse (top left) intermediate (middle) and fine (coast) grid (all in black). The NSC-Coarse model has a much higher resolution and covers the Rotterdam harbour in detail. The Harbor model (blue) is larger in area than the NSC-Coarse model, and covers the entire estuary. It is used to calculate hydrodynamic boundary conditions for the NSC-Coarse model.

the coast of Goeree-Overflakkee South to just before the sand engine North. Upstream, the NSC-Coarse grid reaches up to the towns of Gouda (Hollandsche IJssel), Lekkerkerk (Lek), Papendrecht (Lower Merwede), Dordrecht (Dordtsche Kil), and to (but not including) the Haringvliet (Spui)<sup>1</sup>.

### 3.4 Substances, bed layers, and important model parameters

The starting point of this thesis was an already calibrated version of the ZUNO-DD (WAQ) model. For consistency, all model parameters for the NSC-Coarse (WAQ) model have been set identical to those of the ZUNO-DD model. An overview of the model parameters is given in Table D.1 in appendix D. The potential impact of this decision is evaluated in section 5.3.

To include the effect of different floc sizes and settling velocities, the sediment included in the model is discretized into three 'Inorganic Matter' (IM) sediment fractions, characterized by a unique and constant settling velocity, given in Figure 3.2. Flocculation is not modelled in this thesis, and the different fractions are meant to represent different particle or floc sizes. Each fraction therefore behaves independently from the other fractions. Additionally, sometimes the term 'total inorganic matter' is used. This is the sum of the three fractions (IM1+IM2+IM3).

Besides the sediment fractions, two bed layers are defined, schematized in Figure 3.3. Each bed layer interacts with the sediment fractions in the water column by having a deposition and an erosion flux. Layer 'S2' represents a sandy bed in which sediment may be buried, while layer 'S1' represents a thin 'fluff' layer of mud that deposits on top of layer S2 during calm conditions. Layer S2 is characterized by longer sediment residence times than layer S1. This is reflected by the fact that layer S1 is given a critical shear stress of  $\tau_{c,S1} = 0.2N/m^2$  and layer S2 has  $\tau_{c,S2} = 0.8N/m^2$ . For the calculation of the deposition and erosion fluxes, as well as a list of all model parameters, the reader is referred to appendix D.

To save computational resources, it is desirable to choose as large as possible a timestep while maintaining sufficient accuracy. To make an informed choice, test computation have been repeated with timesteps of  $\Delta t = 5m$ ,  $\Delta t = 2m$ ,  $\Delta t = 1m$ , and  $\Delta t = 30s$ . The difference between the

<sup>1</sup>The discharge of the Haringvliet sluices into the North sea is included in the model as a separate discharge.

Sediment fraction	Settling velocity
IM1	10.8 m/d
IM2	86.4 m/d
IM3	0.1 m/d

Table 3.2: Sediment fractions included in the WAQ models. Each fraction is characterized by a unique and constant settling velocity that will influence its transport behaviour. Note that fraction IM2 has the largest settling velocity the heaviest fraction and IM3 the smallest.

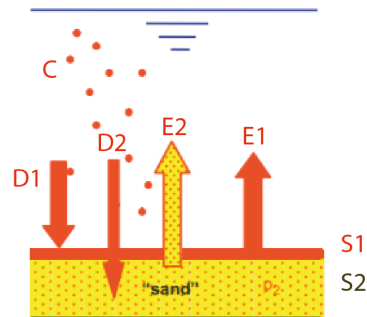


Figure 3.3: Overview of the bed layers S1 and S2. S2 is a sandy layer with a longer residence time (coloured yellow), while S1 is a muddy 'fluff' layer with a much shorter residence time (thin red line on top of S2). Each layer has an erosion and deposition flux, so there are four exchange fluxes between the bed and the water column (van Kessel et al., 2010).

results of  $\Delta t = 1m$  and those of  $\Delta t = 30s$  was considered sufficiently small to accept a timestep of  $\Delta t = 1m$ .

## 3.5 Forcing conditions

The environmental forcing conditions that are applied to the hydrodynamic models (both NSC-Coarse and ZUNO-DD) are comprised of wind, waves, river discharges, and tides (water levels). All are based on measurements of the year 2007. The ZUNO-DD (FLOW) model is supplied with a spatially varying wind field, while the wind field of the NSC-Coarse model is measured at Noorderpier (Hook of Holland). River outflows consist of measured discharge time series, and tides are imposed as time varying water levels at the model boundaries. For the NSC model, these water levels are corrected with a Kalman filter, using measured water levels at five measurement stations in front of the Dutch coast.

### 3.5.1 Treatment of wind waves

Special care needs to be taken with the treatment of wind waves. Wind waves are not automatically resolved in the hydrodynamic model (the model is based on the shallow water equations) but are very important for the resuspension of sediment. Its influence can therefore not be neglected. The most accurate way to include short wave effects is to run a short wave resolving model online with the long wave model, but this is deemed too computationally expensive. To circumvent this issue, a wave field has been generated by using a SWAN averaged wave field corrected by a data assimilation based on wave height measurements of the year 2007 from 18 available wave buoys. The wave buoy locations are given in Figure 3.4. Out of this wave field, a scalar field of bottom shear stresses is computed, which is interpolated onto the model grid and added to the bottom velocity shear stresses in the WAQ model. This procedure was implemented by Deltares for the ZUNO-DD (WAQ) model, and has been repeated for the NSC-Coarse model in this thesis. Besides most likely being less accurate than a wave model, the method has a number of consequences.

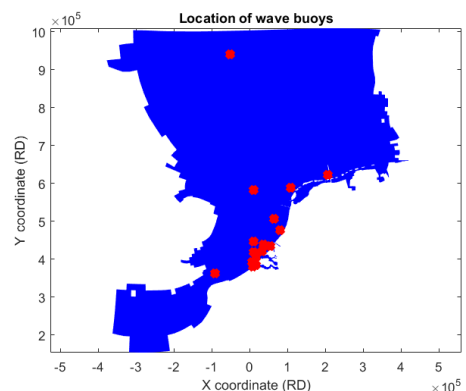


Figure 3.4: Location of the wave buoys used for assimilating the wave field. Though the number of buoys for the entire North Sea is small, the concentration near the Dutch coastline is high.

First, the stirring effect of wind waves on the salinity structure is lost. The shear stress field is added after the hydrodynamic computation, and affects only the resuspension of sediment. Since

wind waves have a mixing influence, this may lead to an overestimation of the stratification during stormy conditions.

Second, the wave bottom shear stresses are computed as a scalar field, meaning that the directional relationship between velocity shear and wave shear is lost. During periods when either shear stress dominates (storms, quiet conditions), this is deemed harmless, but when they are of equal magnitude this may lead to significant errors.

One should therefore regard the wave field more as a means to take into account the effects of storms on the resuspension of sediment than as a precise representation of a wind wave field.

### 3.6 Boundary conditions

The ZUNO-DD model is characterized by two large open boundaries in the Dover strait and between the Danish and British coasts. At both sides, a water level boundary representing the tidal forcing and a constant salt concentration are applied for the ZUNO-DD (FLOW) model. Furthermore, hourly freshwater discharges are applied at all river outflows that lie within the model. For the WAQ model, sediment concentrations are applied for the three distinct sediment fractions (IM1, IM2, IM3) presented in Figure 3.2.

The NSC-Coarse (FLOW) model receives its boundary conditions from the Harbor model, which is run first. At the seaside, this model is supplied with astronomical tide water levels, which are improved further using a Kalman filter that uses 10 minute interval water level measurements supplied by the Ministry of Infrastructure and Water Management (Rijkswaterstaat) at five measuring stations (Hoek van Holland, Lichteiland Goeree, Haringvliet 10, Scheveningen, and Brouwershavensegat 08). On the river side, the model is supplied with daily averaged discharge measurements for the rivers Waal (measured at Tiel), Lek (Hagestein boven), and Meuse (Lith). The salt concentrations are calculated using a discharge dependent formula for the Meuse and Rhine.

The SPM boundaries at sea will be calculated with the ZUNO-DD (WAQ) model. To do so, the cross-shore seaside boundaries of the NSC-Coarse grid have been divided into 6 sections, while the alongshore boundary consists of 4 sections. The 12 layers of the ZUNO-DD model have been kept intact, to preserve the variations over depth. The NSC-Coarse boundary is thus discretized into 192 sections. For each section, the suspended sediment concentrations (IM1, IM2, and IM3) are extracted from the ZUNO-DD (WAQ) output, and are averaged over that section and written to a boundary conditions file with timesteps of one hour. An overview of the boundary sections is given in Figure 3.5.

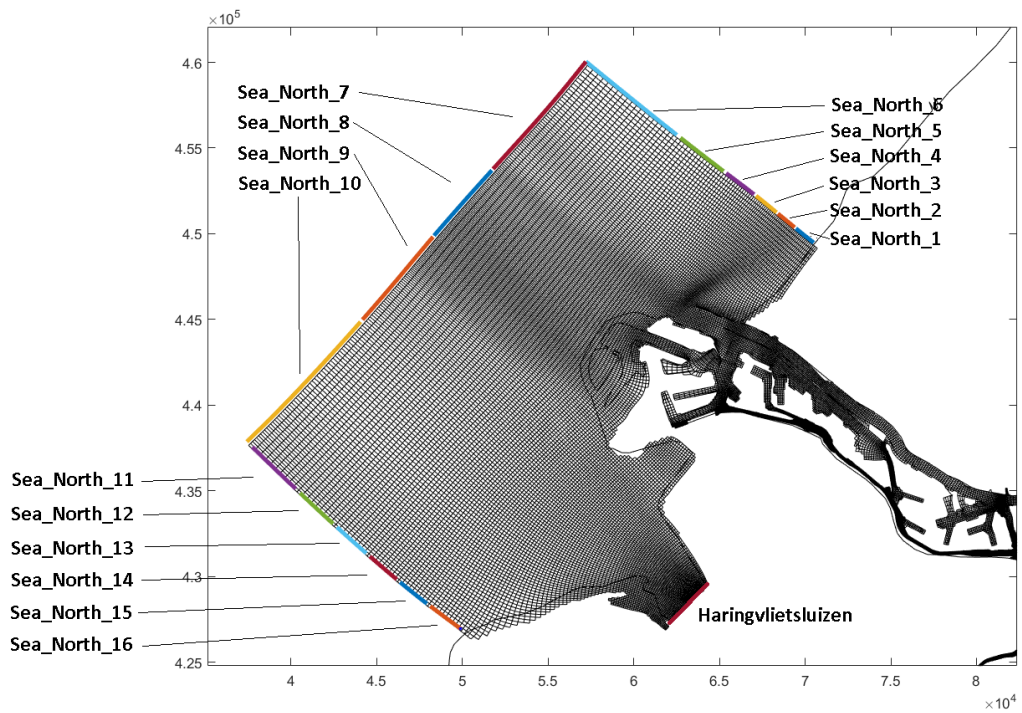


Figure 3.5: The seaside boundaries of the NSC-Coarse grid have been divided into six sections for the cross-shore boundaries and four sections for the alongshore boundary. For each section, SPM concentrations are averaged over the section and supplied as boundary conditions at each hour and for each of the 12 depth layers. Thus, the North Sea open boundary of the NSC-Coarse (WAQ) model is spatially discretized into 192 segments. This will allow for more variability than the previously used boundary conditions which were constant in time and depth. Note that Maasvlakte 2 is added to the model through the bathymetry, and is therefore not included in the model grid.

### 3.7 Initial conditions and spin-up of NSC-Coarse (WAQ) model

Each model will need initial conditions for both the FLOW and the WAQ simulation. The hydrodynamic initial conditions consist of water levels, water velocities, temperature, and salt concentrations. The initial conditions of the WAQ models consist of concentrations of all three SPM fractions in all 12 sigma layers, as well as the concentration of each SPM fraction in each of the two bed layers.

For all models except the NSC-Coarse (WAQ) model, there are restart files available with the required initial conditions. These models therefore do not need to be spun up. For the NSC-Coarse (WAQ) model, no initial conditions for SPM concentrations and bed layer compositions are available. Hence, the WAQ model will be initialized through a cold start (all concentrations set to zero, and the model is run until a dynamic equilibrium is reached). To assess when the model has spun up sufficiently, a single spring-neap tidal cycle will be repeated cyclically. For this process, the third period has been selected, as it is considered to be most representative of average weather conditions (see Table 3.3). In this process, it is important that sediment masses are conserved during the transition from one cycle to the next. The Delft3D (WAQ) module computes sediment concentrations, and a mismatch in water levels would produce a sediment mass imbalance. For that reason, the time period of scenario three has been chosen such that the start and end times occur at high water (to minimize flow velocities), and the water levels at start and end naturally match as closely as possible, interpolating over a few hours to match the water levels exactly. Delft3D-WAQ has an inbuilt function to guarantee mass conservation, but it is nevertheless desirable to have a naturally smooth transition. In this manner, all hydrodynamic input conditions are repeated cyclically.

In correspondence with the hydrodynamic conditions, the SPM boundary conditions (IM1, IM2, and IM3) and the bottom wave shear stresses have been repeated cyclically as well. For the time period of scenario three, the SPM concentrations and wave shear stresses have been extracted from the ZUNO-DD (WAQ) output and the wave stress data assimilation respectively, and these are repeated in line with the hydrodynamics.

The spin-up procedure consists of a number of successive runs of the spin-up scenario. For a single model run, the spin-up conditions of Period 3 are repeated for ten spring neap cycles. A single run therefore has a length of 140 (virtual) days, creating a pattern such as shown in Figure 3.6 (only four cycles are shown). This model run can then be repeated a number of times, with each run using the end of the previous run as initial conditions. The model runs can then be compared at different observation stations. When the difference between model run  $n$  and  $n-1$  is sufficiently small, the spin-up of the model has been completed. The result is an initial conditions file that can be used as the starting point for each subsequent scenario.

Spin-up of the NSC-Coarse (WAQ) model was considered complete after five model runs. The total spin-up time of the model is therefore 700 days. In Table A.1 to Table A.5, the relative increase in concentration from one cycle to the next (taken at the last timestep of each cycle) is displayed for 21 observation points in and outside the harbour (locations are shown in Figure A.6). For the station Hook of Holland, the development of the concentrations of the five successive runs is plotted in Figure 3.7. After 5 runs, the substance IM2S2 (sediment fraction IM2 in bed layer S2), which responds the slowest to forcing conditions, showed an increase of about 5% relative to the previous run for the relevant observation points. This was deemed to be sufficiently small.

It is important to note that a dynamic equilibrium will not be reached at all observation points. Erosion occurs in the model when the computed bottom shear stress exceeds the prescribed critical shear stress for erosion  $\tau_{shields}$ . Harbor basins are sheltered regions by design, and in these areas the bottom shear stresses may never or rarely exceed the critical shear stresses. The result is continuous sedimentation and no erosion, and hence no equilibrium. This is understandable, since harbour basins are dredged deeper than their natural depth, and thus never reach a dynamic equilibrium. Because of this, the tables in appendix A show some stations which do not or very slowly converge to an equilibrium. These stations have been excluded from the assessment of the model spin-up.

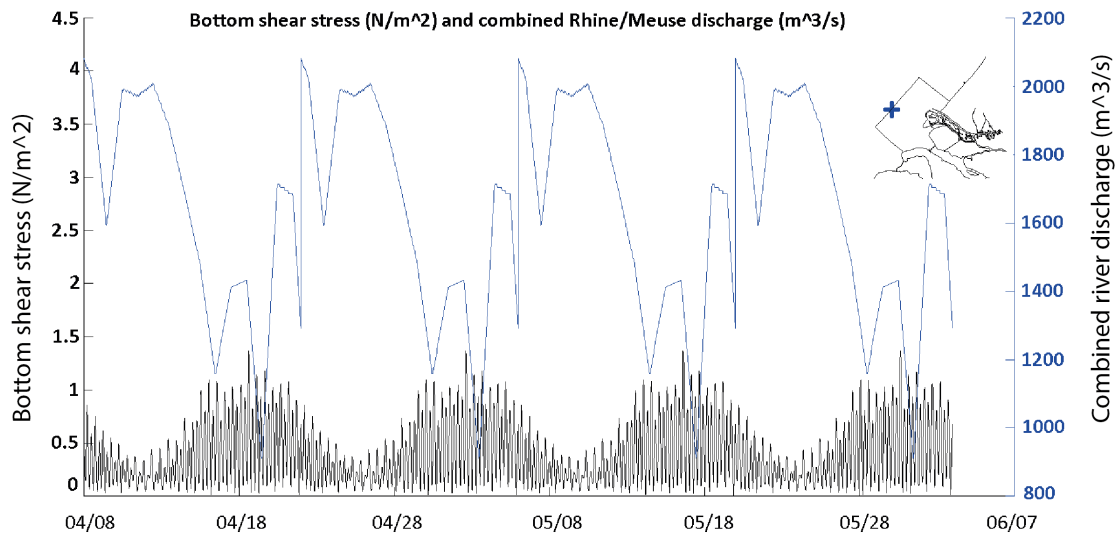


Figure 3.6: Overview of the forcing conditions used for model spin-up. Period 3 (a single spring-neap tide, representative of quiet weather conditions) has been repeated cyclically to create a period of 10 spring-neap cycles (140 days, not all of them shown in this picture). Mass conservation has been ensured from one cycle to the next. The black line (left axis) shows the bottom shear stress, with short oscillations representing the semidiurnal tide and the longer term amplitude modulations representing the spring-neap tidal cycle. The blue line (right axis) depicts the combined Rhine-Meuse discharge.

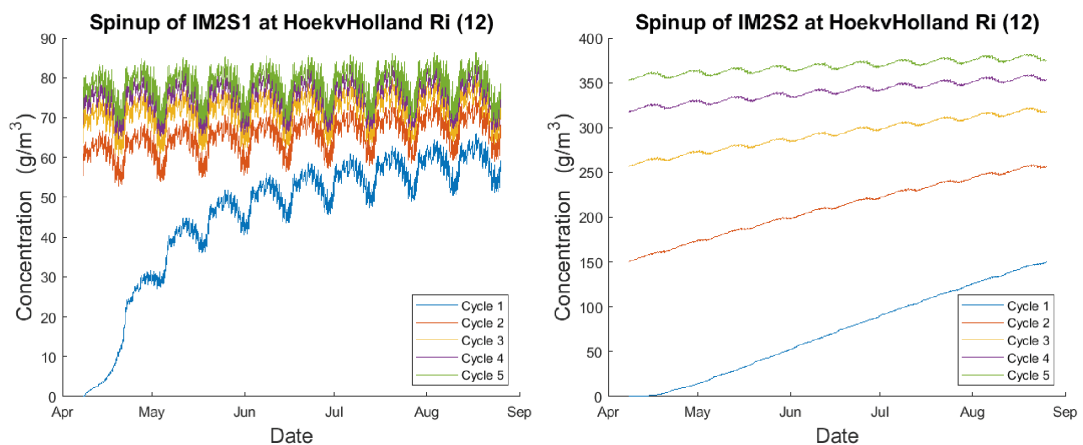


Figure 3.7: Two plots showing the spin-up of sediment fraction IM2 for the two bed layers S1 and S2 at observation point Hook of Holland (see Figure A.6 for the exact location) over five repeated spin-up runs. The 'fluff layer' S1 responds much faster than the deeper layer S2. The waves in the plotted lines are caused by successive spring-neap cycles, while the small scale fluctuations correspond with daily tidal cycles.

### 3.8 Model Scenarios

For this thesis, four periods of 14 days have been selected out of the environmental conditions of 2007. They will be used as forcing conditions for the NSC-Coarse (WAQ) model. They have been chosen based on their combination of wind, bottom shear stress, and river discharge. An overview is given in Table 3.3.

Scenario number	Period	Description
Period 1	17-01-2007 to 31-01-2007	High discharge, High waves
Period 2	08-03-2007 to 22-03-2007	High discharge, low waves
Period 3	07-04-2007 to 21-04-2007	Low discharge, low waves
Period 4	03-11-2007 to 17-11-2007	Low discharge, high waves

Table 3.3: Overview of the different scenarios extracted from the forcing conditions of the year 2007.

Period 3 is representative of quiet conditions, and is used to spin up the model, as has been described in the previous section. After spin-up, this period is not run again, as the dynamic equilibrium that is used as initial condition is based on this period. Instead, the other three periods will be run starting from the initial conditions of period three to see how they change this equilibrium. The shear stresses, wind velocities and directions, water levels, and river discharges belonging to these forcing conditions can be found in Appendix A.

It is important to recognize that none of these periods are 100% true to their description, since measured environmental conditions have been used instead of idealized scenarios. Period 1 actually is comprised of two periods of high wave action (18/1/07 to 23/1/07 and, to a lesser degree 27/1/07 - 30/1/07), and the river discharge is generally high, but not constant. Period 2 represents a river discharge starting at  $6000m^3/s$ , but declining to  $3000m^3/s$  at 20/3/07. Furthermore, wave action increases towards the end of the period. Finally, the wave action in Period 4 is concentrated between 6/11/07 and 13/11/07 rather than being uniformly spread over the time period. River discharge is generally low, but increases to  $2500m^3/s$  towards the end of the period.

This means that the influence of waves and discharge on harbour sedimentation cannot be completely separated. Nevertheless, the forcing periods have been chosen to highlight the individual conditions as much as possible.



# Chapter 4

## Analysis of model results

*This chapter presents an analysis of the model results. Section 4.1 discusses the response of Rhine ROFI to the environmental forcing and the response of SPM concentrations at sea. The ZUNO-DD results are compared to results of the NSC-Coarse model in section 4.2. Section 4.3 discusses SPM fluxes through the harbour mouth. Sedimentation inside the harbour is treated in section 4.4. Section 4.5 provides an assessment of the acting bottom shear stresses inside the harbour. Finally, the salinity, velocity, and SPM profiles along the Rotterdam Waterway are assessed in section 4.6.*

### 4.1 ZUNO-DD: Salinity and SPM structure at Sea

The model simulations that were carried out are based on measured environmental conditions of the year 2007. Because of this, simulation results are always the result of the complex interaction of all forcing conditions, rather than coming from a controlled setup where each parameter is varied independently. The advantage of this method is that it produces more realistic forcing scenarios. The downside is that it is more difficult to trace observed effects back to individual forcing mechanisms. Nevertheless, some patterns emerge from the salinity and SPM structures. Special attention is given to the boundaries of the NSC-Coarse model, since this is where the SPM boundary conditions of the NSC model are generated and applied.

#### 4.1.1 Frictional and Ekman response of salinity field to wind forcing

(Wiechen, 2011) carried out controlled tests with the ZUNO-DD (FLOW) model to study the frictional and Ekman response of the salinity structure to different wind directions and magnitudes. These responses are also observed when applying measured environmental data as forcing.

Under the influence of alongshore Southerly winds, the ROFI is pushed North by the frictional wind stress and on-shore by the on-shore directed Ekman transport. This confines the ROFI against the coast. In these cases, the northern NSC-Coarse boundary is virtually always stratified, while the Western and Southern boundaries remain well-mixed (see Figure B.5 to Figure B.7). In extreme cases however, the ROFI is confined so much that all NSC boundaries (including the Northern section) are well mixed. This occurs only during strong ( $> 10m/s$ ) Southwesterly or on-shore winds. It appears to be caused by a wind induced water level setup against the coast restricting the river outflow, in combination with enhanced stirring due to wind shear at the water surface. This pattern is best seen in Figure A.1 to Figure A.4. Peaks in the wave bottom shear stress oftentimes coincide with sharp declines and subsequent rises in river outflow, which in turn are related to peaks in the wind speed. Furthermore, Figure A.5 shows that these instances correspond to water level setups computed at the mouth of the Rotterdam Waterway. Without exception, these situations coincide with strong alongshore Southerly or on-shore winds. An example of this occurs on 9/11/2007, which is illustrated in Figure B.8 to Figure B.10.

Conversely, when an alongshore wind is blowing from the North, the ROFI is pushed across the Southern boundary, and can extend far across the Western boundary by a frictional force directed South and an off-shore directed Ekman response. This behaviour is summarized in Figure 4.1. Snapshots of full tidal cycles are shown in Appendix B.

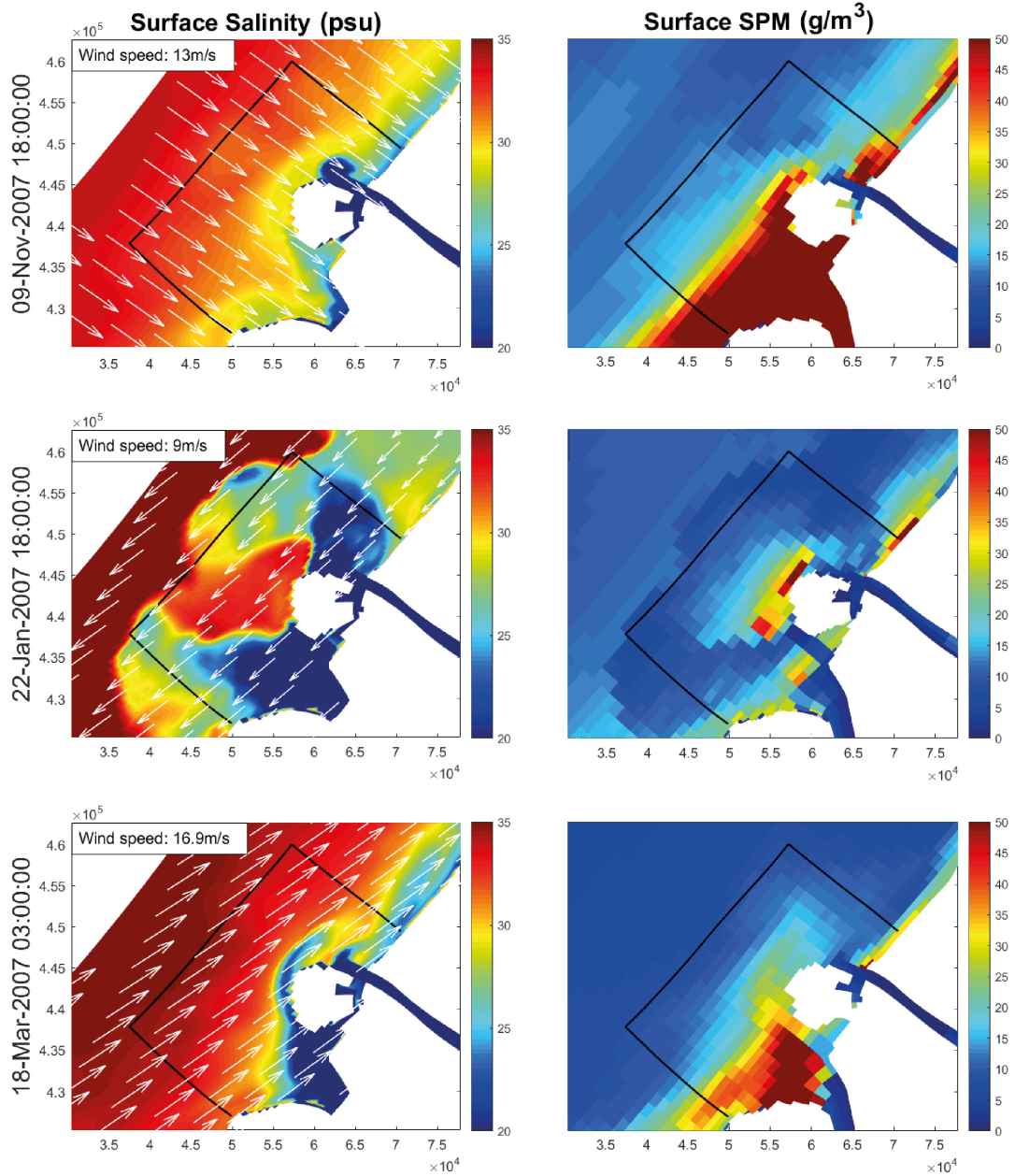


Figure 4.1: Three momentary snapshots from the ZUNO-DD model, illustrating the response of the surface salinity field (left) to a strong wind forcing from different directions and the response of the surface SPM profile (right) to the salinity structure. Wind vectors have been plotted over the salinity field in white, and the boundary of the NSC-Coarse model has been denoted in black. The strong wind forcing induces significant stirring at the surface, limiting the size of the ROFI. on-shore and alongshore Southerly winds push water against the coast through a frictional and Ekman response, and restricts stratification. As a result, the water column is almost entirely well mixed in the top left panel, and severely reduced in the bottom left panel. off-shore and alongshore Northerly winds move water off-shore and enhance stratification. When stratification is strong, turbulence damping confines SPM below the pycnocline, and an absence in surface SPM is seen (middle panel). Persistent off-shore winds were not observed in the reference periods, and are therefore not included.

Figure 4.1 shows the response of the Rhine ROFI under strong wind conditions. This induces significant mixing due to the high wind friction at the water surface (Wiechen, 2011). A summary of the response under calmer conditions is given in Figure 4.2. With less wind stirring, the ROFI remains larger under all wind directions. The Northern NSC boundary is always stratified, while the Western and Southern boundaries are intermittently stratified, depending on the phase of the tide and wind direction. A mild Northeasterly wind in combination with a high river discharge (Figure 4.2, middle panel) is able to stratify nearly the entire NSC-Coarse grid area at sea.

#### 4.1.2 Relationship SPM and the salinity structure and bottom shear stresses

As may be expected, bottom shear stresses are the most important driver of suspended sediment concentrations. Periods of large bottom shear stresses (storms) result in nearshore TIM concentrations of up to  $200 \text{ g/m}^3$ , while they are very low during periods of low bottom shear stresses.

The bottom shear stresses are, besides the presence of currents and waves, largely controlled by the local bathymetry. The bathymetry controls the local water depth, and thereby the degree to which shear stresses penetrate to the bottom and resuspend sediment. This leads to different sediment concentrations on the Northern and Southern boundaries of the NSC-Coarse model. While the bottom depth at the Southern boundary decreases gradually to around -20m, the Northern boundary sees a rapid decline in bed level to around -13m near the coast, followed by a relatively flat plateau of approximately 10km and another rapid decline to -20m. This causes the first 6km of the Southern cross-shore section to be more shallow than the Northern section, the rest of the section to be deeper. The near-shore part of the Southern cross-shore section is therefore more susceptible to suspension.

Besides bottom shear stresses, the effect of stratification on surface SPM (total inorganic matter) can be observed. When stratification is large, turbulence damping at the pycnocline causes large areas of the ROFI to be devoid of surface SPM (Geyer, 1993). This can be seen in Figure 4.1 (middle panel) and Figure 4.2 (all panels), where the shape of the surface salinity field (left) is recognizable as an area of low SPM concentration in the surface SPM field (right). Conversely, in periods of low stratification this restriction of surface SPM is not seen (see Figure 4.1, top and bottom panels). Figure B.8 shows snapshots over one tidal cycle of the surface salinity and total SPM fields on November 10<sup>th</sup>. Strong on-shore winds cause high wave induced bottom shear stresses in combination with very low stratification, and a water buildup against the coast (frictional response). The result is large amounts of surface SPM, with higher concentrations on the Southern (shallow) boundary due its shallower bathymetry. These model results are in line with (Pietrzak et al., 2011; Eleveld et al., 2008), who constructed plots with a similar pattern using satellite imagery.

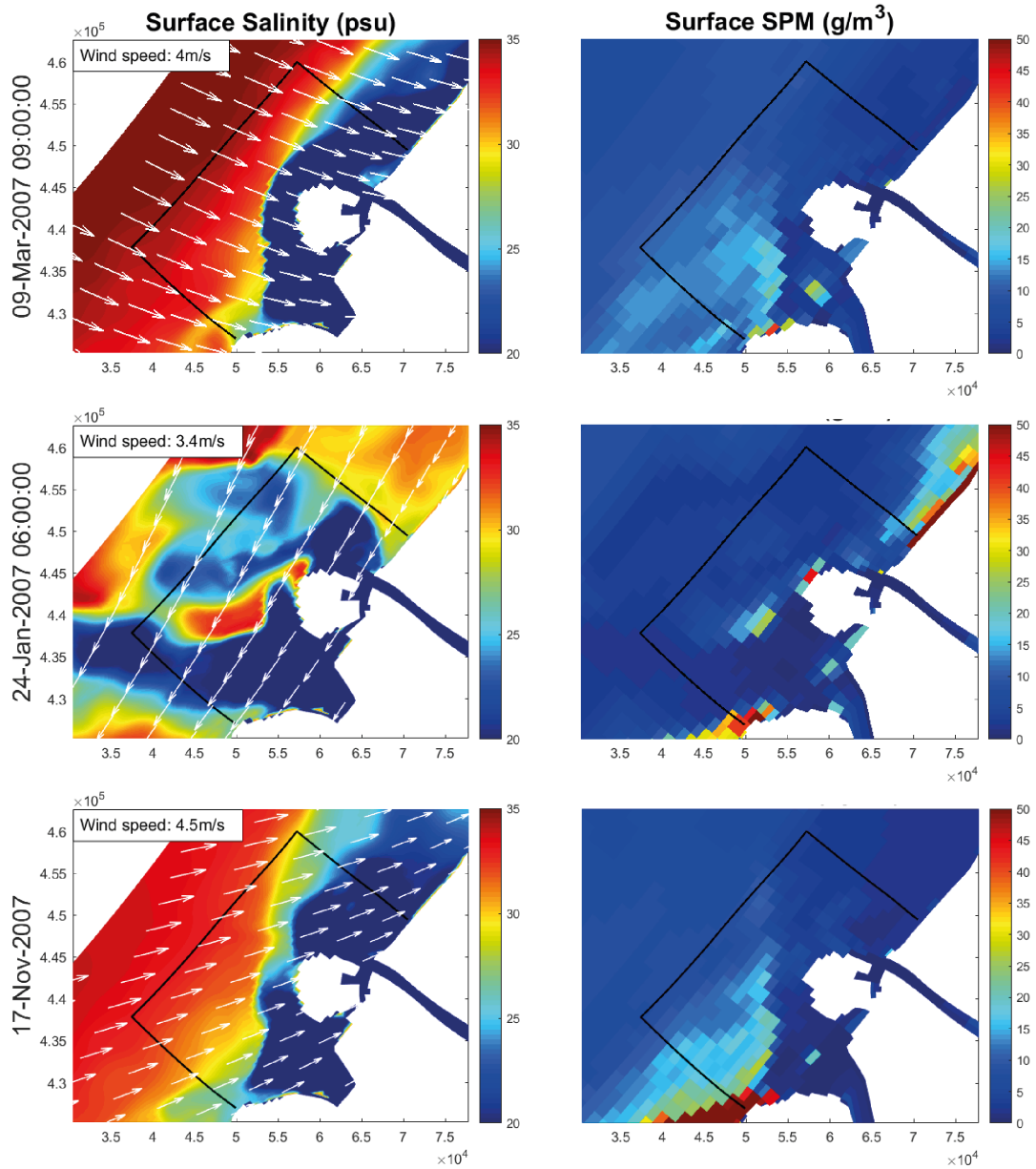


Figure 4.2: Three momentary snapshots from the ZUNO-DD model, illustrating the response of the surface salinity field (left) to a moderate wind forcing from different directions and the response of the surface SPM profile (right) to the salinity structure. Wind vectors have been plotted over the salinity field in white, and the boundary of the NSC-Coarse model has been denoted in black. The moderate wind forcing imposes much less wind stirring at the surface than Figure 4.1, which allows for a much larger region of stratification. on-shore and alongshore Southerly winds push water against the coast through a frictional and Ekman response, and restricts stratification (top and bottom panels). off-shore and alongshore Northerly winds move water off-shore and enhance stratification (middle panel). When stratification is strong, turbulence damping confines SPM below the pycnocline, and an absence in surface SPM is seen. Persistent off-shore winds were not observed in the reference periods, and are therefore not included.

## 4.2 Comparison with NSC-Coarse model

Part of the NSC-Coarse model overlaps with the ZUNO-DD model on the sea side. The models use roughly the same forcing conditions<sup>1</sup>, but apart from that the models strongly differ in resolution and model domain. It is therefore worthwhile to compare to what degree the models behave similarly at the area of overlap. To that end, the surface plots of the three tidal cycles that were plotted for the ZUNO-DD model (Figure B.2 to Figure B.10) have been repeated for the NSC-Coarse model. The results are shown in Figure B.11 to Figure B.15.

Though the surface salinity are considerably different between the two models, the large scale structures seem to be reproduced. Interestingly, the NSC-Coarse model produces much sharper concentration gradients than the ZUNO-DD model. This is likely due to the coarse resolution of the ZUNO-DD model, which will introduce some diffusion.

The WAQ calculations show more deviation. Most notably, there is generally more surface SPM present in the NSC-Coarse model, especially during storms and high discharges. There are three possible explanations for this observation.

- The environmental forcing conditions that were used for the spin-up of the model were almost completely devoid of (wind) wave action. This means that a lot of sediment has deposited on the seabed during the spin-up period, creating a very large sediment availability during storm events. This is unrealistic, since the high frequency of wave events on the North Sea limits the amount of sediment available for resuspension during storm events.
- Both the velocity and wave induced shear stresses turn out to be higher on the NSC-Coarse model than on the ZUNO-DD model.
- During and after storm events, large amounts of sediment fraction IM1 are emitted from the Rotterdam Waterway, creating a sediment plume on the North Sea. In the ZUNO-DD model, this sediment is eroded from the harbour basins (see Figure 4.5 and Figure 4.4).

Besides this, the surface SPM concentrations in the NSC-Coarse model can be seen to be separated into distinct bands, whereas the concentrations in the ZUNO-DD model vary more smoothly. This is a result of the horizontal aggregation of the NSC-Coarse boundary into 16 boundary sections (2x6 cross-shore, 4 alongshore, see Figure 3.5). When little mixing is present, these sections remain intact at sea.

Apart from these observations, NSC-Coarse and ZUNO-DD (WAQ) models show some correspondence too. The relation between surface salinity and SPM at sea is visible in the surface profile of the NSC-Coarse results as well as in the ZUNO-DD model. Where there is stratification, surface SPM is largely absent and fronts in the salinity field often coincide with fronts in the surface SPM concentrations. This is in line with observations such as (Eleveld et al., 2008; Pietrzak et al., 2011).

## 4.3 Interactions at the mouth

To investigate SPM fluxes within the model more closely, the NSC-Coarse domain has been divided into observation areas. For each of these areas, all internal sediment fluxes are aggregated, so that only the sedimentation within each area and the sediment fluxes between each area and its neighbouring areas remain. An overview of these predefined observation areas is given in Figure 4.3.

All SPM fluxes between the sea and port area go through the Maasmond. Therefore, studying the SPM fluxes between the observation areas 'MMD' (Maasmond) and 'ZEE' (sea, not labelled) will shed light on the port's total import or export of sediment via the North Sea<sup>2</sup>.

By studying the time development of the sediment exchange through the Maasmond, it becomes clear that the influx of sediment is not uniformly distributed in time. Figure 4.4 shows the import flux (1<sup>st</sup> and 3<sup>rd</sup> panel) and the cumulative import (2<sup>nd</sup> and 4<sup>th</sup> panel) for sediment fractions IM1 and IM2 respectively. Negative import denotes the export of SPM through the Maasmond. It

<sup>1</sup>The ZUNO-DD model specifies the outflow of the Rotterdam Waterway and the Haringvliet at the mouth, while the NSC-Coarse model does this at the upstream end of the Harbour model.

<sup>2</sup>In Figure 4.3 it looks as though the NWW-w area interacts with the sea as well. However, the model includes a dam along the NWW-w boundary preventing any exchanges between that area and the sea side.

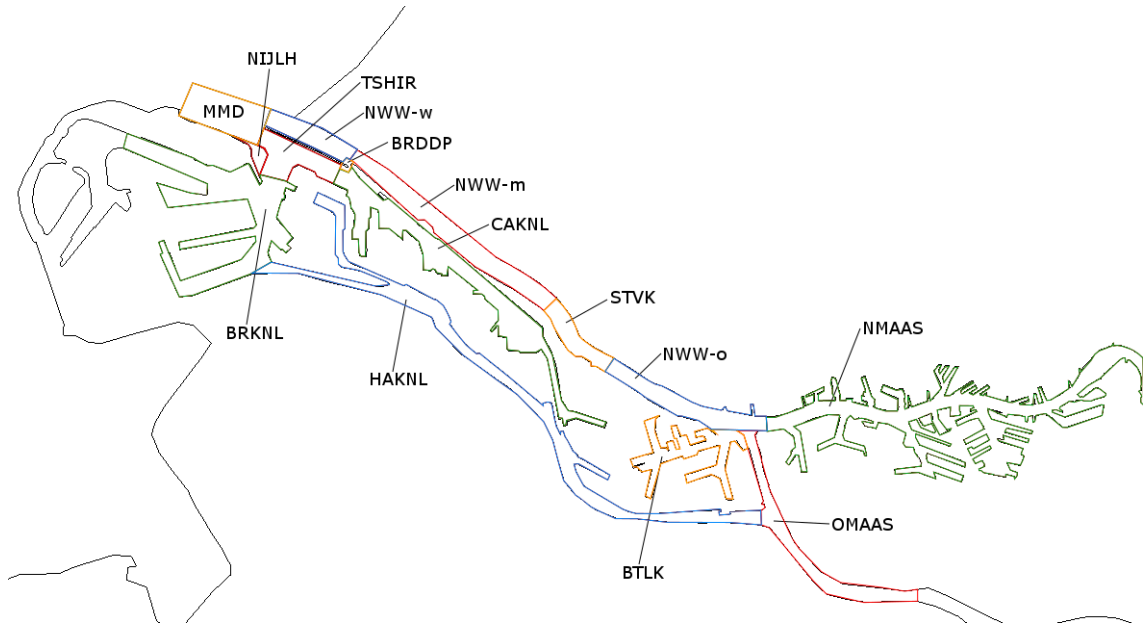


Figure 4.3: Overview of the predefined observation areas. For each observation area, all fluxes between the cells are aggregated. In that way, a given area shows the sedimentation within that area, and the sediment exchange fluxes with neighbouring areas, rather than showing the individual cell interactions. Plots of the SPM exchange in the Maasmond area ('MMD') are shown in Figure 4.4, Figure C.14, and Figure C.15. Plots of total sedimentation in the relevant observation areas are shown in Figure 4.5 and Figure 4.6. Plots of the development of sedimentation over time are shown in Figure C.16 to Figure C.21.

can be seen that almost all sediment exchange is concentrated in a short period of time (around 6 days in Period 4), and exchanges are very low for the rest of the period (around 8 days in Period 4). This is in line with (Verlaan et al., 2000), who noted that the import of Marine sediment is dominated by episodic events rather than a steady influx. Furthermore, Figure 4.4 shows that when the sediment exchange peaks, the heavier sediment fraction IM2 is imported, but an almost equal amount (in mass) of the lighter fraction IM1 is exported to sea. This export of IM1 must either be due to an increase in sediment inflow from the upstream side (being advected all the way through the Rotterdam Waterway) or due to erosion inside the port. In all periods, the export of SPM correlates to an increase in bottom shear stresses when compared with Figure A.4. It is therefore very likely that the lighter sediments (IM1) that accumulated inside the harbour during the calm spin-up conditions are eroded at certain places inside the harbour during storms and are exported to sea. This would be unrealistic, as harbour basins are designed to be sheltered, and are not subjected to high wind waves during storms.

In section 4.4 it will be shown that the sediment that settles at the bed in most harbour basins is predominantly comprised of IM2. Despite the fact that the net exchange of sediment (IM1 + IM2) is very little (they more or less cancel each other out in mass), the import of IM2 is therefore still considered important. Similar plots for all periods have been included in Figure C.14 and Figure C.15. In all instances, increases in sediment exchange in the Maasmond area can be related to peaks in the bottom shear stress at sea.

Figure 4.4 shows the import of SPM to be in phase with the water level (import during flood and export during ebb). The influence of the spring-neap cycle can not be observed in all instances. In Period 1 and 4, spring tides coincide with increased wave action, making it impossible to isolate the two effects. However, Period 2 shows a transition from spring tide to neap tide with negligible wave stresses (see Figure A.2). In this instance, spring tide corresponds to an increased exchange of SPM through the Maasmond, and an export of fraction IM1. IM2 shows a small influx, but the effect is dwarfed by the effect of the waves that occur later on.

The picture that emerges is that the influx of SPM through the Maasmond is controlled by the tide and by the SPM availability in the water column.

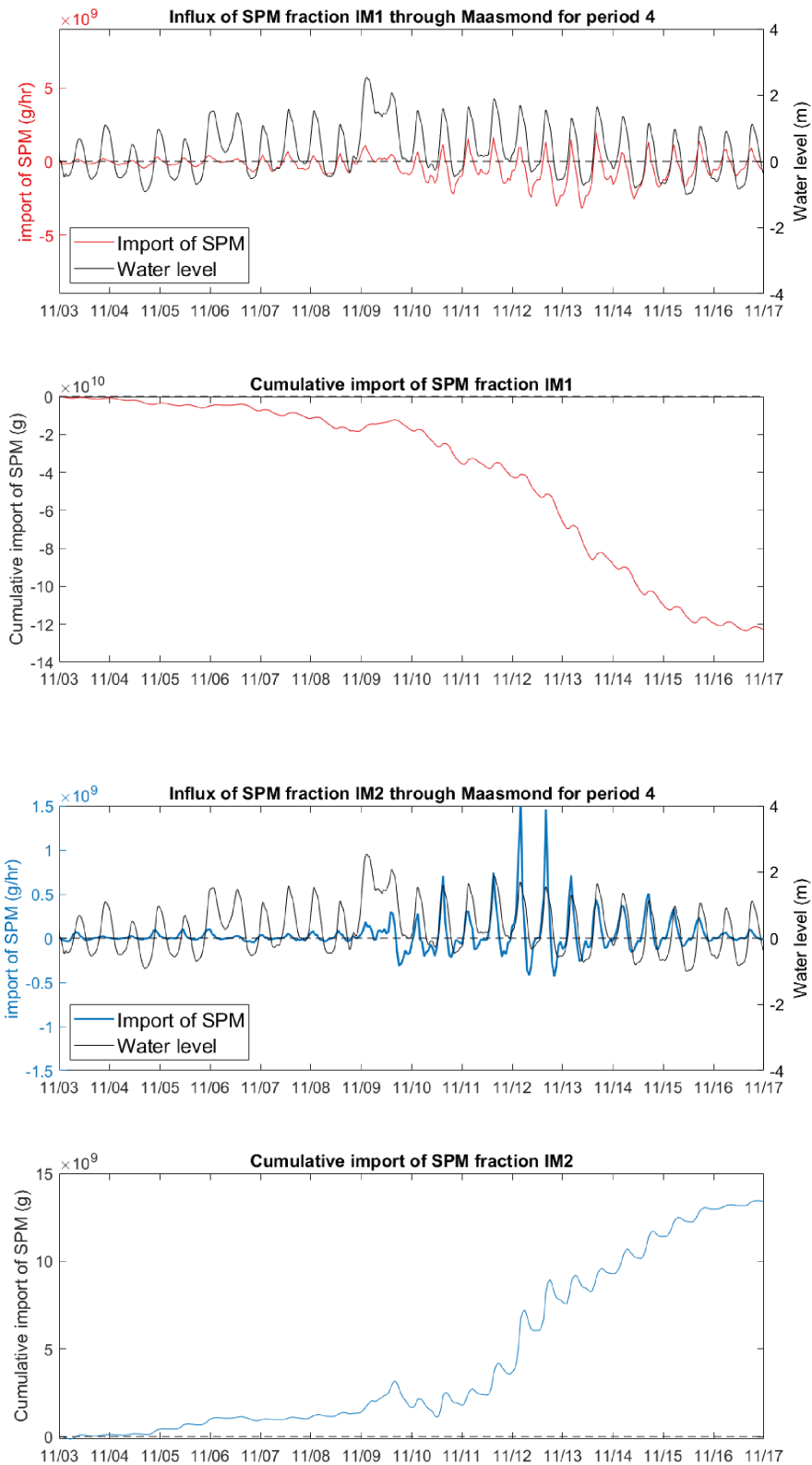


Figure 4.4: Plot showing the exchange of SPM fractions IM1 (red) and IM2 (blue) between the North sea and the port over time for Period 4. For each fraction, the top panel shows the influx (top) and the cumulative import (bottom), where negative values imply export. This figure is best compared with the forcing diagram in Figure A.4. Very little sediment is exchanged up to the storm and subsequent rise in discharge starting around 9/11/2007. After this point, sediment exchange spikes, and the heavier sediment fraction IM2 is imported, while the lighter fraction IM1 is exported.

## 4.4 Assessment of sedimentation and dredging loads within the Port area

To assess the impact of the defined scenarios on harbour sedimentation, the same observation areas that were introduced in Figure 4.3 are used. Sedimentation takes place in bed layers S1 and S2, which have been described in section 3.4. Due to the sheltered nature of the harbour, both the 'fluff layer' S1 and the deeper layer S2 are important for harbour siltation. However, the two layers respond rather differently to the applied forcing and will therefore be discussed separately. Sediment fractions IM1, IM2, and IM3 are combined in Figure 4.5 and Figure 4.6 to form the total sedimentation in each observation area as a result of each scenario.

Figure 4.5 shows significant erosion of bed layer S1 for all observation areas. This figure is compared with the export of IM1 in Figure 4.4, it seems likely that large amounts of IM1 which have deposited during the quiet spin-up period are eroded and exported to the North Sea during the model scenarios. This is only possible if bottom shear stresses inside the harbour basins are significantly larger during the model periods than during the spin-up period, and exceed the predefined critical shear stress for erosion  $\tau_{S1,c} = 0.2N/m^2$ . The critical shear stress for erosion of bed layer S1 is defined lower than that of layer S2, which explains why layer S1 erodes more easily than S2.

In contrast with Figure 4.5, Figure 4.6 shows sedimentation in bed layer S2 for most areas. In absolute terms, the New Meuse section dominates over the other observation areas. This is largely due to the fact that many of smaller inland basins and even the main waterway which is not maintained by Port of Rotterdam are included in this observation area. Part of this large sedimentation figure will be in the main waterway, but Figures C.3 to C.12 show strong sedimentation in the harbour basins lining the New Meuse as well. This is out of line with dredging data, and an inquiry at the dredging department's staff revealed that these sedimentation figures are likely overstated. In this thesis, focus is given to the areas under marine influence, and by a lack of better knowledge the sediment concentrations on the river boundaries are held constant. For that reason, no further attention will be given to this area.

It is useful to compare computed sedimentation with archived dredging records. The computations are based on relatively infrequent events (storm, high discharge) of a single spring neap-cycle, and are computed in grams of dry matter. Conversely, the dredging records are kept in cubic meters of dredged material, and are highly influenced by dredging strategies and year round conditions. A quantitative comparison of dredged quantities and computed sedimentation loads is therefore deemed unreliable. However, the orders of magnitude of dredging sections amongst themselves can be compared. Figure 4.6 shows the computed sedimentation in Calandkanaal ('CAKNL' in Figure 4.3) of equal order of magnitude, though slightly smaller, as the computed sedimentation in Botlek harbour ('BTLK'). This is in line with annually dredged quantities of Botlek and Europoort respectively, as shown in Figure 1.1. Dredging records also show virtually no dredging activity in the Hartel channel ('HAKNL'). This is confirmed in all model scenarios, where slight erosion as a result of high wave/discharge conditions is predicted.

The dredging loads of Figure 1.1 also show the Maasvlakte area ('BRKNL' in Figure 4.3) to be the dominant deposition area since the completion of Maasvlakte 2 in 2013. This is not confirmed in the model results, which place the Maasvlakte area below the Europoort area ('CAKNL') and below Botlek.

Finally, it is noteworthy that while Botlek harbour takes a large share in computed sedimentation, this picture becomes even more pronounced when discounted for surface area (bottom Figure 4.6). This fact aligns with (de Nijs et al., 2011), who showed that Botlek harbour has a very high sediment trapping efficiency, and attributed it to its position at the limit of saltwater intrusion in the Rotterdam waterway and the presence of an estuarine turbidity maximum (ETM).

In line with the ZUNO-DD (WAQ) model, three sediment fractions have been included in the NSC-Coarse model, each with its own settling velocity. Although in reality the distinction between floc sizes is lost once the sediment is consolidated, the use of a model enables the decomposition of the bed layer into its original particle components<sup>3</sup>.

---

<sup>3</sup>In the WAQ models, the fact that the distinction between particle sizes is lost once particles have consolidated is expressed by the fact that all sediment fractions have the same critical shear stress for resuspension, while they have different sedimentation rates (due to their settling velocities).

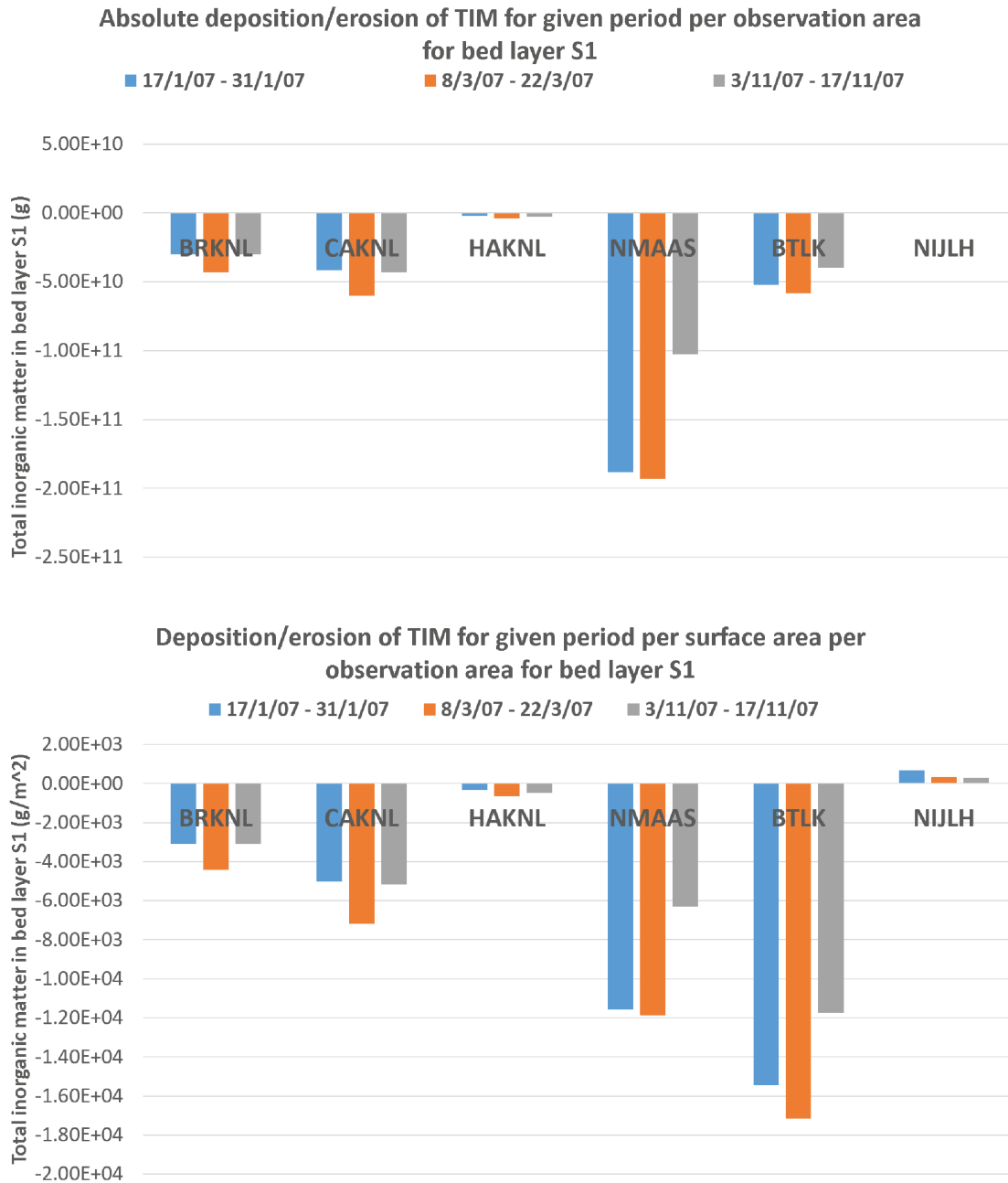


Figure 4.5: Overview of the total sedimentation in bed layer S1 as a result of the three model scenarios. IM1, IM2, and IM3 are combined in this figure. The top histogram shows the absolute sedimentation per area, while the bottom histogram shows sedimentation per square meter surface area. There is net erosion in all areas for all scenarios. Apparently, the model scenarios induce bottom shear stresses in the harbour basins, which resuspends sediment that has deposited during the quiet spin-up conditions.

4.4. ASSESSMENT OF SEDIMENTATION AND DREDGING LOADS WITHIN THE PORT AREA

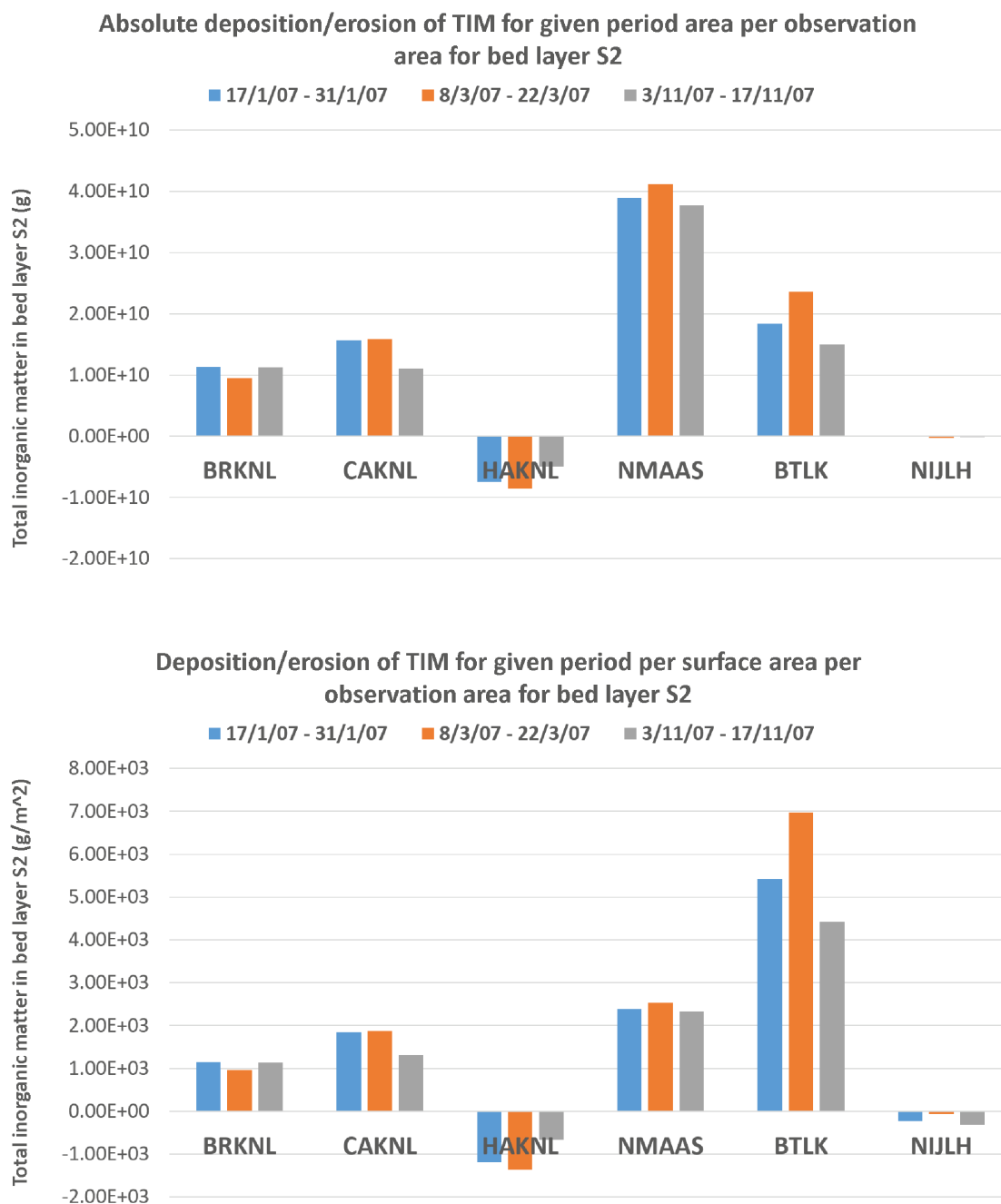


Figure 4.6: Overview of the total sedimentation in bed layer S2 as a result of the three model scenarios. IM1, IM2, and IM3 are combined in this figure. The top histogram shows the absolute sedimentation per area, while the bottom histogram shows sedimentation per square meter surface area. 'HAKNL' and 'NIJLH' show slight erosion or no effect, while all other areas show sedimentation.

### 4.4.1 Role of settling velocity

The lightest SPM fraction IM3 virtually never settles, and plays no role in harbour sedimentation. This can be seen in Figure C.13, where the sedimentation in the four most relevant areas is decomposed into its sediment fractions for each period. For brevity, Figure 4.7 only shows IM1 and IM2 for period 2, but it is considered to be illustrative of the total picture. IM2 is the dominant SPM fraction for sedimentation in most of the port area, although the distribution varies over the harbour basins. The most striking exception is the Europoort area ('CAKNL'), where IM1 is the dominant sediment fraction. It is expected that this is caused by the fact that the Caland channel forms a long closed basin, while the other basins are located more directly on the main waterway.

To get a sense of how fractions IM1 and IM2 spread within the harbour area, the difference in sediment concentration between the first and last timesteps of a model scenario in bed layers S1 and S2 have been computed. The result is a plot showing the total deposition and erosion resulting from each model scenario. For Period 1, the changes in bed concentrations of sediment fractions IM1 and IM2 layer S2 are shown in Figure 4.8 and Figure 4.9. The general picture that emerges is that of erosion at sea and sedimentation inside the port area. The storm in Period 1 resuspends sediment at sea, which is consequently advected into the harbour with the incoming tide. A striking exception from this trend is the erosion of IM1 in Maasvlakte 2 area. This is not to be expected, as Maasvlakte 2 is a very sheltered basin. However, section 4.5 will show that the wave induced bottom shear stresses in this area have been strongly overstated, leading to unphysical erosion.

Without exception, the lighter IM1 fraction is found in the end of the basins, while the heavier fraction IM2 settles closer to the mouth. This is reasonable, as the back of the harbour basins is usually more sheltered. Fraction IM2 generally settles before it reaches the back of the basins, while the lighter fraction IM1 is not able to settle inside the basin mouth. For brevity, only 2 plots have been included in the main text, but for similar plots of all bed layers and model scenarios, the reader is referred to Figure C.1 to Figure C.12.

The bed changes in layer S1 show a very different picture (see Figure C.1, Figure C.5, and Figure C.9). For all periods, IM1 is eroded from bed layer S1 inside the port area, and only very little is deposited. This can only mean that during the model scenarios, bottom shear stresses inside the harbour basin have increased relative to the spin-up scenario (either due to waves or due to increased velocity), and is eroding fraction IM1 which was previously able to settle. This sediment is subsequently exported to sea, where remains largely in suspension because it is not able to settle. In contrast, sediment fraction IM2 shows both deposition and erosion.

Physically, the sheltered nature of the harbour basins is such that large scale erosion of (unconsolidated) mud inside the harbour basin as a result of stormy conditions is unlikely. In this light, the erosion of layer S1 is problematic. The cause of this problem hinges on which types of sediment are important for harbour siltation (i.e. should IM1 be able to settle inside the port in the first place?) and what the critical shear stress for resuspension should be. A too low value will result in non-physical erosion, while a too large value will overstate siltation rates. This parameter also highly influences where sediment is deposited (more to the back of basins or closer to the waterway).

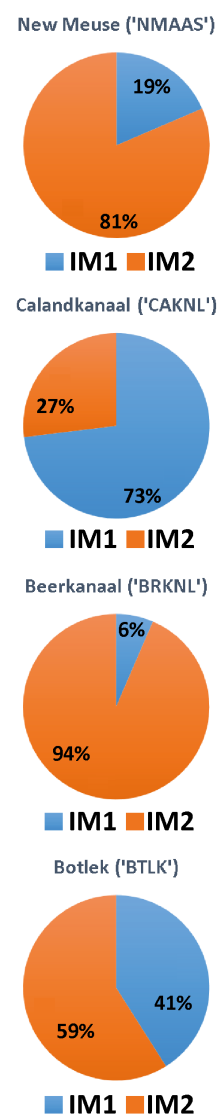


Figure 4.7: Distribution of IM1 and IM2 deposited in the observation areas defined in Figure 4.3.

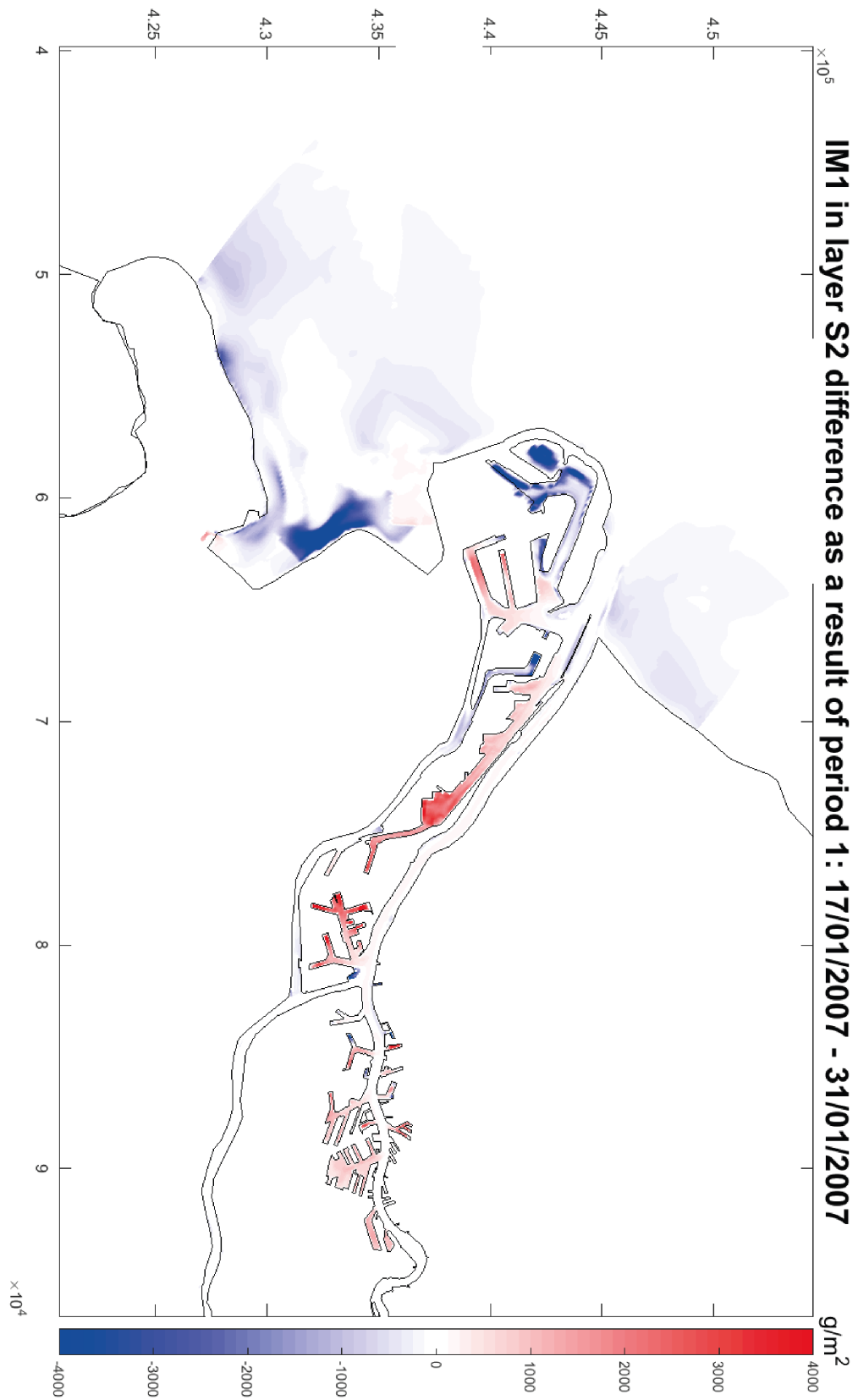


Figure 4.8: Difference map over period 1 of IM1 concentration in layer S2, showing the difference in concentration between the last and first time steps. This forcing scenario contained a storm, marked by high bottom wave shear stresses. The result is net erosion at sea and net deposition in the harbour basins.

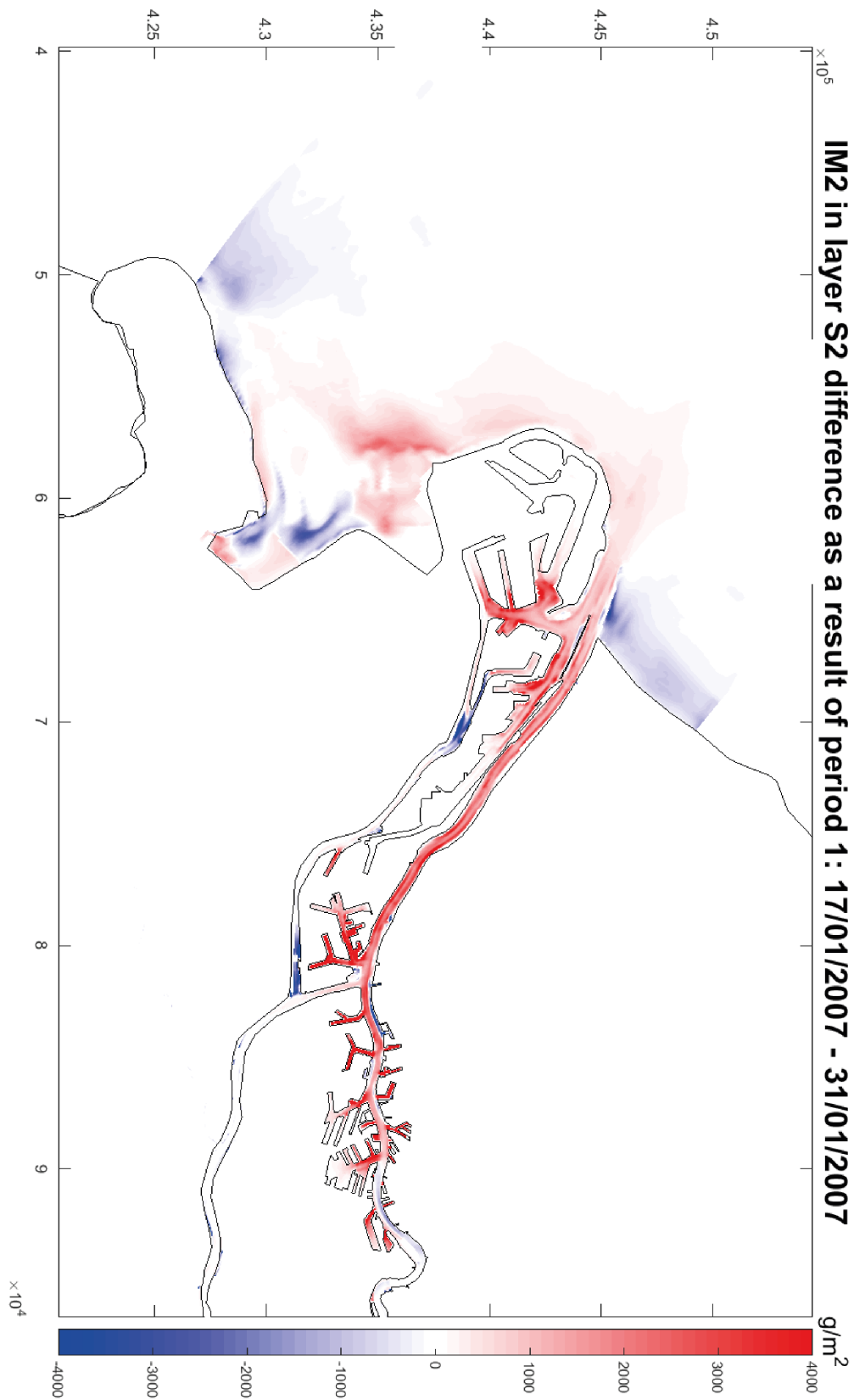


Figure 4.9: Difference map over period 1 of IM2 concentration in layer S2, showing the difference in concentration between the last and first time steps. This forcing scenario contained a storm, marked by high bottom wave shear stresses. The result is net erosion at sea and net deposition in the harbour basins. Sediment fraction IM2 has a higher settling velocity than fraction IM1. As a result, this fraction settles in more active areas than fraction IM1.

### 4.4.2 Time development of sedimentation

In this section, the time variability of the deposition in the previously described harbour basins will be analyzed. Plots of the temporal development of sediment concentrations in both bed layers are shown in Figure C.16 to Figure C.21. Like the import of SPM through the harbour mouth, the sedimentation in the harbour basins generally consists of relatively brief episodes of rapid sedimentation rather than a steady deposition flux. The following observations can be made:

- The bottom shear stress at sea (see Figure A.1 to Figure A.4 shows a strong correlation with sedimentation rates (both positive and negative) in the harbour basins. In layer S1, peaks in the bottom shear stress induced by waves correspond with strong erosion peaks of sediment fraction IM1, causing the aforementioned export of IM1 to sea. In layer S2, storms included in the various scenarios can be traced to peaks in sedimentation rates.
- A weak response of bed concentrations to the tidal cycle is visible. Bed concentrations are generally out of phase with the tidal cycle, meaning that concentrations are generally higher during low tide and lower during high tide.
- It was expected that more sediment would be imported and trapped during spring tide than during neap tide. However, no clear relation between sedimentation rates and the spring-neap cycle is observed. This may be due to the large area of the observation areas, as well as the other environmental conditions distorting the signal. For single observation points, especially those in more dynamic areas, both the spring-neap cycle and the tidal cycle can very clearly be discerned. This was observed during the spin-up of the model (see Figure 3.7).
- (de Nijs et al., 2011) concluded that sedimentation in Botlek harbour is not related to import of SPM from sea, but rather to the timing and availability of fluvial SPM in the ETM. However, Figure C.16 to Figure C.21 a response of the sedimentation as a result of storms at sea. Unless this the advection of the salt wedge is modified by a storm, this response should not be visible. It is expected that this is the result of an overestimation of the wave bottom shear stresses, as will be elucidated in section 4.5.

IM1 and IM2 sedimentation rates react differently to forcing conditions and harbour basins. Peaks in bottom shear stresses at sea cause erosion of IM1 in the Maasvlakte ('BRKNL') area, but deposition in the Europoort ('CAKNL') and Botlek ('BTLK') areas. On the other hand, IM2 is virtually never eroded. It is expected that the latter areas are more sheltered, allowing for the deposition of the lighter sediment fraction.

## 4.5 Bottom shear stresses

The previous sections revealed that the model scenarios result in increased harbour sedimentation (mainly SPM fraction IM2 and mainly layer S2), but also in harbour erosion and export of sediment to sea (mainly SPM fraction IM1 and layer S1). Bottom shear stresses are the sole driver of sediment resuspension, and they are therefore analyzed in this section. The bottom shear stresses have been generated with the wave assimilation technique that has also been used for the ZUNO-DD (WAQ) model. Figure 4.10 shows maps of the total (wave + velocity) and wave induced bottom shear stresses during quiet, average, and storm conditions. The colour scale is chosen such that areas where erosion of bottom layer S2 takes place are dark red.

During periods of significant wave action, wave induced bottom shear stresses exceed the critical stresses almost everywhere inside the harbour, which is unrealistic. Furthermore, there also appears to be a phase shift of about one day compared to the stresses generated for the ZUNO-DD (WAQ) model. These wave stresses are inducing the erosion that has been observed previously (Figure 4.4 and Figure 4.5 among others). The (most likely) produced errors are particularly strong in the Maasvlakte area. Maasvlakte 2 has been included in the bathymetry and not in the model grid. The wave stresses are in part generated by resolving the dispersion relation based on nearby wave buoys, and the water depth is therefore an important parameter. As a result, Maasvlakte 2 is generating large wave stresses in the wave stress assimilation, which is clearly erroneous.

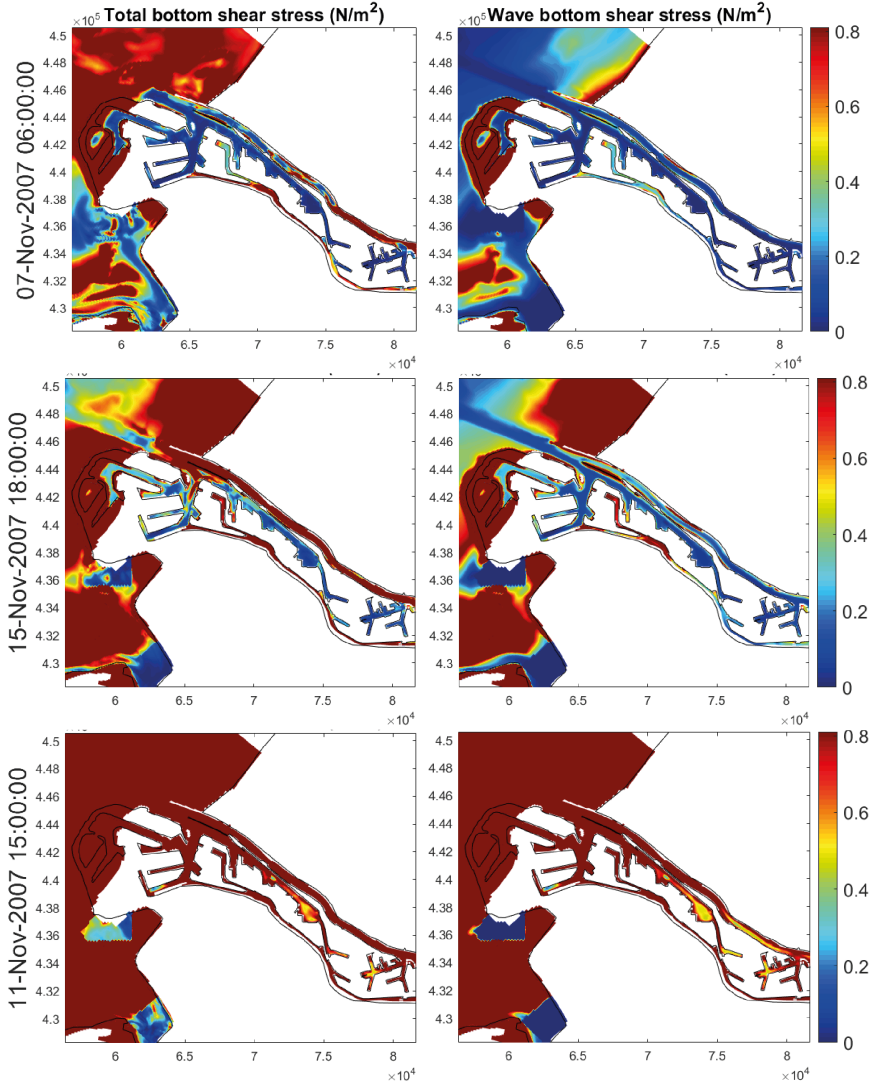


Figure 4.10: Total and wave bottom shear stresses taken from Period 4 during calm (top), average (middle) and storm (bottom) conditions. The upper colour limit is set at the critical shear stress for resuspension of layer S2 ( $\tau_{c,S2} = 0.8N/m^2$ ). Hence, Erosion from the bottom layer will occur in the dark red patches. In general, wave induced bottom stresses protrude much too far into the harbour, creating unrealistic resuspension in especially the Maasvlakte and Europoort areas. The critical shear stress for bed layer S1 is much lower at  $\tau_{c,S1} = 0.2N/m^2$  so layer S1 is even more sensitive to the wave stresses.

In section 4.4 it was observed that when compared to dredging records, the model severely underpredicts sedimentation in the Maasvlakte area. It is very likely that the unrealistic protrusion of wave induced bottom shear stresses into the port area is responsible for this fact.

## 4.6 Advection in the Rotterdam Waterway

To analyze the advection of salinity and SPM in the Rotterdam Waterway three different observation points have been chosen along the Rotterdam Waterway, as shown in Figure 4.11. For these locations, the time and depth varying profiles of salinity, along-shore velocity, and SPM have been plotted for the first ten days of forcing period 1. The results are shown in Figure 4.12 to Figure 4.14.

### 4.6.1 Salinity

As may be expected, salinity concentrations and concentration gradients are highest near the mouth of the Rotterdam Waterway (observation point 1) and decrease in the upstream direction (observation points 2 and 3). Furthermore, it is clearly visible that the distance over which the

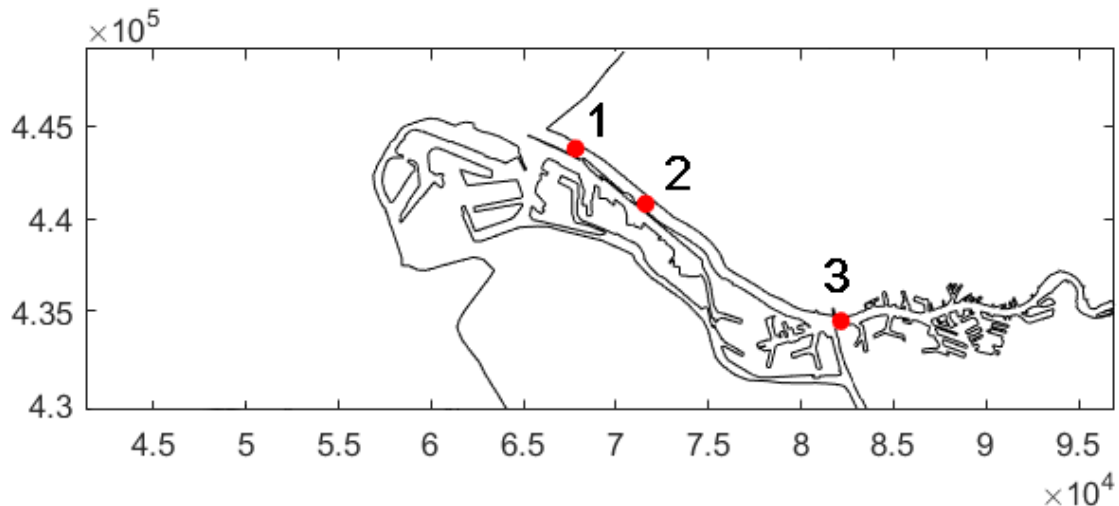


Figure 4.11: Location of the observation points of Figure 4.12 to Figure 4.14

salt wedge is advected into the Rotterdam Waterway is variable. Near the mouth, near bottom water is permanently salty, while at observation points 2 and 3 the water column is intermittently stratified. At station 3, stratification is only present when the salt wedge is advected far upstream. Around 19/01/2007, a storm occurs which induces a significant onshore transport of water at sea (see Figure A.1). This causes the salinity structure to be advected far into the Rotterdam Waterway, and observation point 1 to be well-mixed.

#### 4.6.2 Along channel velocity

The along channel water velocity is closely tied to the salinity structure. During the storm on 19/01/2007, the water column at observation point 1 is completely saline, and water velocities into the harbour persist throughout the water column for some time. This results in a rise in water level, which can also be observed. Furthermore, when stratification is present it can be seen that exchange currents develop. This phenomenon is strongest near the mouth (observation point 1), where near bottom velocities are almost always directed inland or zero. During flood, virtually no negative velocities are observed. River water therefore enters the North Sea through a pulsating surface current that is cut off during flood. The exchange flow weakens in the upstream direction, and at observation point 3 the along channel velocities are more or less homogeneous over the water column. However, when the salinity structure is advected further upstream the velocities can still be seen to be modified by the salinity intrusion.

#### 4.6.3 Suspended sediment and the ETM

Salinity concentrations in the water column have a very strong episodic nature. Storms correspond to very high concentrations in the water column. In section 4.5 it was shown that the assimilated wave stresses penetrate far into the harbour, which means that the high concentrations are likely the result of local resuspension. A time lag of about a day can be observed between the onset of high SPM concentrations and the storms in the hydrodynamic forcing. This is in line with the observation made in section 4.5 that the assimilated wave forcing is phase shifted with a day compared to the rest of the model forcing. However, in between storm events the advection of an ETM can be observed. This can be seen as a periodic increase in near-bottom SPM which varies on a semi-diurnal time scale and coincides with the onset of flood and the increase of near bottom salinity concentrations. The timing of the ETM could not be related to increases in harbour siltation rates.

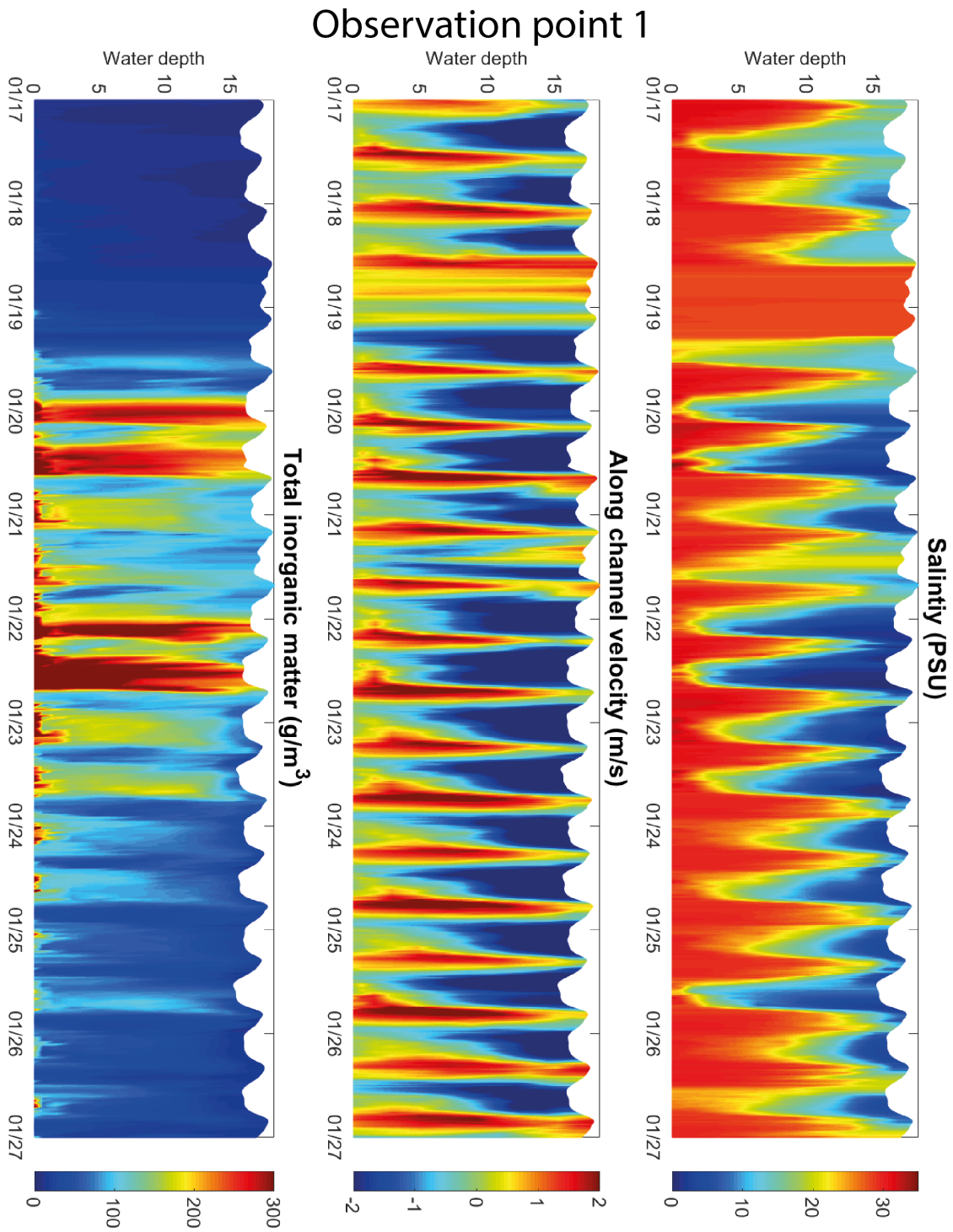


Figure 4.12: Salinity, along channel velocity, and total SPM concentrations at observation point 1 for a period of 10 days. Positive velocities are into the harbour. Differential advection of the density structure in the Rotterdam Waterway can be seen, in combination with exchange velocities in the water column. The SPM concentrations show a strong episodic character due to the high wave shear stresses that penetrate into the harbour, but at times also show the advection of an ETM.

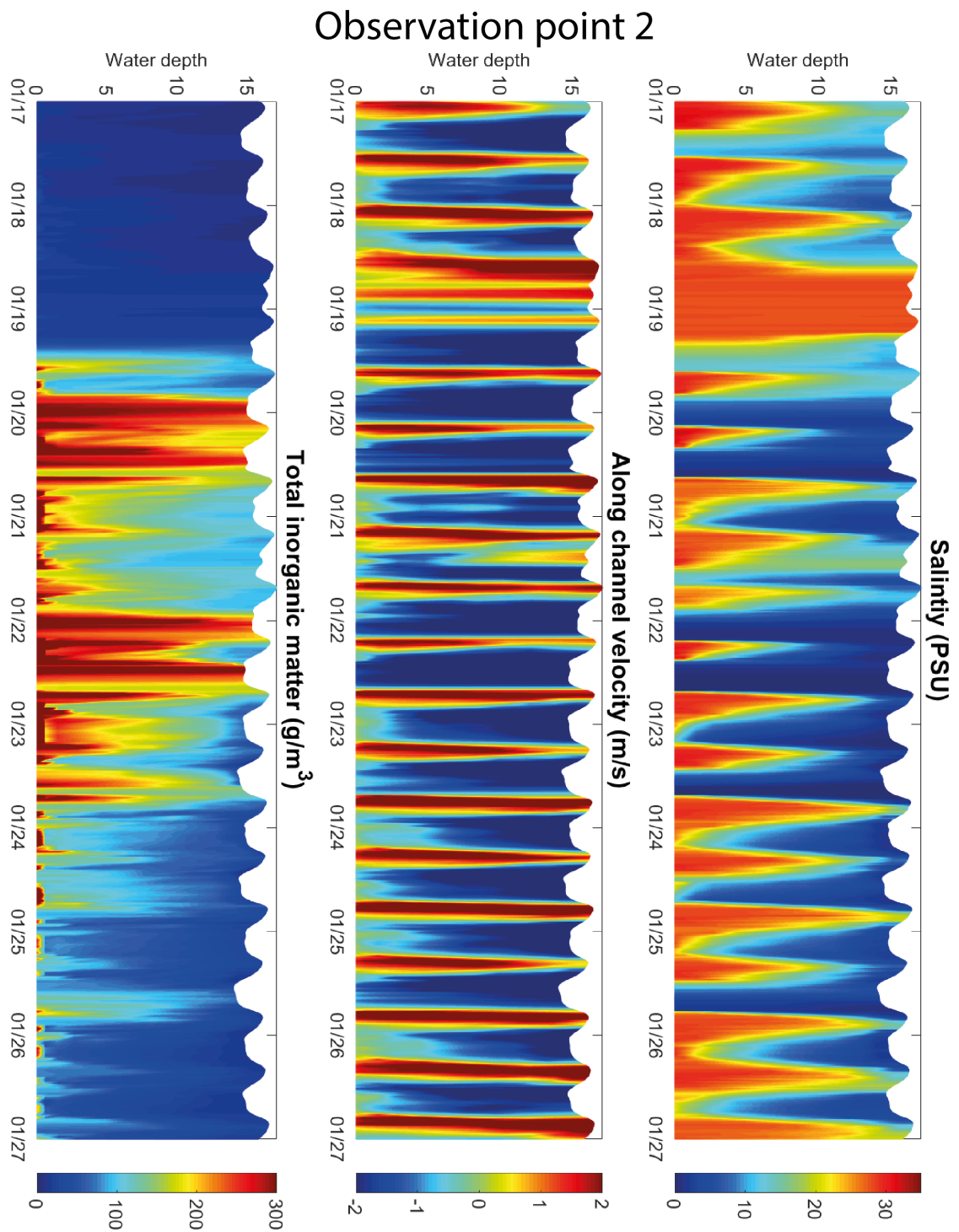


Figure 4.13: Salinity, along channel velocity, and total SPM concentrations at observation point 2 for a period of 10 days. Positive velocities are into the harbour. Differential advection of the density structure in the Rotterdam Waterway can be seen, in combination with exchange velocities in the water column. The SPM concentrations show a strong episodic character due to the high wave shear stresses that penetrate into the harbour, but at times also show the advection of an ETM.

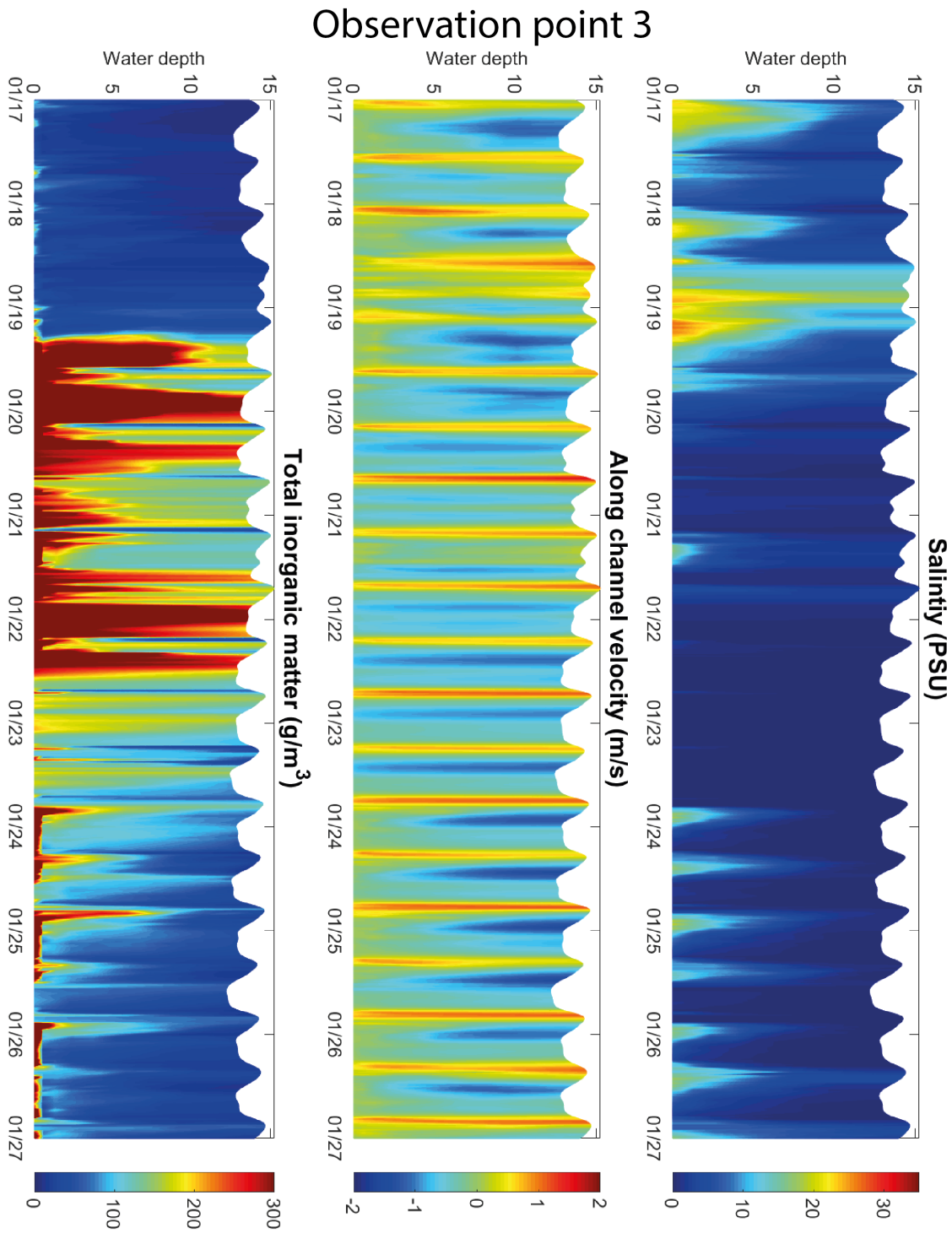


Figure 4.14: Salinity, along channel velocity, and total SPM concentrations at observation point 3 for a period of 10 days. Positive velocities are into the harbour. Differential advection of the density structure in the Rotterdam Waterway can be seen, in combination with exchange velocities in the water column. The SPM concentrations show a strong episodic character due to the high wave shear stresses that penetrate into the harbour, but at times also show the advection of an ETM.



# Chapter 5

## Discussion

*This chapter establishes the relationship between chapter 2 and chapter 4. It connects the outcome of the model results to the known physics, and discusses the underlying assumptions and applicability of the model. First, the model reproduction of highly variable SPM concentrations and its impact on harbour siltation are discussed. Then, the implications of a number of model choices are evaluated,*

### 5.1 Modelling SPM variability

The model setup described in this thesis includes physical behaviour which has not been modelled before in the Port of Rotterdam. Modelled scenarios consist of 14 day periods, allowing for spring-neap and wind/wave variability to be included in the environmental forcing. Furthermore, effect of waves on sediment suspension is included through time and space varying boundary conditions and independently generated wave shear stresses. As a result, SPM concentrations show large variations and correlate strongly to wave forcing, in line with observations by (Flores et al., 2017; Suijlen et al., 2002). The increased influx of SPM into the harbour during storms as described by (Verlaan et al., 2000) is also visible in the model results, as is shown by figures such as Figure C.15 (in combination with Figure A.2). The import of SPM is governed not purely by the volume of water exchanged, but also by the availability of suspended sediment near the harbour mouth. This principle is similar to (de Nijs et al., 2009), who concluded that the import of SPM into Botlek harbour was controlled mainly by the availability of SPM near the harbour mouth<sup>1</sup>. Siltation rates in Europoort and Maasvlakte match this behaviour, and increase during storm events.

### 5.2 Marine processes

However, (Verlaan et al., 2000) notes two mechanisms for the import of SPM. Besides the advection of SPM by currents, they note that during storms, a wave induced boundary layer of approximately 0.1m high forms near the bed, marked by high wave induced shear stresses. This boundary layer is able to suspend large amounts of sediment, forming a layer of high near bottom SPM concentrations, marked by a lutocline at the height of the boundary layer (where shear stresses decrease). This highly concentrated SPM layer is transported into the Maasmond by residual currents, and settles due to the increased depth in the Maasmond. Upon settling, it forms a fluid mud layer that spreads to adjoining harbour basins through density driven currents. The wave boundary layer is not resolved in the current model setup. Instead, bottom shear stresses are computed as a function of the free stream velocity above the boundary layer and a friction coefficient (see Equation D.19). Wave stresses are only included as a separately generated time varying scalar field that is added to the velocity shear for the computation of sediment resuspension fluxes. Nevertheless, because the stresses only act on the bottom the model does at times produce high SPM concentrations in the lowest  $\sigma$  layer, producing something akin to a lutocline (though no sediment density induced

---

<sup>1</sup>The two cases diverge in the fact that near the harbour mouth (Maasmond), SPM availability is controlled by wave and current induced bottom shear stresses, whereas at the mouth of Botlek harbour the availability is governed by the location of the ETM.

processes are resolved). It is unknown to what degree the transport of this highly concentrated sediment layer is reproduced.

Furthermore, it is important to note that the formation and spreading of fluid mud is not resolved by the model due to the one way coupling between the hydrodynamics and SPM transport. This means that there is no feedback between sediment and flow, and that many phenomena associated with high sediment concentrations, such as hindered settling, sediment density induced currents and turbulence damping are not resolved. This means the model performs best for low SPM concentrations and will produce transport errors for high concentrations. This was confirmed by (Winterwerp et al., 2003) through model simulations. They modelled SPM transport in the Maasmond with an uncoupled model set up and with a coupled setup, and found siltation rates to be up to 3 to 5 times larger for the coupled runs. This increase was attributed to the inclusion of hindered settling, buoyancy destruction, and increased water density due to sediment concentrations. Furthermore, they concluded that sediment density effects play a role at concentrations as low as  $100g/m^3$ . This may lead to an underestimation of siltation rates in the harbour basins lining the Maasmond. Whether the resulting error is truly as large as the factor three to five suggested by (Winterwerp et al., 2003) remains to be seen. However, it is clear that only one of the two transport mechanisms proposed by (Verlaan et al., 2000) is fully represented. If SPM transport rates of the current model setup turn out to be unsatisfactory, one may consider creating a local model with sediment-flow coupling.

Besides the absence of a wave boundary layer, the treatment of wind waves in the current model setup has another consequence. The wave stresses only affect sediment resuspension, and do not impact the hydrodynamics. However, (Souza et al., 1996) concluded that wind waves have a strong mixing effect on stratification, and showed that stratification in the Rhine ROFI can be significantly reduced by wave mixing. This process is neglected in the current model setup, which should in principle lead to an overestimation of stratification and the processes associated therewith. Furthermore, the effect of wave induced momentum transport on the mean flow through radiation stresses is neglected, which is known to induce sediment transport (Holmedal et al., 2009). (Flores et al., 2017) used measurements to link storm events to an off-shore transport of SPM and attributed it to a combination of barotropic and baroclinic processes. It is unknown to what degree these processes impact the advection of SPM into the Rotterdam harbour. A way to investigate these processes could be to repeat a simulation period with the inclusion of a short wave resolving module, and compare outputs.

### 5.3 Inside the port

In the Rotterdam waterway, fluvial SPM is trapped by the density structure that is advected up and down the waterway, and accumulates in an ETM which exchanges sediment with the harbour basins lining the waterway (de Nijs et al., 2009; de Nijs et al., 2010; de Nijs et al., 2011). (de Nijs et al., 2012) performed model simulations to reproduce the previously measured advection of SPM in the Rotterdam Waterway. They found that they underpredicted saltwater intrusion and stratification and overpredicted the height of the pycnocline above the bed. As a result, they underpredicted the trapping of fluvial SPM by the salt wedge. Svasek Hydraulics performed a model validation of the NSC-Fine model (which uses a three times finer grid than the NSC-Coarse model but has only 7 sigma layers in the vertical), and concluded that computed salinity concentrations were within the 5% accuracy range (Rotsaert, 2010). Interestingly, they included a comparison with the NSC-Coarse model, and concluded that the NSC-Coarse model was more accurate in terms of salinity. However, the only measurement station in the Rotterdam Waterway is located at Hook of Holland (see Figure A.6 for the location 'HoekVHolland Rivier'), and the station only includes three measurement points in the vertical. The conclusion based on this measurement point is that the density difference between the bottom and surface of the Rotterdam Waterway is overstated, but more measurements are needed to truly verify this claim.

Because an important model application is harbour siltation, the assessment of bed concentrations forms an important part of this thesis. The two layered sediment bed implemented in the current model setup is a schematization of a sandy bed onto which a thin layer of mud may form during quiet conditions such as may be found on the North Sea (van Kessel et al., 2010). There can be exchange between bed layer S2 and the water column even when there is sediment present in S1.

The rationale behind this is that on the North Sea, the muddy layer S1 usually does not cover the entire bed, but instead accumulates in the troughs of the sandy bed forms. Besides layer thickness, the amount of sediment that can be stored in bed layer S2 depends on the sand porosity and density. Sediment in layer S2 is considered to be trapped in sand pores, and is released when the sand is mobilized. The erosion flux of layer S2 is therefore based on the mobilization of sand, as has been described in Appendix D. This is a good representation of the North Sea, but one could question its physical resemblance to muddy harbour basins where the underlying sand layer is rarely exposed. It is unknown if this poses a problem for siltation studies, but one could envision a model where the S2 layer can be deactivated when a certain amount of SPM accumulates in layer S1. Another consideration is that this bed schematization was used in the ZUNO-DD model, and this model has been calibrated and used for suspended sediment concentrations and not for sediment bed concentrations. For the ZUNO-DD model, this is desirable, as it is used to compute suspended sediment concentrations on the NSC-Coarse model boundary, and bed concentrations are not important. However, bed concentrations are important inside the harbour, and this may require new calibration of model parameters.

Finally, the settling velocities of the three sediment fractions are an important model parameter. They have been used in the ZUNO-DD model to investigate the spreading and settling of different particle and floc sizes, and for consistency they have been left unchanged in this thesis. However, floc formation is a complex process which depends on the salinity, acidity, organic matter content, and shear rate in the water column (Mietta et al., 2009). These properties change significantly as particles travel from their source (sea or river) to the harbour basins where they are deposited, and it may therefore not be assumed that floc sizes remain unchanged as they travel from the model boundaries to the basins. Floc measurements will need to clarify if this creates a large discrepancy between the sediment characteristics inside and outside the harbour. In the meantime, a sensitivity analysis could be done to establish the response of the model to different settling velocities. Flocculation aside, marine and fluvial sediments have different origins and compositions. It is therefore probable that they have different settling velocities as well. To include this effect, sediment fraction IM3, which plays no role in harbour siltation, could be removed from the model setup, and a new fraction that is applied only on the river boundary could be applied with its own settling velocity<sup>2</sup>.

---

<sup>2</sup>The Dleft3D-WAQ module only enables the inclusion of three sediment fractions.



## Chapter 6

# Conclusions and recommendations

The objective of this thesis is to investigate sediment dynamics in the Rhine ROFI and in the Port of Rotterdam by setting up a sediment model for the NSC-Coarse grid. To make this possible, a new sediment model has been set up for Port of Rotterdam, with the following changes with respect to their previous model setup:

- The open sea SPM boundary conditions have been generated with the ZUNO-DD model to allow for variations in space and time.
- The effect of wind waves on the resuspension of sediment has been included through a wave stress assimilation model.
- The model period has been enlarged from one day to a full spring-neap cycle (14 days) to allow for variable forcing conditions.
- The sediment fractions have been expanded from one to three distinct settling velocities to include some effects of differential settling.
- The bed schematization has been updated from a single bed layer to a double layer to allow for different sediment residence times in the bed.

This is the first model setup that includes the dynamic nature of SPM concentrations at sea in combination with a detailed representation of the Rotterdam Harbor. Four spring-neap cycles in the year 2007 have been selected to be used as forcing conditions (Table 3.3). One of these contained very calm weather, which was cyclically repeated for 50 times to spin up the model, yielding a set of initial conditions to be used for the other periods. The other three periods contained storms, discharge peaks, or combinations of the two, and were used to assess the behaviour of the model.

### 6.1 Conclusions

Chapter 2 gives a detailed description of the physical behaviour of suspended sediment in the Rhine-Meuse estuary and provides an answer to research question 1. In summary, fine sediments are eroded from the English channel and from the banks of the Rhine-Meuse river systems, and are transported to the Rhine-Meuse estuary through residual North Sea currents (marine) and through the Rhine and Meuse (fluvial) (van Alphen, 1990; M. Visser et al., 1991; Suijlen et al., 2002; Otto et al., 1990). In the estuary, marine sediments are eroded by waves and currents, and are confined below the pycnocline when stratification is present (Pietrzak et al., 2011; Eleveld et al., 2008; Joordens et al., 2001). They enter the Rotterdam harbour through advection of suspended sediment, and through the advection of a highly concentrated sediment layer that form in the wave boundary layer during storms, and spreads through fluid mud processes once inside the Maasmond region (Verlaan et al., 2000). On the river side, SPM is advected over a salt wedge that moves up and down the Rotterdam Waterway, forced by the tidal signal imposed at the harbour mouth (de Nijs et al., 2010). Turbulence damping at the pycnocline causes fluvial sediment to sink to the lower salty layer, and accumulate in an ETM (de Nijs et al., 2011; Geyer, 1993). This ETM exchanges sediment with the various harbour basins lining the Rotterdam Waterway, resulting in

fluvial siltation in these basins (de Nijs et al., 2009). This mechanism traps about 65% to 85% of fluvial sediment, and the remaining fluvial SPM settles in the Maasmond (de Nijs et al., 2011). Conversely, marine SPM does not penetrate far into the Rotterdam Waterway, and only affects the harbour basins lining the Maasmond (Verlaan et al., 2000).

Research questions two and three (section 1.3) deal with the extent to which the model setup of this thesis is able to reproduce the sediment dynamics and siltation rates in the Port of Rotterdam. In this early stage of model development, the model assessment has been done principally by comparing the model results to known physical behaviour and dredging statistics. Dredging statistics (see Figure 1.1) show Maasvlakte 1 to be the dominant siltation site since the construction of Maasvlakte 2 in 2013<sup>1</sup>. After that, Europoort and Botlek follow, with dredging loads of roughly half that of Maasvlakte 1. These two basins are in the same order of magnitude in terms of dredging loads. In the NSC-Coarse (WAQ) model, these areas are included as monitoring areas ('BRKNL', 'CAKNL', and 'BTLK' in Figure 4.3). One should expect more or less the same proportionality from the model simulations. However, it was concluded in chapter 5 that sedimentation in the marine influenced areas could also be overstated, since 14 day scenarios including storms have been modelled, but could also be understated since (Verlaan et al., 2000) identified fluid mud processes (not resolved in this model) as an important mechanism for marine siltation besides suspended transport.

Under these considerations, the following conclusions about the model results can be drawn:

- The wave bottom shear stresses assimilated for the NSC-Coarse (WAQ) model turn out higher and penetrate further into the harbour than expected and are not at a satisfactory level. Specifically, the generated wave shear stresses are higher than those generated for the ZUNO-DD model in the area of overlap, and wave shear stresses in excess of the critical shear stress for resuspension from bed layer S2 (which has the highest  $\tau_c$  of the two layers) are seen as far as Botlek harbour during storms (Figure 4.10). Furthermore, wave stresses show a time delay of approximately one day with respect to the rest of the model forcing. Harbour basins are sheltered areas by design, and should not erode significantly during storms. Maasvlakte 2 is included through the bathymetry of the model, and this is not properly handled by the wave stress assimilation. It is treated as an extremely shallow area and almost permanently generates high shear stresses in the Maasvlakte 2 area. Through this error, sediments are eroded and exported to sea in bed layer S1, which is undesirable.
- The effect of stratification on SPM concentrations at sea can be confirmed qualitatively. Surface plots show the absence of surface SPM when stratification is present (see Figure 4.1, Figure 4.2, appendix B). The concentration of sediment in the lower layer is confirmed by cross-sections (see cross-sections in appendix B. This is in line with observations by (Eleveld et al., 2008; Suijlen et al., 2002; Pietrzak et al., 2011). Furthermore, the trapping of fluvial SPM in the Rotterdam Waterway as described by (de Nijs et al., 2011) was observed in section 4.6. However, the presence of an ETM could not be related to harbour siltation rates along the Rotterdam Waterway. Botlek harbour responded strongly to storm events, which is attributed to the wave stress assimilation. This generated large amounts of local resuspension far upstream the Rotterdam Waterway, which is considered nonphysical behaviour. This made it difficult to distinguish individual siltation mechanisms in this area.
- The model qualitatively reproduces the episodic sedimentation events such as described by (Verlaan et al., 2000). During quiet conditions, figures like Figure 4.4 show very little exchange of SPM through the harbour mouth and figures like Figure C.21 show little sedimentation. When high wave bottom shear stresses occur, both SPM exchange through the harbour mouth and sedimentation rates in bed level S2 peak. This is a significant improvement from previous WAQ simulations performed with the NSC-Coarse model, and results from the imposed wave shear stresses and SPM concentrations at the open sea boundary. However, especially in bed level S1, erosion and export of SPM to sea is observed inside the harbour. This is expected to be caused by the aforementioned unrealistically wave shear stresses inside

---

<sup>1</sup>(de Bruijn, 2018) performed an analysis of historical dredging data, and showed that the increase of dredging loads at Maasvlakte 1 since the construction of Maasvlakte 2 coincides with a decrease in the adjoining Maasmond area, which is maintained by the Ministry of Infrastructure and is not included in Figure 1.1. He concluded that the increase is likely a result of an internal redistribution of sedimentation patterns and not of an increased influx of SPM.

the harbour. The model significantly underestimates siltation in the Maasvlakte 1 area compared to the Europoort and Botlek areas, which together form the three dominant siltation sites in terms of dredging loads. In Figure 4.6, which shows total siltation in bed layer S2 as a result of each period, Europoort ('CAKNL') and Botlek ('BTLK') correctly show the same proportionality, but Maasvlakte 1 ('BRKNL') is significantly lower, which is in contrast with dredging statistics. Furthermore, Figure 4.5 shows erosion of IM1 in bed layer S1, which is problematic. Both the underestimation of Maasvlakte 1 and the erosion from bed layer S1 are again expected to be caused by the erroneously computed wave shear stresses. It, it was concluded in chapter 5 that only one of the two transport mechanisms of marine SPM into the harbour as observed by (Verlaan et al., 2000) is resolved in the current model setup. This should in principle lead to an underestimation of marine SPM transport and siltation during storm events

- During storms a large amount of sediment is suspended at sea when compared to suspension of the overlapping area of the ZUNO-DD model. This is expected to be caused in part by the larger shear stresses mentioned before, and in part by the virtually waveless conditions that were used for the spin-up of the NSC-Coarse (WAQ) model. In total, 700 days of calm conditions were simulated to reach a state of dynamic equilibrium for the sediment concentrations in the water column and bed layers. This creates an unrealistically large sediment availability, which is brought in suspension when a storm is modelled. In reality, the frequency of waves on the North Sea limits the amount of sediment available for resuspension, which known as a starved bed condition.

Despite the critical notes above, a considerable amount of physics have been added to the model with respect to previous model studies, and the fact that clear responses to variable environmental conditions can be observed is encouraging. In general, it is recommended to solve the issues listed above to the point where the qualitative expectations formulated in section 6.1 are met. From there the model can be calibrated to match siltation rates and can develop in a useful tool for future applications. To further improve the model, the following steps are recommended, in descending order of importance.

## 6.2 Recommendations

- **Reconstruct the assimilation of the wave bottom shear stresses.** The wave stress assimilation performed for this thesis was based on the same wave buoys that were used for the ZUNO-DD (WAQ) model, under the assumption that only waves on the sea side of the NSC-Coarse grid would be generated and velocity induced stresses would dominate inside the harbour. It turned out that the wave stress assimilation produced significant errors inside the harbour, creating unrealistically large bottom shear stresses in supposedly sheltered harbour basins. It is expected that this error is the cause of a lot of the issues described in section 6.1. The largest model improvement can be made by reassessing this assimilation technique inside the harbour. Including a short wave model in the hydrodynamic simulation would be the best option, but this could require unrealistically large computational resources. If this is the case, a better wave stress assimilation, possibly including wave buoys inside the harbour and with proper treatment of Maasvlakte 2 is expected to yield a very large improvement. Alternatively, if the above cannot be realized or if quick results are desired, one could interpolate the shear stresses of the ZUNO-DD model directly onto the NSC-Coarse grid, leaving the shear stresses inside the harbour at zero. It is expected that this will resolve current issues such as the erosion of layer S1, the strong response of Botlek harbour to wave stresses, and the comparatively low sedimentation in Maasvlakte 1. Furthermore, it could be that expected sediment transport mechanisms are more noticeable when there is less local resuspension by waves. This interpolation of wave stresses has been carried out during the course of this thesis work, but has not been included in this thesis due to time constraints. The output has been supplied to Port of Rotterdam to be used in future model studies.
- **Include a separate sediment fraction for fluvial SPM.** Sediment transport paths and siltation mechanisms are much more easily distinguished if sediment can be traced to its origin. Furthermore, marine and fluvial sediment are known to have different compositions, and are therefore unlikely to have the same settling velocities. It was concluded in chapter 4

that SPM fraction IM3 plays no role in harbour siltation. It is therefore recommended that this fraction is removed from the model setup, and instead a new fraction is added only the open river boundaries of the model. The remaining two SPM fractions should be removed from the riverine boundaries and will be indicative of marine sediment. This will allow SPM in the model to be traced back to its origin at all times, and will give the potential for different marine and riverine settling velocities, increasing the applicability of the model and improving the relation of the model to the physical system.

- **Assess the types and concentrations of SPM found in the harbour through measurements.** The best model confirmation is through measured data. It is advised to make a thorough assessment of the measured data that is currently available, and perform new measurements if desired. It would be valuable to have measurement data of SPM concentrations in the main pathways. Furthermore, it would be valuable to have salinity measurements over the vertical, to assess how well stratification in the Rotterdam Waterway is reproduced by the SIMONA model. This is important for the reproduction of the trapping of SPM. In addition, it would be valuable to characterize settling velocities in different locations of the port area. This can then be compared to the spreading of the modelled sediment fractions IM1 and IM2. Furthermore, it would be interesting to know how the floc sizes found inside the harbour compare to those at sea. In chapter 2 it was noted that floc sizes are amongst other factors dependant on turbulent shear, salinity, and organic matter content. These parameters undergo strong changes between the sea and the harbour basins, and it may be that flocculation causes the input sediment at sea to have different settling behaviour from the sediment found in the harbour. Flocculation not yet included in this thesis, but the WAQ module offers options to this end. However, this may be unrealistic and impractical for the near future, and its usefulness will depend on the desired model application. (Winterwerp, 2002) notes that the settling velocity in this type of model is usually regarded as a calibration parameter.
- **Adjust the critical shear stresses for resuspension for bed layers S1 and S2.** A crucial parameter for the calibration of the model for dredging purposes will be the critical shear stress for resuspension for bed layers S1 and S2. This parameter controls how much sediment deposits, and where it deposits. An important consideration in this step will be to determine what the relative importance of bed layer S1 and S2 should be, since both have different critical shear stresses for resuspension. However, this step has not yet been considered in detail.

# Appendices



## Appendix A

# Supporting figures: Model Forcing Conditions and spin-up of NSC model

### A.1 Forcing conditions

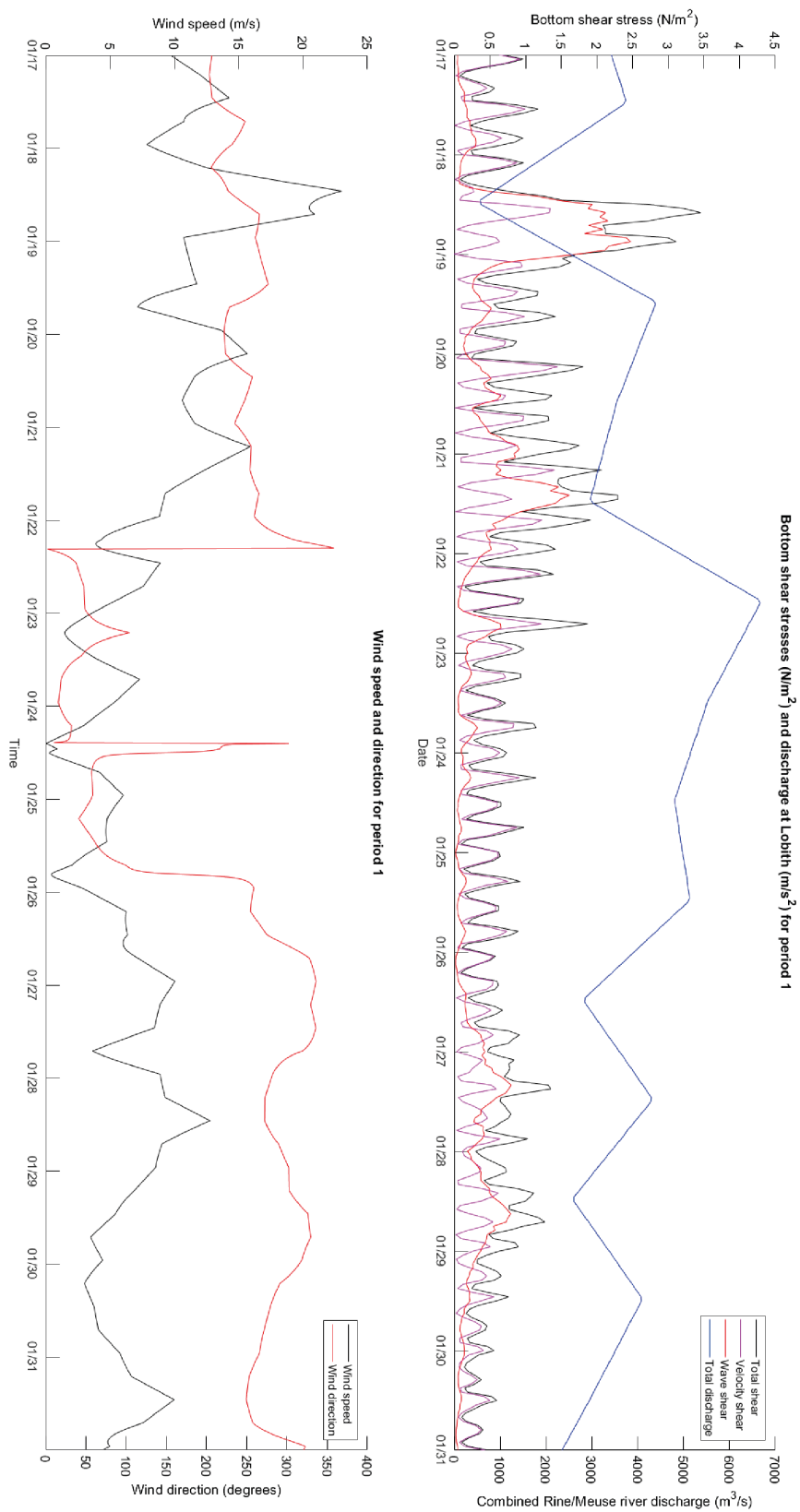


Figure A.1: Model forcing conditions for Period 1. Bottom shear stresses (velocity and waves) and wind speed are displayed on the left axes, while river discharge and wind direction are shown on the right axes.

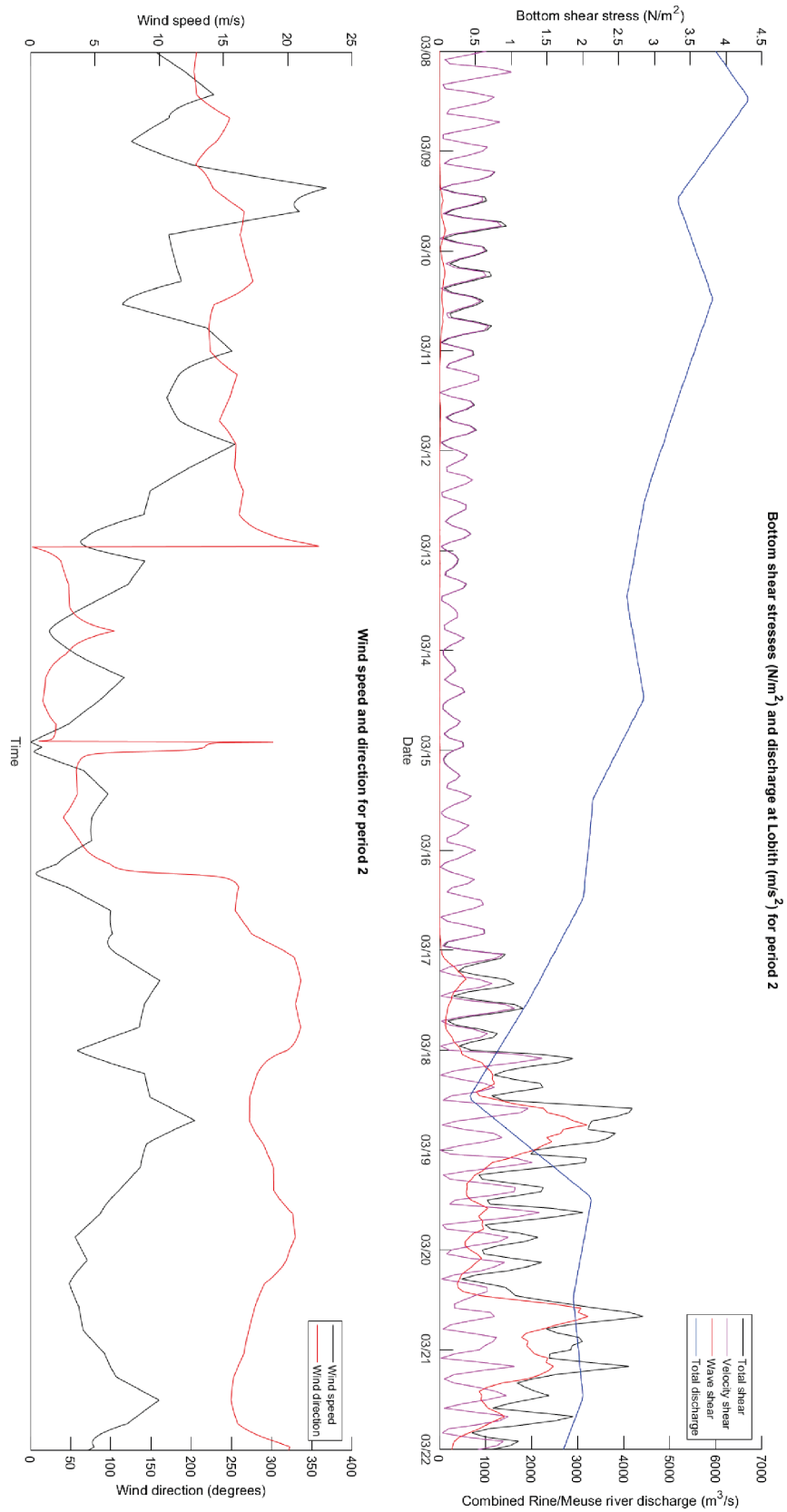


Figure A.2: Model forcing conditions for Period 2. Bottom shear stresses (velocity and waves) and wind speed are displayed on the left axes, while river discharge and wind direction are shown on the right axes.

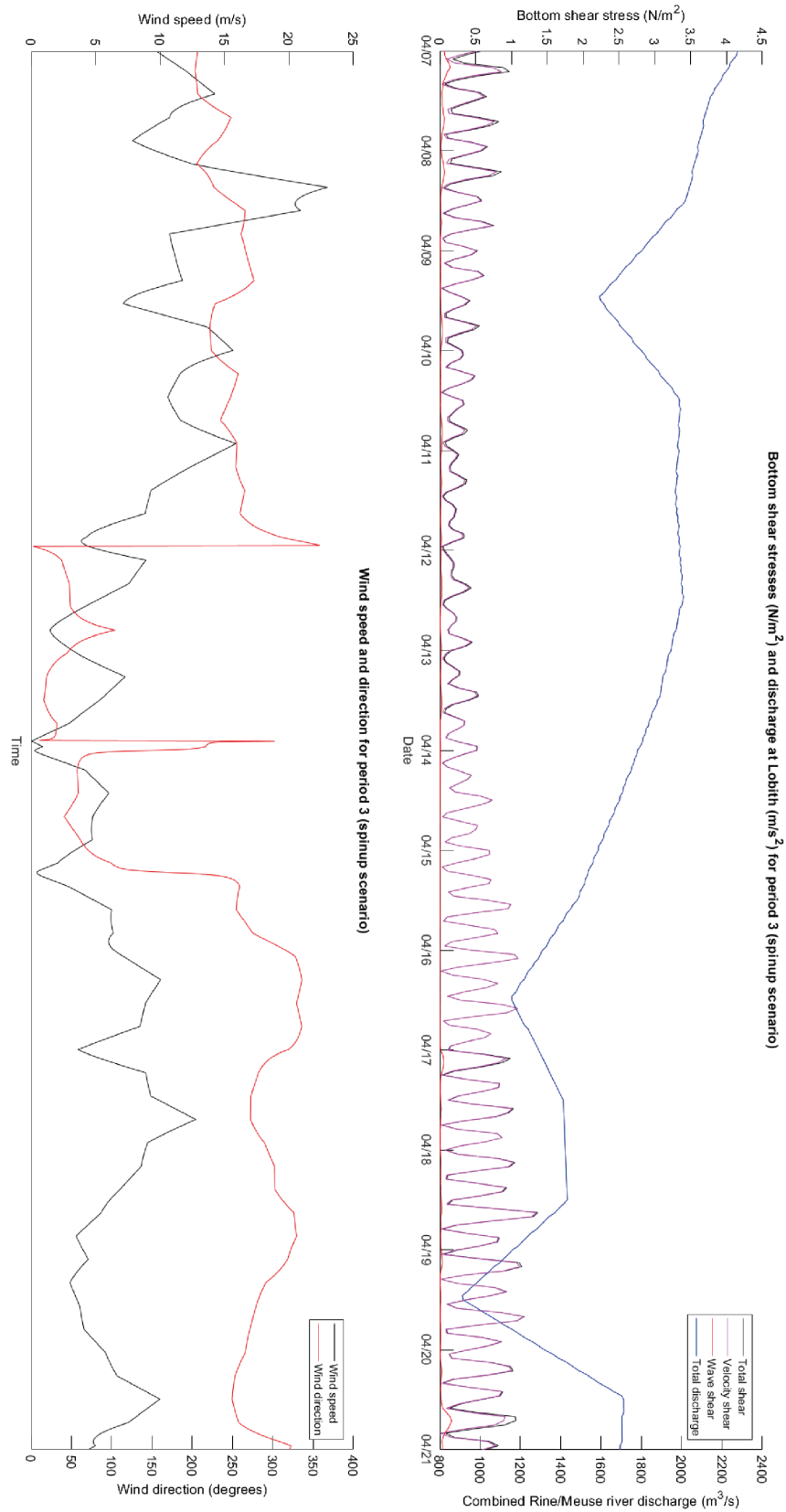


Figure A.3: Model forcing conditions for Period 3. This period is used only for the spin-up of the model. Bottom shear stresses (velocity and waves) and wind speed are displayed on the left axes, while river discharge and wind direction are shown on the right axes.

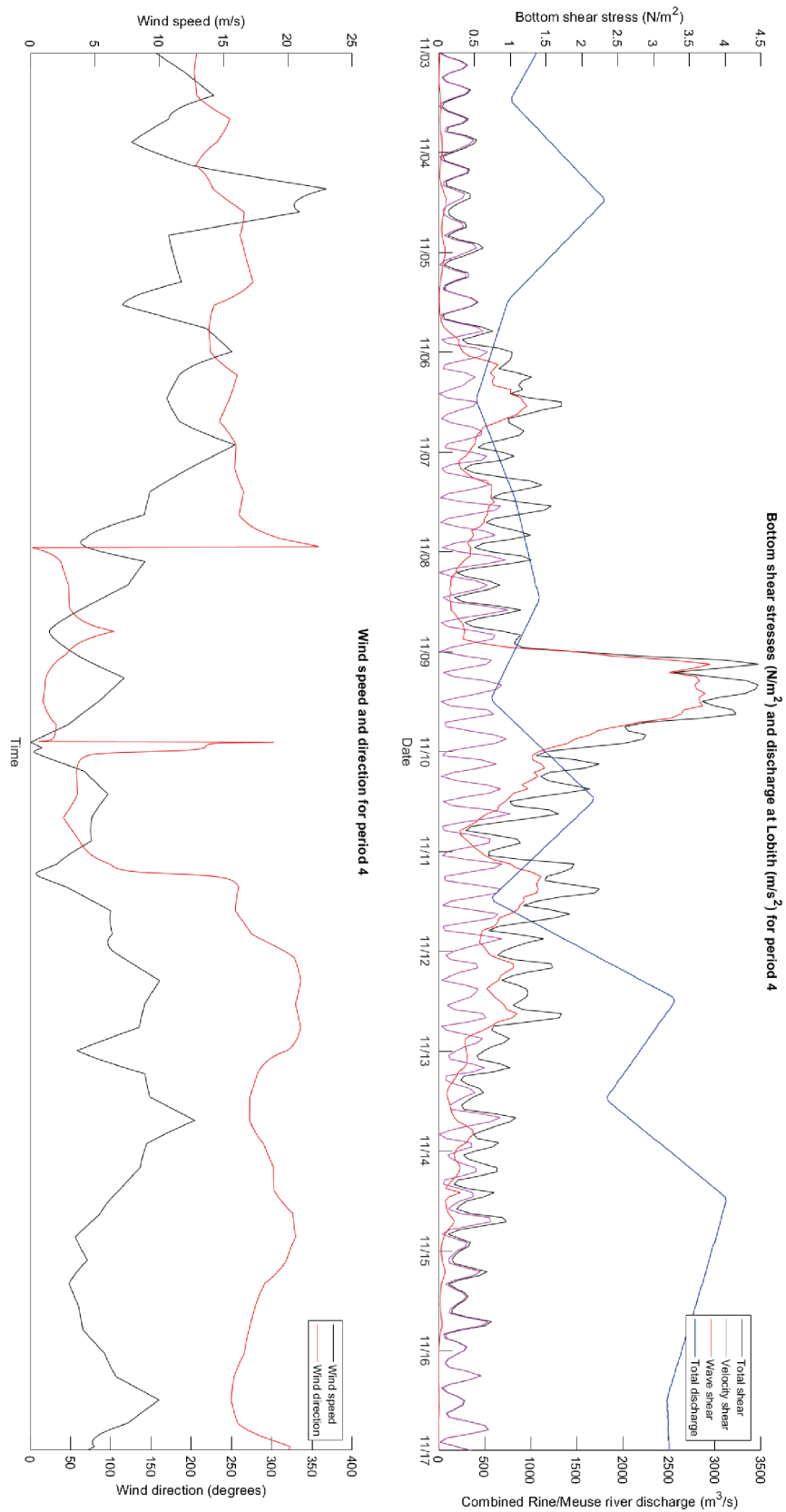


Figure A.4: Model forcing conditions for Period 4. Bottom shear stresses (velocity and waves) and wind speed are displayed on the left axes, while river discharge and wind direction are shown on the right axes.

## A.1. FORCING CONDITIONS

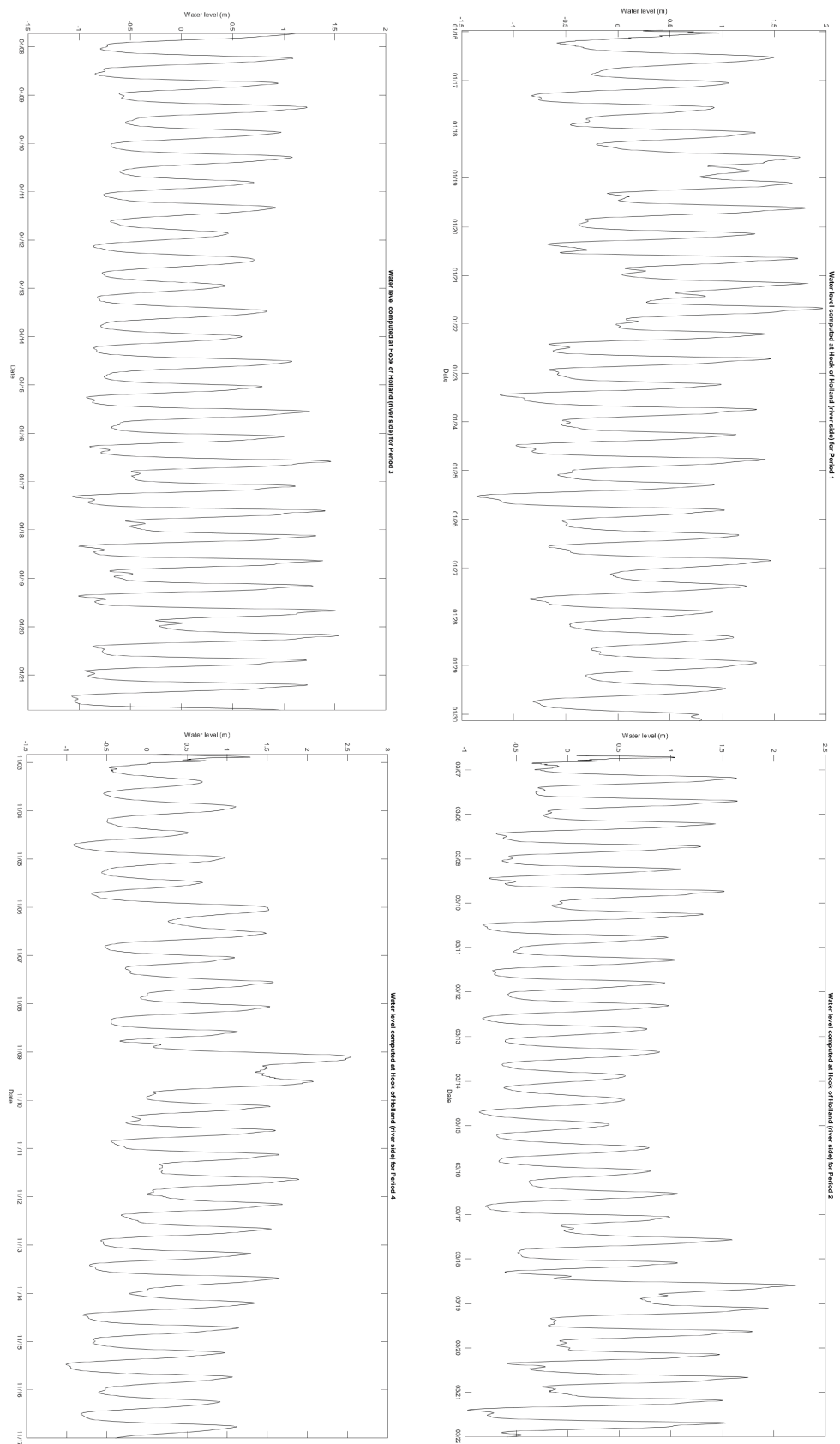


Figure A.5: Model forcing conditions. Computed water levels at Hook of Holland (river side) for all periods.

## A.2 Tables showing the spin-up of the NSC-Coarse (WAQ) model

The following tables show the relative increase in concentrations of different substances at different observation points from one spin-up cycle to the next. One spin-up cycle consist of ten repetitions of Period 3 (140 days). This has been repeated five times in order to reach a dynamic equilibrium. For each repetition, the concentrations of the final timestep of the previous run have been used as initial conditions (restart file).

In these tables, the percentages for each cycle show the percentual increase in concentrations at the last timestep with respect to the previous cycle. Hence, the diminishing percentages as more cycles are run shows how fast the substance reaches a dynamic equilibrium. This determines the spin-up time of the model.

For observation points, some substances appear not to spin up, or spin up very slowly. These are stations in very sheltered areas, where bottom shear stresses never or rarely exceed the critical shear stress for resuspension. If this is the case, the area experience constant siltation and an equilibrium cannot be reached. This can be understood from the fact that most harbour basins are permanently dredged, and are therefore always out of equilibrium. For that reason, these observation points have been left out of consideration for the model spin-up, and mainly the stations at sea and the more active parts of the harbour are assessed for spin-up.

In total, the spin-up scenario has been repeated five times, leading to a total spin-up time of 700 days. The tables show that especially bed layer S2 is responsible for the large spin-up time. This can be understood from the fact that this layer has the longest sediment residence time, and therefore responds to changes in forcing conditions the slowest.

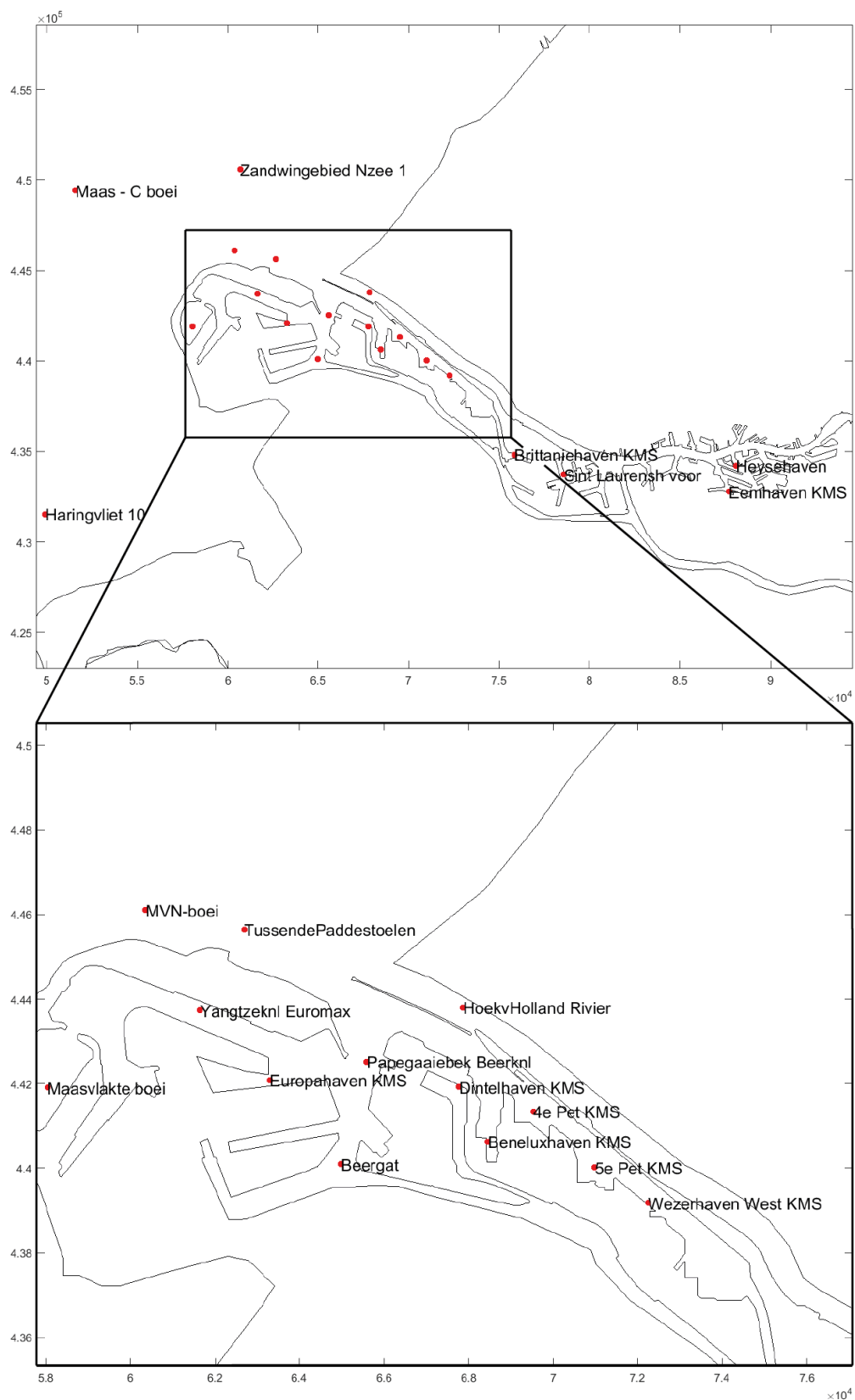


Figure A.6: Location of observation points used for the assessment of the spin-up time of the NSC-Coarse (WAQ) model.

<b>Substance: IM1S1</b>	Cycle 1	Cycle 2	Cycle 3	Cycle 4	<b>Cycle 5</b>
HoekvHolland Ri (12)	[-]	1.6%	0.9%	0.6%	<b>0.4%</b>
Beergat (12)	[-]	53.8%	35.8%	26.7%	<b>21.2%</b>
Haringvliet 10 (12)	[-]	1.0%	0.5%	0.3%	<b>0.2%</b>
MVN-boei (12)	[-]	1.0%	0.5%	0.3%	<b>0.2%</b>
Maasvlakte boei (12)	[-]	15.9%	7.1%	4.2%	<b>2.6%</b>
Maas - C boei (12)	[-]	0.6%	0.3%	0.1%	<b>0.1%</b>
TussendePaddest (12)	[-]	0.9%	0.5%	0.3%	<b>0.2%</b>
Papegaaiebek Be (12)	[-]	2.2%	1.1%	0.7%	<b>0.5%</b>
Zandwingebied N (12)	[-]	0.5%	0.3%	0.2%	<b>0.1%</b>
Dintelhaven KMS (12)	[-]	6.1%	3.9%	3.1%	<b>2.6%</b>
Brittaniehaven (12)	[-]	54.7%	36.6%	27.5%	<b>22.0%</b>
Eemhaven KMS (12)	[-]	53.2%	35.6%	26.7%	<b>21.4%</b>
Sint Laurens v (12)	[-]	53.3%	35.5%	26.5%	<b>21.2%</b>
Beneluxhaven KM (12)	[-]	4.9%	2.2%	1.4%	<b>1.0%</b>
7e Pet KMS (12)	[-]	53.9%	35.8%	26.8%	<b>21.4%</b>
4e Pet KMS (12)	[-]	52.6%	35.0%	26.2%	<b>20.9%</b>
Wezerhaven West (12)	[-]	53.3%	35.5%	26.6%	<b>21.2%</b>
5e Pet KMS (12)	[-]	53.0%	35.3%	26.4%	<b>21.1%</b>
Yangtze knl Euro (12)	[-]	10.2%	4.1%	2.3%	<b>1.4%</b>
Heysehaven (12)	[-]	52.5%	35.3%	26.5%	<b>21.2%</b>
Europahaven KMS (12)	[-]	52.8%	33.7%	24.1%	<b>18.3%</b>

Table A.1: Development of the relative increase in concentration of SPM fraction IM1 in bed layer S1 from one spin-up cycle to the next. Each cycle consists of 10 repetitions of model scenario 3 (Figure A.3). Some observation areas (locations given in Figure A.6 are in very sheltered areas and never or very slowly converge to an equilibrium. The model was considered to have spun up sufficiently after 5 runs (700 days).

<b>Substance: IM1S2</b>	Cycle 1	Cycle 2	Cycle 3	Cycle 4	<b>Cycle 5</b>
HoekvHolland Ri (12)	[-]	30.5%	11.4%	4.7%	<b>2.1%</b>
Beergat (12)	[-]	54.0%	36.1%	27.1%	<b>21.6%</b>
Haringvliet 10 (12)	[-]	33.3%	14.0%	6.4%	<b>3.1%</b>
MVN-boei (12)	[-]	33.0%	13.8%	6.3%	<b>3.0%</b>
Maasvlakte boei (12)	[-]	61.8%	40.7%	29.9%	<b>23.4%</b>
Maas - C boei (12)	[-]	38.3%	19.0%	10.4%	<b>6.0%</b>
TussendePaddest (12)	[-]	40.6%	21.3%	12.4%	<b>7.7%</b>
Papegaaiebek Be (12)	[-]	45.9%	27.1%	18.0%	<b>12.6%</b>
Zandwingebied N (12)	[-]	38.7%	19.6%	10.9%	<b>6.4%</b>
Dintelhaven KMS (12)	[-]	56.7%	37.3%	27.9%	<b>22.3%</b>
Brittaniehaven (12)	[-]	54.7%	36.6%	27.5%	<b>22.0%</b>
Eemhaven KMS (12)	[-]	53.2%	35.6%	26.7%	<b>21.4%</b>
Sint Laurens v (12)	[-]	53.3%	35.5%	26.5%	<b>21.2%</b>
Beneluxhaven KM (12)	[-]	54.8%	36.1%	26.9%	<b>21.4%</b>
7e Pet KMS (12)	[-]	53.9%	35.8%	26.8%	<b>21.4%</b>
4e Pet KMS (12)	[-]	52.6%	35.0%	26.2%	<b>20.9%</b>
Wezerhaven West (12)	[-]	53.3%	35.5%	26.6%	<b>21.2%</b>
5e Pet KMS (12)	[-]	53.0%	35.3%	26.4%	<b>21.1%</b>
Yangtze knl Euro (12)	[-]	55.8%	37.0%	27.6%	<b>21.9%</b>
Heysehaven (12)	[-]	52.5%	35.3%	26.5%	<b>21.2%</b>
Europahaven KMS (12)	[-]	55.0%	36.7%	27.4%	<b>21.9%</b>

Table A.2: Development of the relative increase in concentration of SPM fraction IM1 in bed layer S2 from one spin-up cycle to the next. Each cycle consists of 10 repetitions of model scenario 3 (Figure A.3). Some observation areas (locations given in Figure A.6 are in very sheltered areas and never or very slowly converge to an equilibrium. The model was considered to have spun up sufficiently after 5 runs (700 days).

A.2. TABLES SHOWING THE SPIN-UP OF THE NSC-COARSE (WAQ) MODEL

<b>Substance: IM2S1</b>	Cycle 1	Cycle 2	Cycle 3	Cycle 4	<b>Cycle 5</b>
HoekvHolland Ri (12)	[-]	13.1%	6.7%	4.2%	<b>2.9%</b>
Beergat (12)	[-]	69.0%	47.9%	36.4%	<b>29.2%</b>
Haringvliet 10 (12)	[-]	3.5%	2.0%	1.2%	<b>0.8%</b>
MVN-boei (12)	[-]	7.0%	3.8%	2.4%	<b>1.6%</b>
Maasvlakte boei (12)	[-]	83.7%	61.5%	45.8%	<b>35.0%</b>
Maas - C boei (12)	[-]	3.8%	1.9%	1.0%	<b>0.5%</b>
TussendePaddest (12)	[-]	8.1%	4.5%	2.9%	<b>2.0%</b>
Papegaaiebek Be (12)	[-]	12.1%	6.5%	4.2%	<b>2.9%</b>
Zandwingebied N (12)	[-]	5.5%	2.8%	1.6%	<b>1.0%</b>
Dintelhaven KMS (12)	[-]	66.5%	32.9%	17.8%	<b>11.6%</b>
Brittaniehaven (12)	[-]	62.5%	42.4%	31.9%	<b>25.6%</b>
Eemhaven KMS (12)	[-]	66.6%	46.7%	35.7%	<b>28.7%</b>
Sint Laurens v (12)	[-]	63.7%	44.1%	33.3%	<b>26.6%</b>
Beneluxhaven KM (12)	[-]	49.4%	28.3%	19.1%	<b>14.1%</b>
7e Pet KMS (12)	[-]	62.2%	41.7%	31.0%	<b>24.6%</b>
4e Pet KMS (12)	[-]	67.1%	47.5%	36.2%	<b>29.0%</b>
Wezerhaven West (12)	[-]	69.8%	50.6%	39.4%	<b>32.2%</b>
5e Pet KMS (12)	[-]	69.7%	50.5%	39.4%	<b>32.1%</b>
Yangtzeknl Euro (12)	[-]	67.7%	41.8%	27.6%	<b>19.4%</b>
Heysehaven (12)	[-]	64.8%	45.4%	34.9%	<b>28.2%</b>
Europahaven KMS (12)	[-]	66.4%	45.9%	34.6%	<b>27.6%</b>

Table A.3: Development of the relative increase in concentration of SPM fraction IM2 in bed layer S1 from one spin-up cycle to the next. Each cycle consists of 10 repetitions of model scenario 3 (Figure A.3). Some observation areas (locations given in Figure A.6 are in very sheltered areas and never or very slowly converge to an equilibrium. The model was considered to have spun up sufficiently after 5 runs (700 days).

<b>Substance: IM2S2</b>	Cycle 1	Cycle 2	Cycle 3	Cycle 4	<b>Cycle 5</b>
HoekvHolland Ri (12)	[-]	41.5%	19.2%	10.1%	<b>5.9%</b>
Beergat (12)	[-]	69.0%	48.0%	36.5%	<b>29.3%</b>
Haringvliet 10 (12)	[-]	35.2%	15.6%	7.6%	<b>3.9%</b>
MVN-boei (12)	[-]	38.6%	17.9%	9.3%	<b>5.2%</b>
Maasvlakte boei (12)	[-]	91.9%	75.4%	61.1%	<b>50.2%</b>
Maas - C boei (12)	[-]	41.0%	21.0%	11.9%	<b>7.0%</b>
TussendePaddest (12)	[-]	46.3%	25.6%	15.8%	<b>10.3%</b>
Papegaaiebek Be (12)	[-]	52.6%	32.1%	21.8%	<b>15.7%</b>
Zandwingebied N (12)	[-]	41.9%	22.0%	12.7%	<b>7.8%</b>
Dintelhaven KMS (12)	[-]	84.5%	60.3%	43.9%	<b>33.7%</b>
Brittaniehaven (12)	[-]	62.5%	42.4%	31.9%	<b>25.6%</b>
Eemhaven KMS (12)	[-]	66.6%	46.7%	35.7%	<b>28.8%</b>
Sint Laurens v (12)	[-]	63.7%	44.1%	33.3%	<b>26.6%</b>
Beneluxhaven KM (12)	[-]	73.3%	52.4%	40.0%	<b>32.2%</b>
7e Pet KMS (12)	[-]	62.2%	41.7%	31.0%	<b>24.6%</b>
4e Pet KMS (12)	[-]	67.1%	47.5%	36.2%	<b>29.0%</b>
Wezerhaven West (12)	[-]	69.8%	50.6%	39.4%	<b>32.2%</b>
5e Pet KMS (12)	[-]	69.7%	50.5%	39.4%	<b>32.1%</b>
Yangtzeknl Euro (12)	[-]	78.3%	57.6%	44.3%	<b>35.4%</b>
Heysehaven (12)	[-]	64.8%	45.4%	34.9%	<b>28.3%</b>
Europahaven KMS (12)	[-]	66.9%	46.6%	35.5%	<b>28.5%</b>

Table A.4: Development of the relative increase in concentration of SPM fraction IM2 in bed layer S2 from one spin-up cycle to the next. Each cycle consists of 10 repetitions of model scenario 3 (Figure A.3). Some observation areas (locations given in Figure A.6 are in very sheltered areas and never or very slowly converge to an equilibrium. The model was considered to have spun up sufficiently after 5 runs (700 days).

<b>Substance: TIM</b>	Cycle 1	Cycle 2	Cycle 3	Cycle 4	<b>Cycle 5</b>
HoekvHolland Ri (12)	[-]	2.1%	1.1%	0.7%	<b>0.5%</b>
Beergat (12)	[-]	7.5%	4.0%	2.7%	<b>2.0%</b>
Haringvliet 10 (12)	[-]	1.7%	0.9%	0.5%	<b>0.3%</b>
MVN-boei (12)	[-]	0.8%	0.5%	0.3%	<b>0.2%</b>
Maasvlakte boei (12)	[-]	6.3%	2.9%	1.7%	<b>1.1%</b>
Maas - C boei (12)	[-]	0.4%	0.2%	0.1%	<b>0.0%</b>
TussendePaddest (12)	[-]	0.5%	0.3%	0.2%	<b>0.1%</b>
Papegaaiebek Be (12)	[-]	2.2%	1.3%	0.9%	<b>0.6%</b>
Zandwingebied N (12)	[-]	0.2%	0.1%	0.1%	<b>0.0%</b>
Dintelhaven KMS (12)	[-]	3.5%	2.1%	1.6%	<b>1.3%</b>
Brittaniehaven (12)	[-]	4.3%	2.6%	1.9%	<b>1.5%</b>
Eemhaven KMS (12)	[-]	7.2%	4.3%	3.0%	<b>2.3%</b>
Sint Laurens v (12)	[-]	3.4%	1.9%	1.3%	<b>0.9%</b>
Beneluxhaven KM (12)	[-]	4.1%	2.3%	1.5%	<b>1.2%</b>
7e Pet KMS (12)	[-]	4.5%	2.4%	1.7%	<b>1.3%</b>
4e Pet KMS (12)	[-]	2.8%	1.4%	0.9%	<b>0.7%</b>
Wezerhaven West (12)	[-]	3.8%	2.0%	1.4%	<b>1.0%</b>
5e Pet KMS (12)	[-]	3.1%	1.4%	0.9%	<b>0.7%</b>
Yangtze knl Euro (12)	[-]	6.6%	3.1%	1.9%	<b>1.2%</b>
Heysehaven (12)	[-]	5.8%	3.3%	2.1%	<b>1.5%</b>
Europahaven KMS (12)	[-]	6.3%	2.7%	1.6%	<b>1.0%</b>

Table A.5: Development of the relative increase in concentration of total SPM (IM1+IM2+IM3) suspended in the water column in layer 12. Each cycle consists of 10 repetitions of model scenario 3 (Figure A.3). The suspended sediment concentrations respond much faster to the hydrodynamic forcing, and therefore have much shorter spin-up time than the bed layers.



## Appendix B

# Supporting figures: Surface and cross-sectional plots from the ZUNO-DD and NSC-Coarse models

This section illustrates the behaviour of the ZUNO-DD and NSC-Coarse WAQ and FLOW models by plotting the salinity and SPM (total inorganic matter) fields for three tidal cycles. Surface fields of salinity and SPM from the ZUNO-DD model and NSC-Coarse model are presented, as well as cross-sectional plots from the ZUNO-DD model of the Northern and Southern boundaries of the NSC-Coarse model. Finally, a cross-section has been taken through the Rotterdam Waterway to shed light onto the advection of salinity and SPM through the waterway. The location of the cross-section is shown below in Figure B.1.

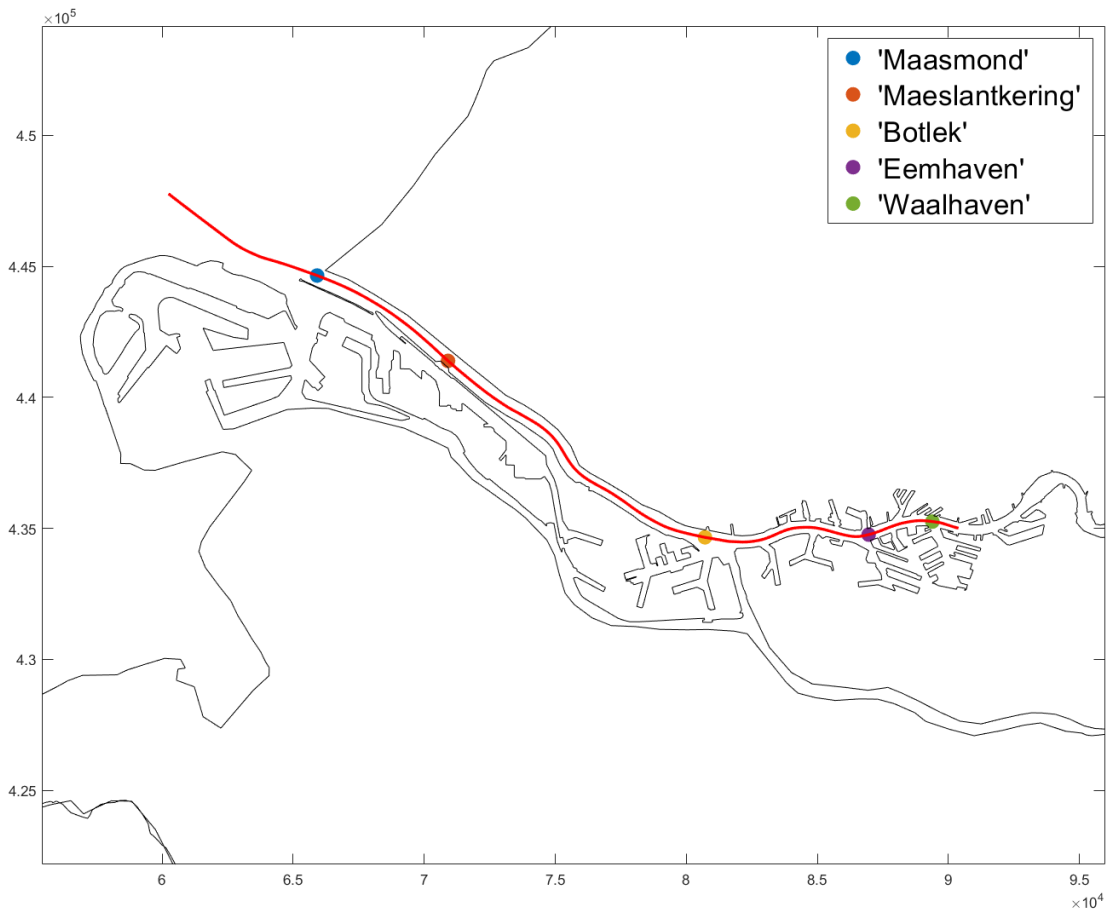


Figure B.1: Cross section location of Figure B.13 and Figure B.14

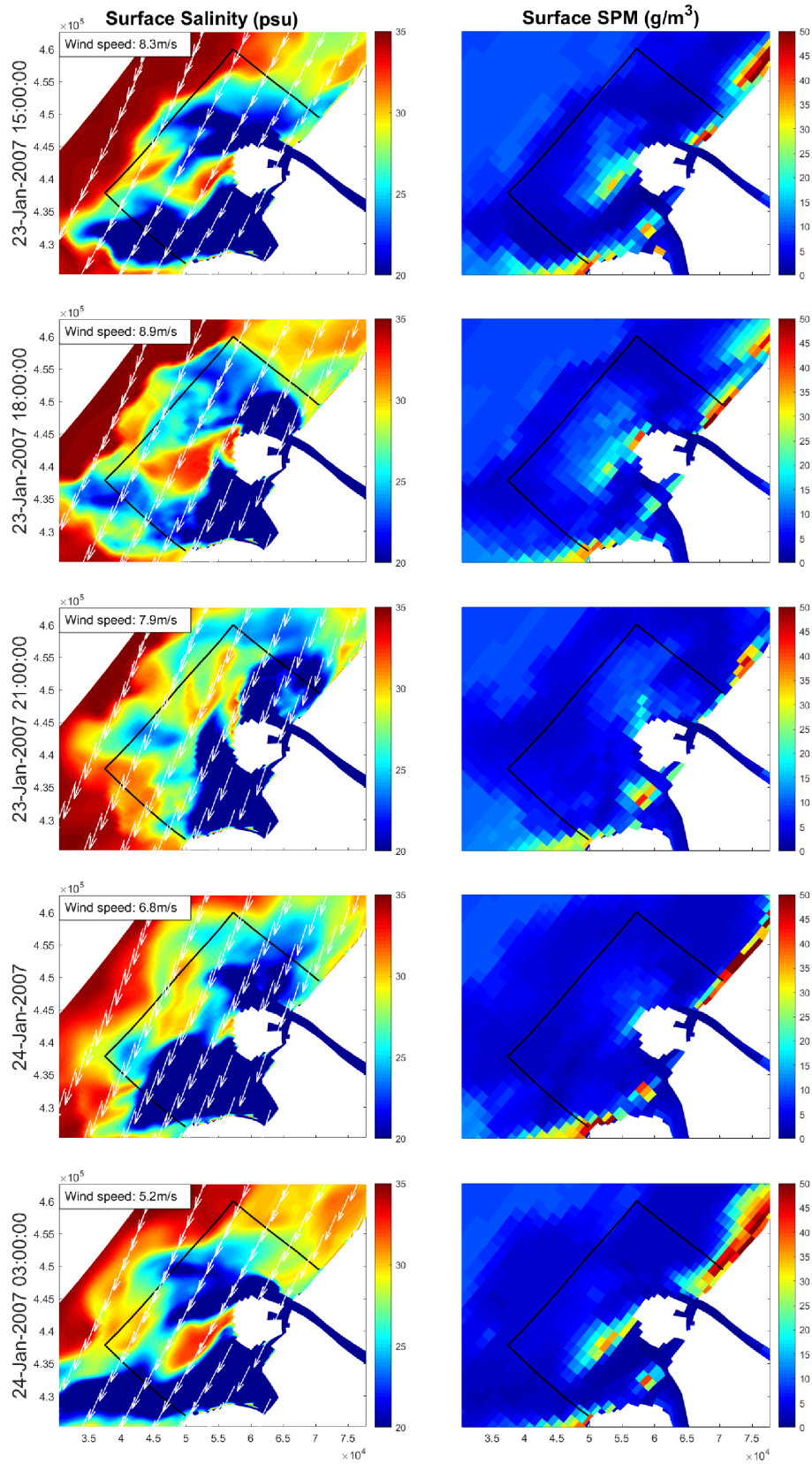


Figure B.2: ZUNO-DD results giving an overview of the development of the surface salinity and total SPM structure during a tidal cycle on January 17<sup>th</sup>. A strong alongshore Southerly wind pushes the ROFI across the Northern boundary (frictional response) and confines it against the coast (Ekman response). Wind vectors have been plotted across the salinity field in white, and a black line denotes the boundary of the NSC-Coarse grid.

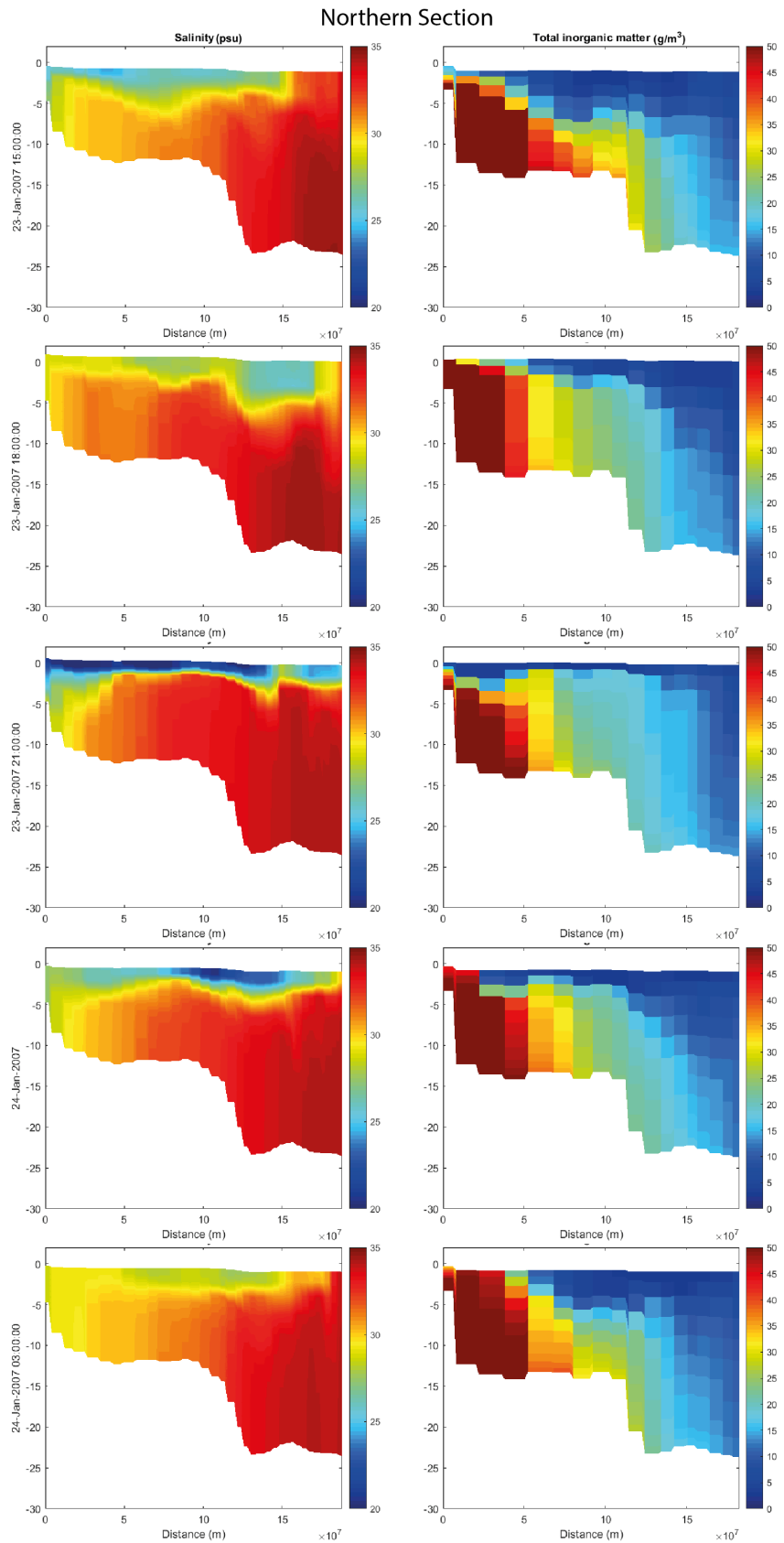


Figure B.3: cross-section of the Northern boundary of the NSC-Coarse model belonging to the tidal cycle of Figure B.2. The left panels show that the water column is stratified throughout the tidal cycle. However, stratification is strongest during flood (21:00), when the ROFI is advected over the Northern boundary. The right panels show the response of the combined SPM concentrations. When stratification is large, SPM is visibly confined below the pycnocline.

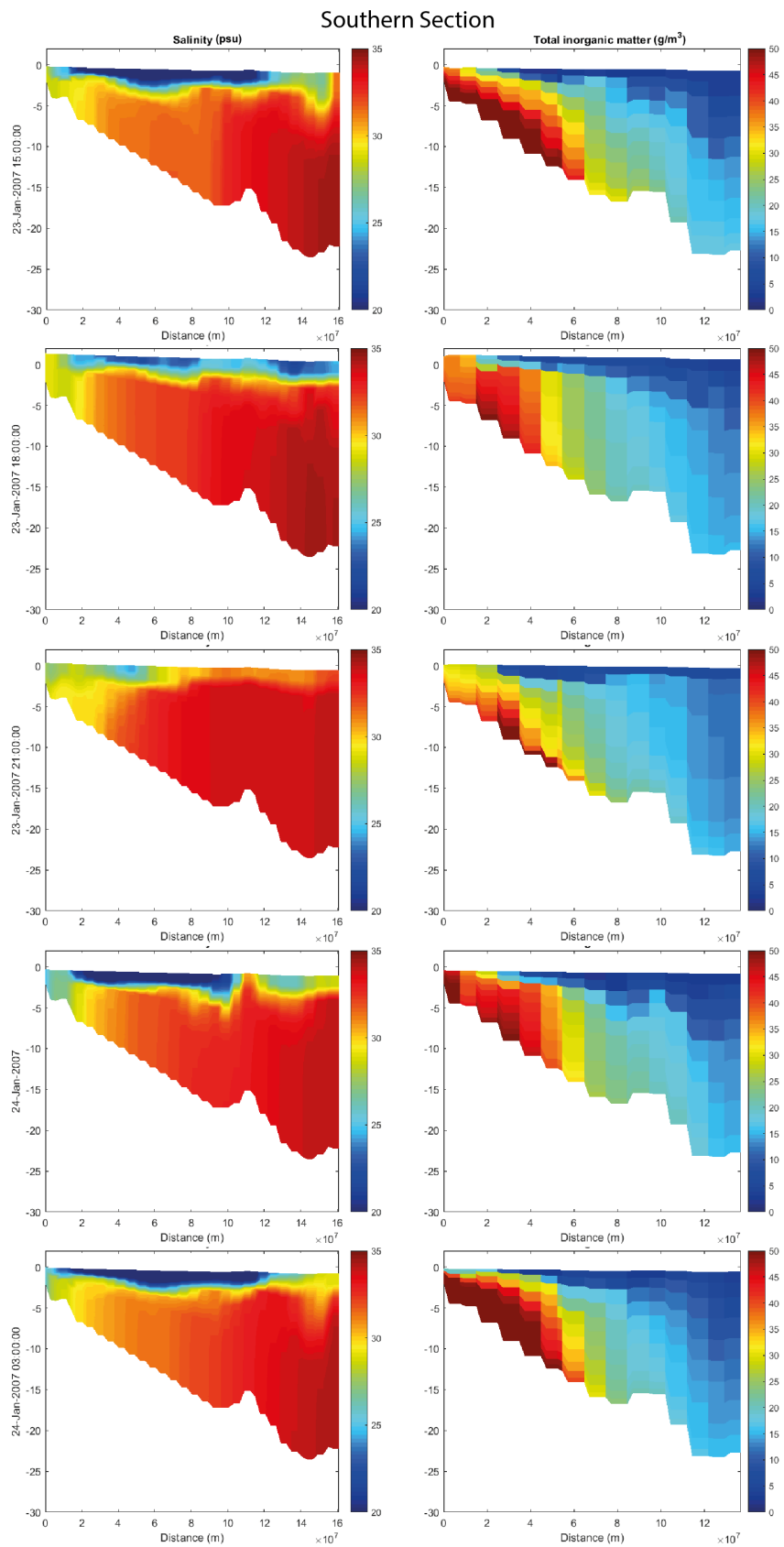


Figure B.4: cross-section from the ZUNO-DD model on the Southern boundary of the NSC-Coarse model belonging to the tidal cycle of Figure B.2. The left panels show that the water column is stratified throughout the tidal cycle. This only occurs during periods of large stratification. Stratification is strongest during ebb (15:00 and 03:00), when the ROFI is advected over the Southern boundary. The right panels show the response of the combined SPM concentrations. When stratification is large, SPM is visibly confined below the pycnocline.

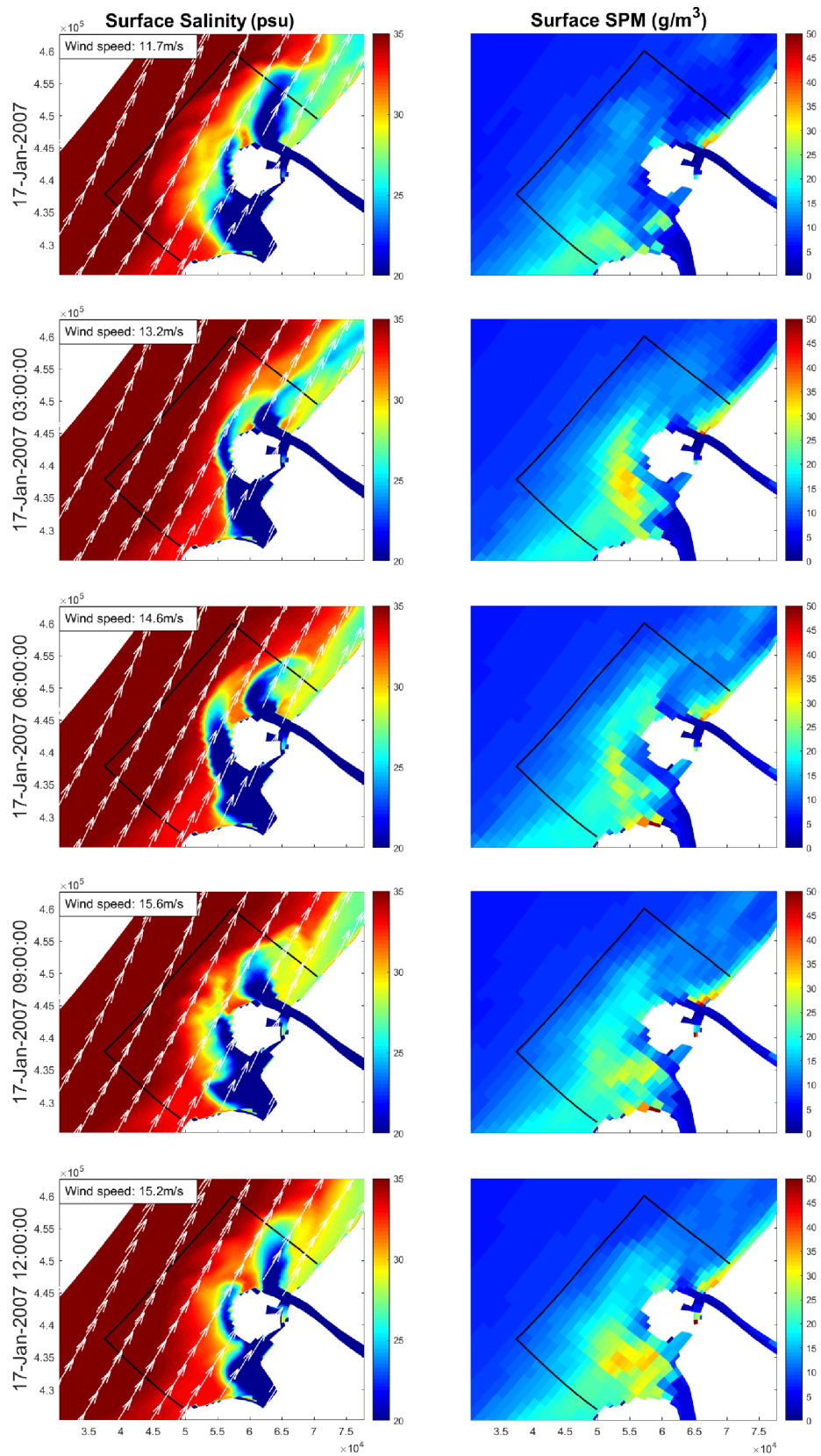


Figure B.5: ZUNO-DD results giving an overview of the development of the surface salinity and total SPM structure during a tidal cycle on January 17<sup>th</sup>. A strong alongshore Southerly wind pushes the ROFI across the Northern boundary (frictional response) and confines it against the coast (Ekman response). Furthermore, high wind velocities impose significant mixing at the water surface, limiting the size of the ROFI. Wind vectors have been plotted across the salinity field in white, and a black line denotes the boundary of the NSC-Coarse grid.

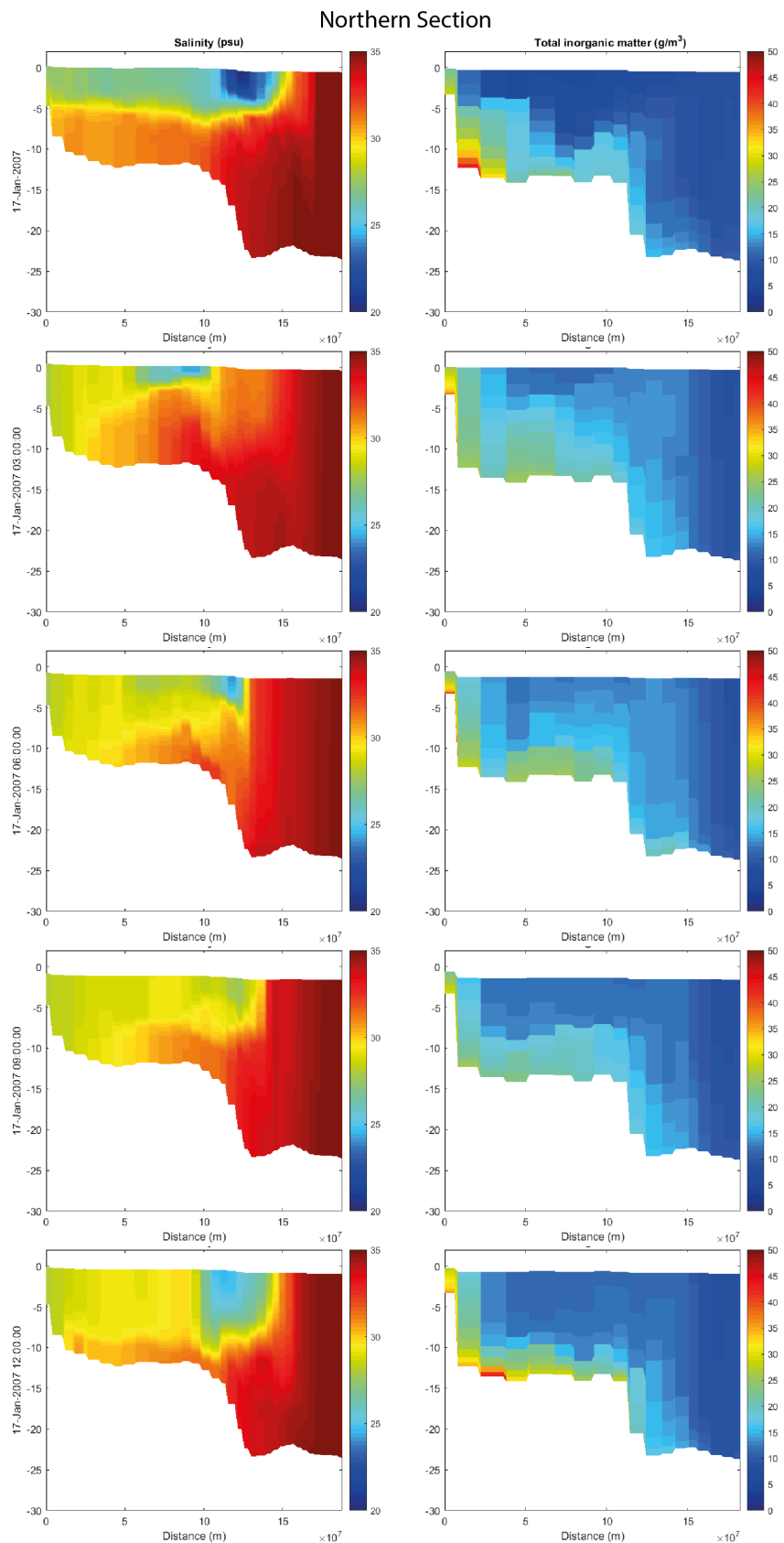


Figure B.6: ZUNO-DD cross-section of the Northern boundary of the NSC-Coarse model belonging to the tidal cycle of Figure B.5. The left panels show that the water column is stratified throughout the tidal cycle, but more mixing is present than in Figure B.3. Stratification is strongest during flood (00:00 and 12:00), when the ROFI is advected over the Northern boundary. The right panels show the response of the combined SPM concentrations. When stratification is large, SPM is visibly confined below the pycnocline.

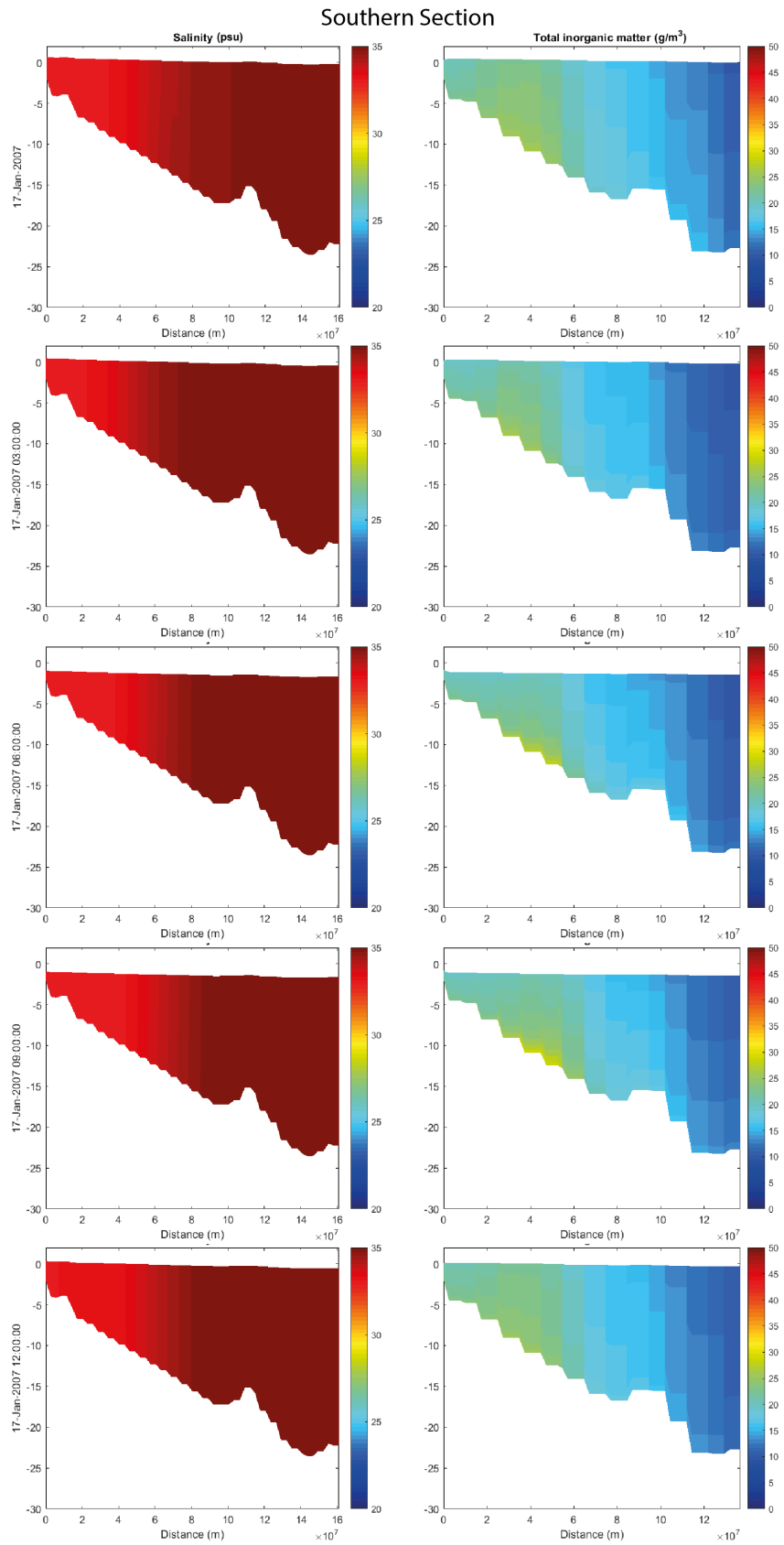


Figure B.7: ZUNO-DD cross-section of the Southern boundary of the NSC-Coarse model belonging to the tidal cycle of Figure B.5. Due to the restricted size of the ROFI and the residual current directed North, the Southern boundary remains well mixed throughout the water column (left panels). This is in contrast to Figure B.4, when a large ROFI induces stratification on this boundary. During these well-mixed conditions, SPM is divided more homogeneously over the water depth.

APPENDIX B. SUPPORTING FIGURES: SURFACE AND CROSS-SECTIONAL PLOTS FROM THE ZUNO-DD AND NSC-COARSE MODELS

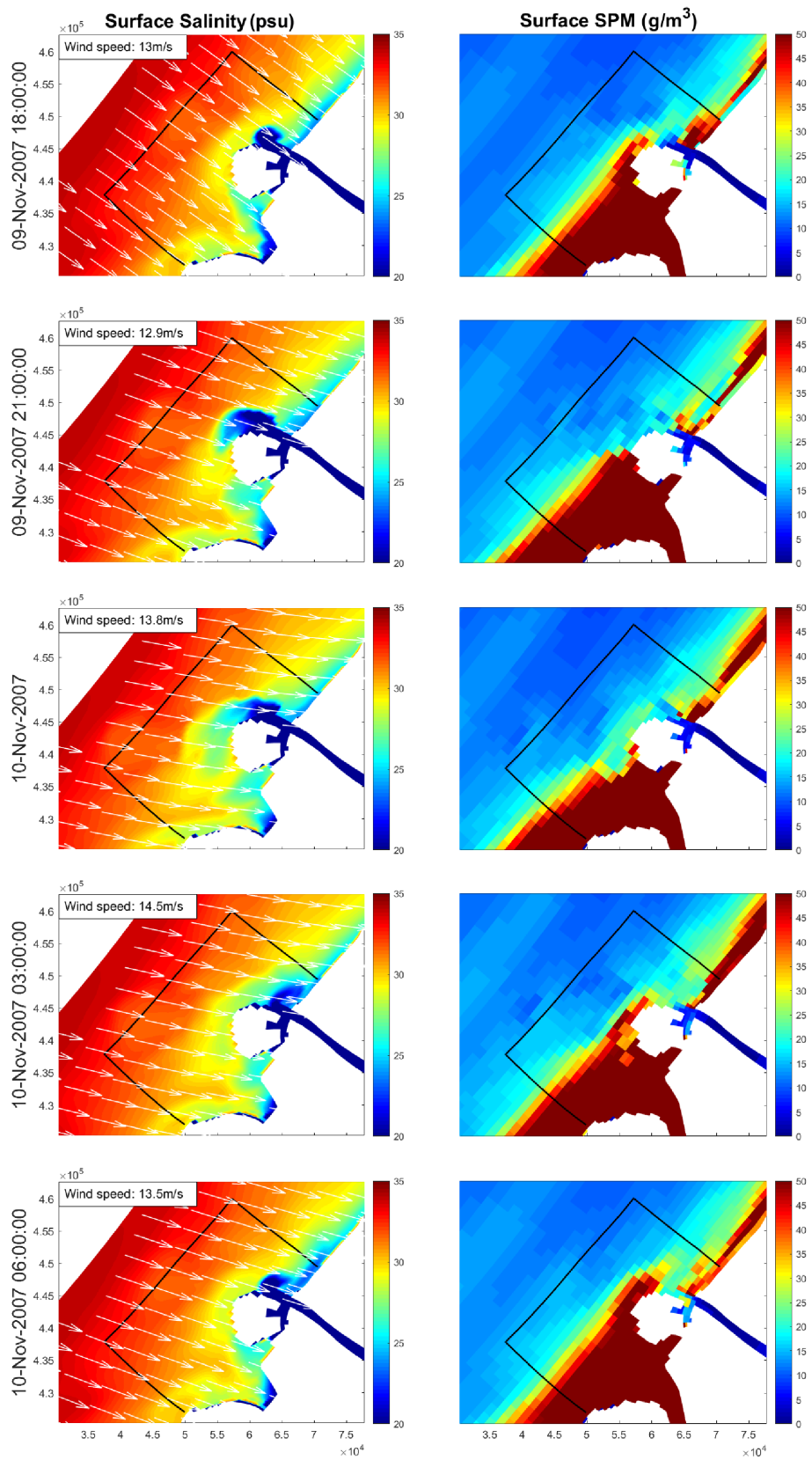


Figure B.8: ZUNO-DD results giving an overview of the development of the surface salinity and total SPM structure during a tidal cycle on January 17<sup>th</sup>. A strong on-shore wind induces a water level setup which restricts the outflow of the Rotterdam Waterway, and imposes strong surface stirring at the water column (frictional response). Wind vectors have been plotted across the salinity field in white, and a black line denotes the boundary of the NSC-Coarse grid.

### Northern Section

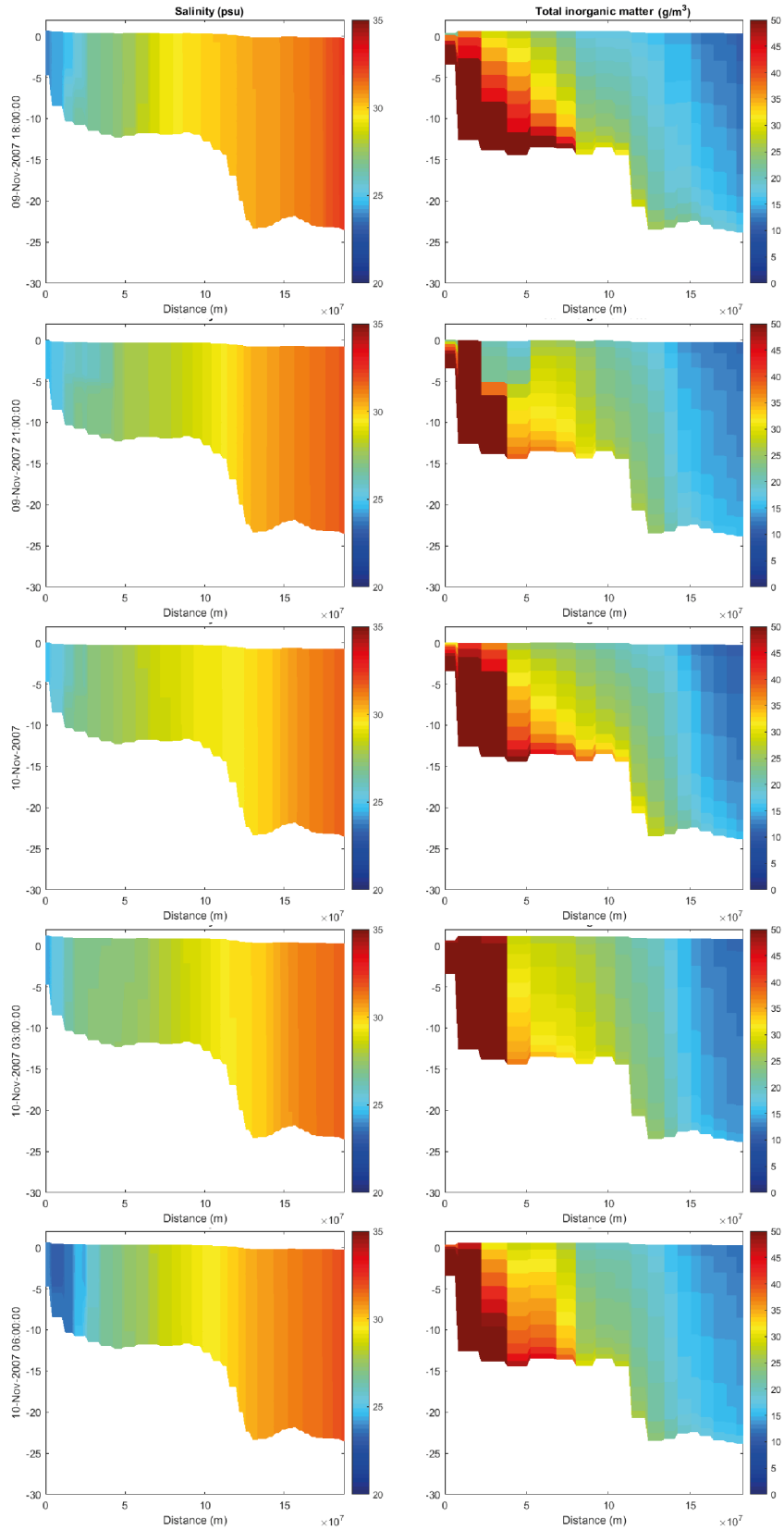


Figure B.9: ZUNO-DD cross-section of the Northern boundary of the NSC-Coarse model belonging to the tidal cycle of Figure B.8. Due to the restricted river discharge and strong surface stirring, the Northern boundary is well mixed throughout the tidal cycle (left panels). Furthermore, large wave stresses resuspend a large amount of sediment. Due to the well-mixed state of the ROFI, this is visible as surface SPM.

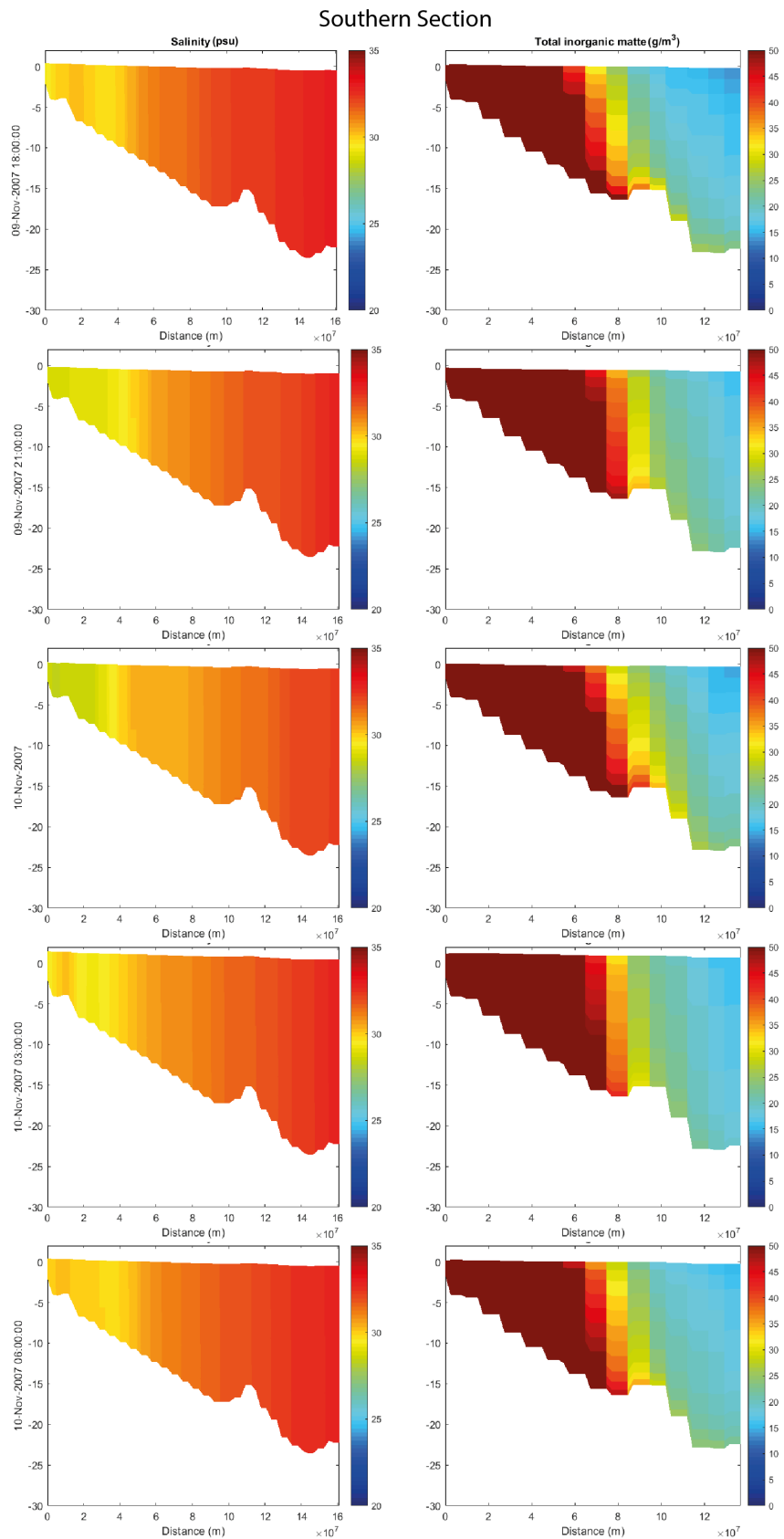


Figure B.10: ZUNO-DD cross-section of the Southern boundary of the NSC-Coarse model belonging to the tidal cycle of Figure B.8. As is the case with Figure B.7, the Southern boundary is well mixed throughout the tidal cycle (left panels). Furthermore, large wave stresses resuspend a large amount of sediment. Due to the well mixed state of the ROFI, this is visible as surface SPM.

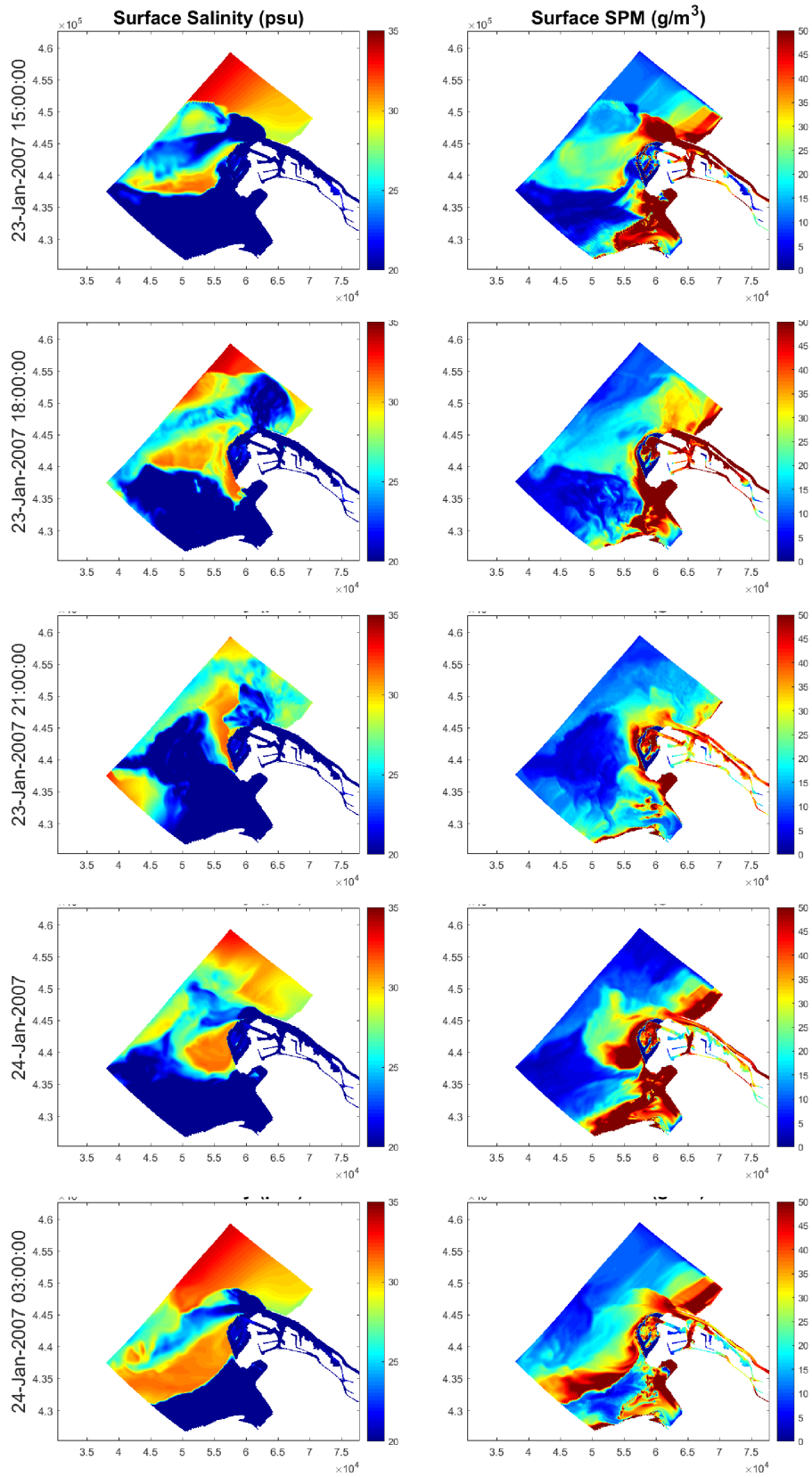


Figure B.11: NSC-Coarse surface plot of salinity and SPM corresponding to the ZUNO-DD plot of Figure B.2.

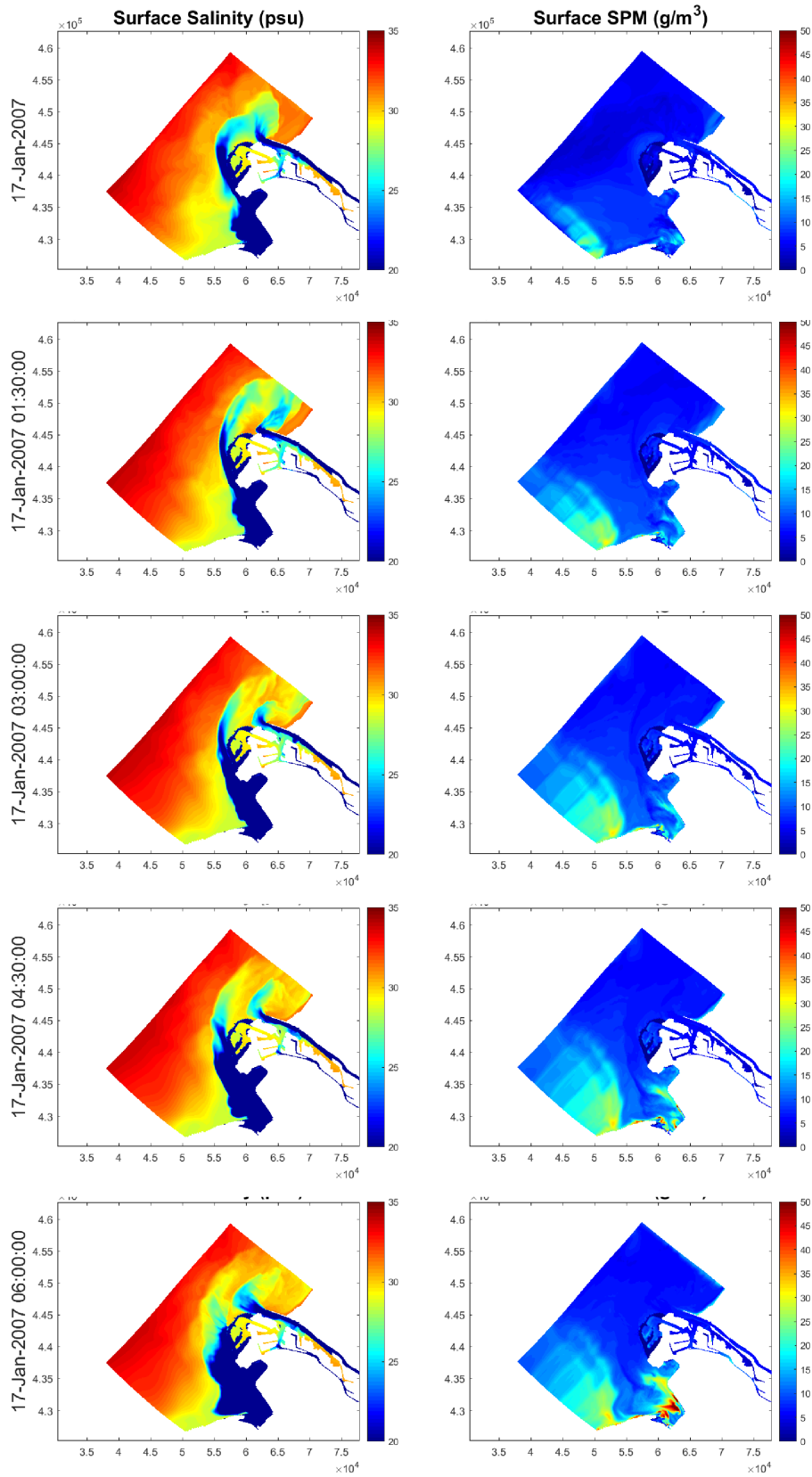


Figure B.12: NSC-Coarse surface plot of salinity and SPM corresponding to the ZUNO-DD plot of Figure B.5.

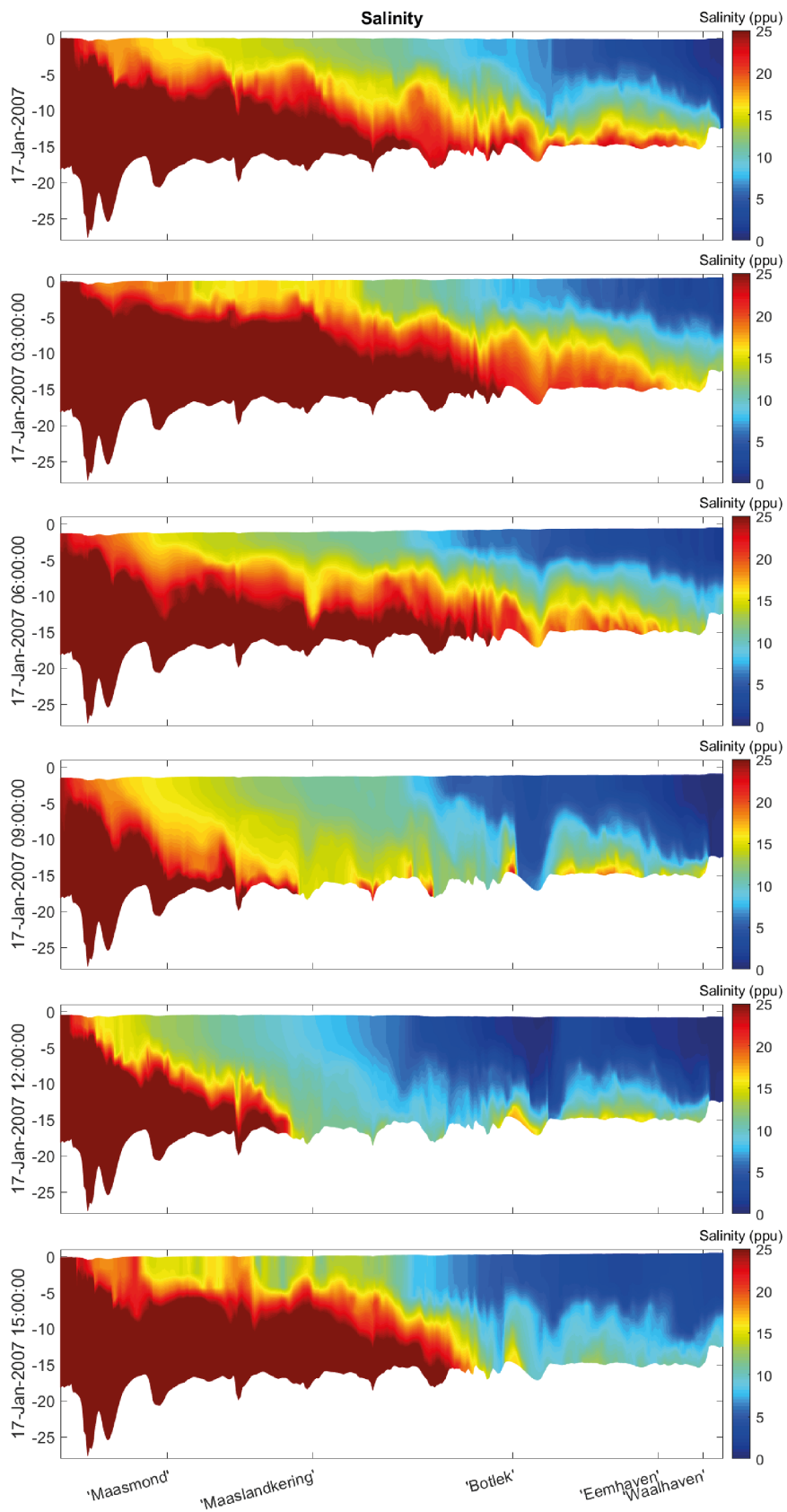


Figure B.13: Salinity cross-section of the Rotterdam Waterway on 17/01/2007

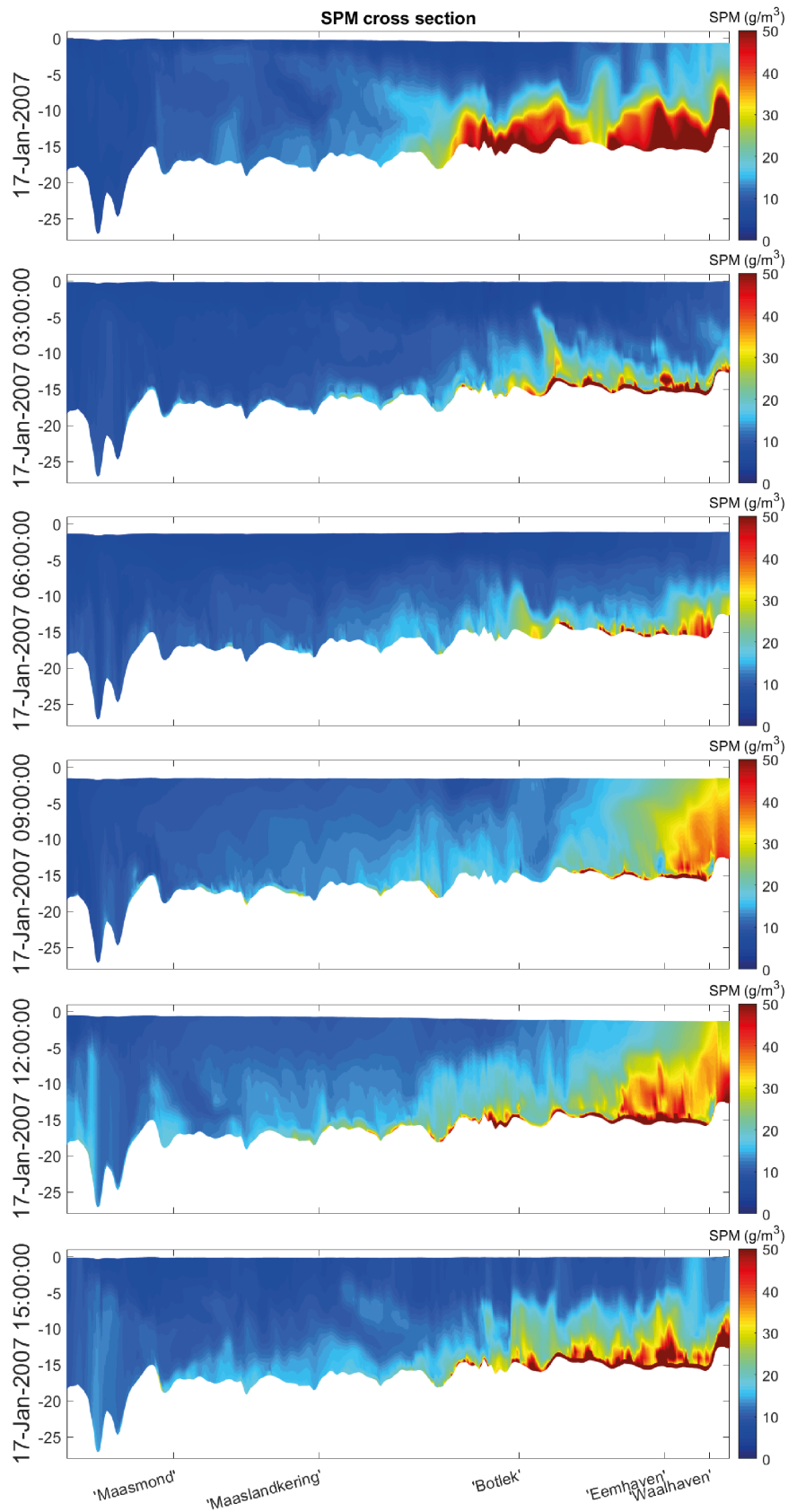


Figure B.14: SPM cross-section of the Rotterdam Waterway on 17/01/2007

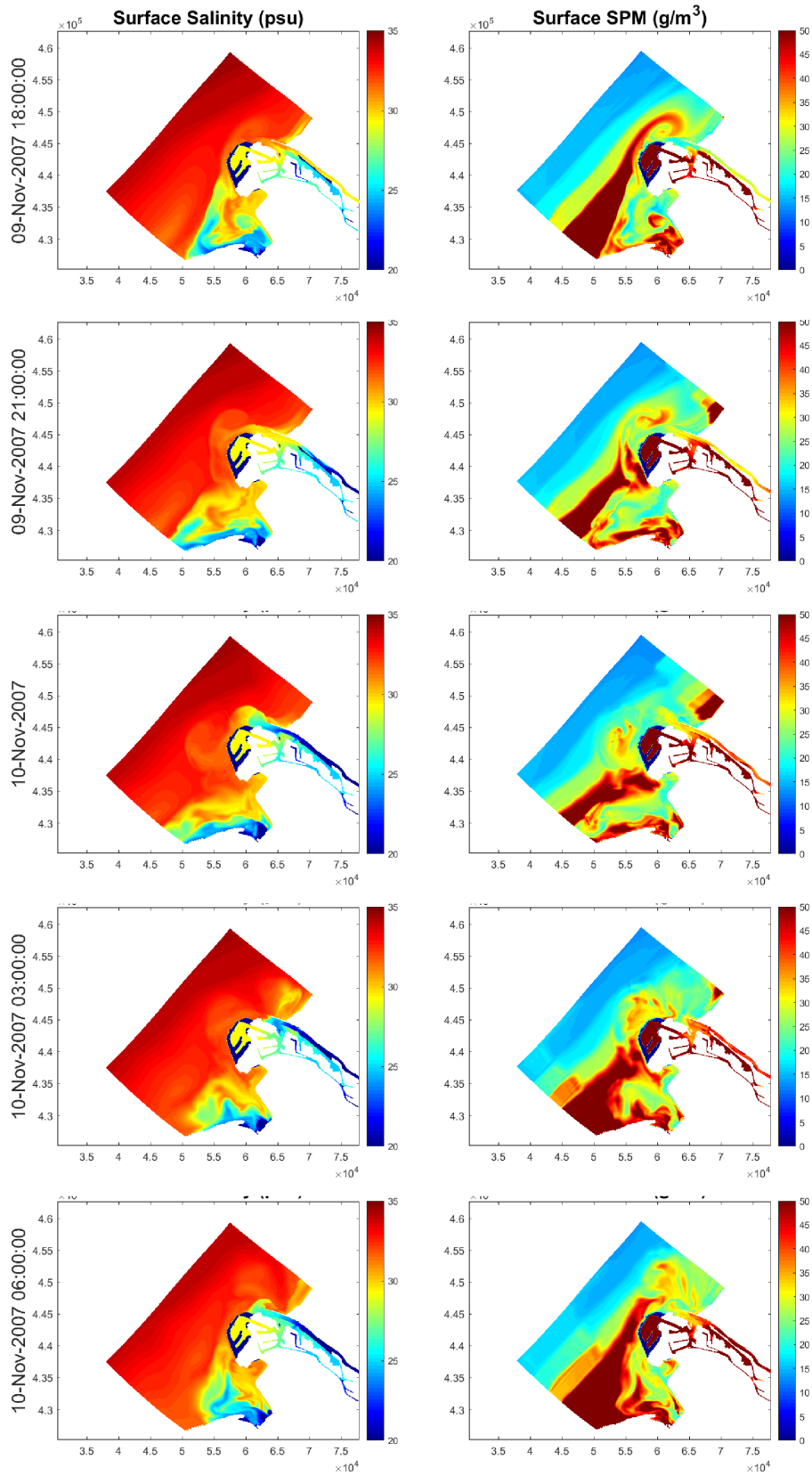


Figure B.15: Surface salinity and surface SPM on 10/11/2007

## Appendix C

### Supporting figures: Plots and charts relating to harbour sedimentation

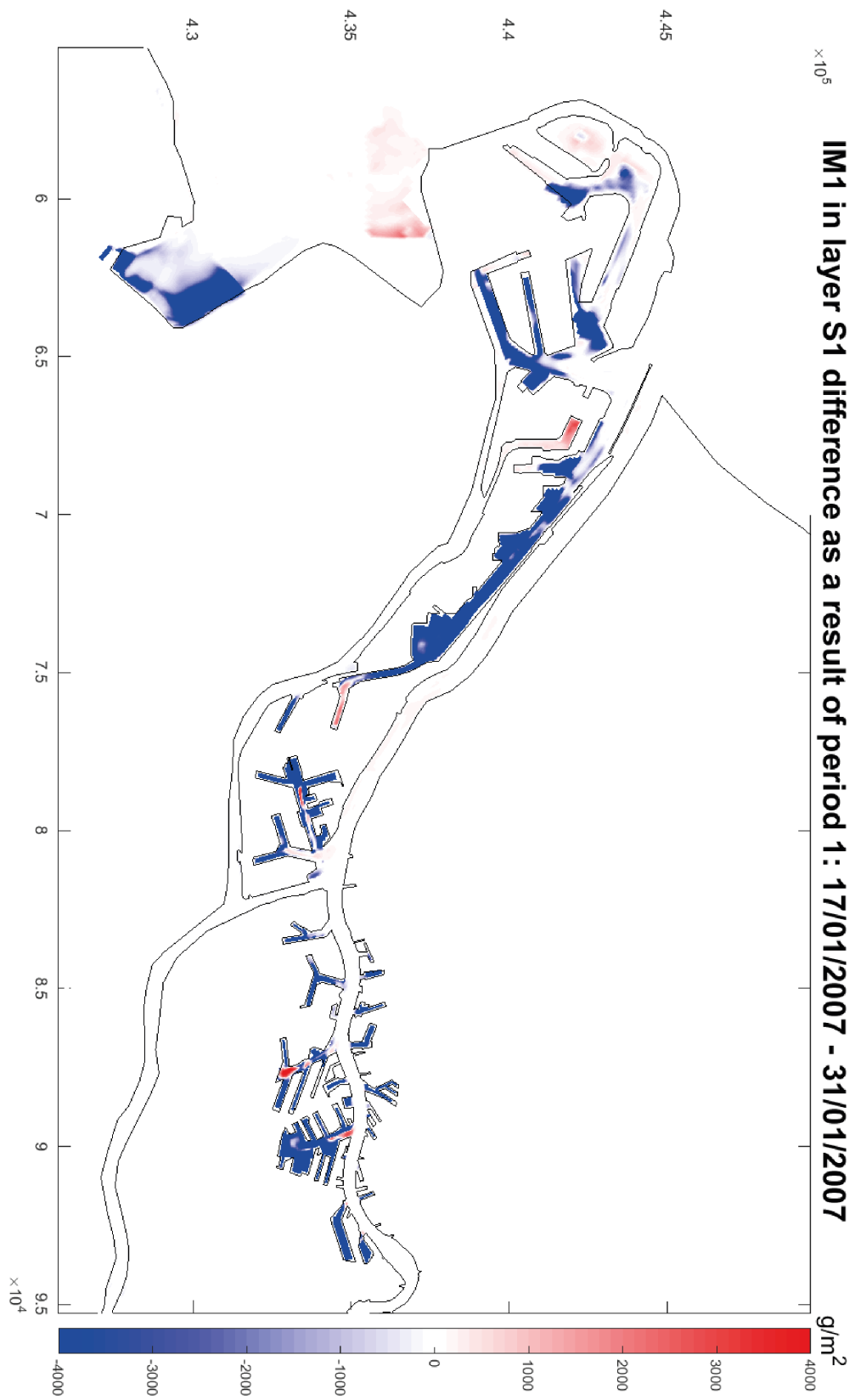


Figure C.1: Difference plot of the concentration of sediment fraction IM1 in bed layer S1 for Period 1. Layer S1 is the most responsive layer of the two, and fraction IM1 is lighter than fraction IM2. As a result, this plot is the most sensitive to bottom shear stresses of this series of plots. Period 1 includes a storm scenario, and as a result there is erosion in virtually all harbour basins. This is an effect of the erroneous wave shear stress assimilation.

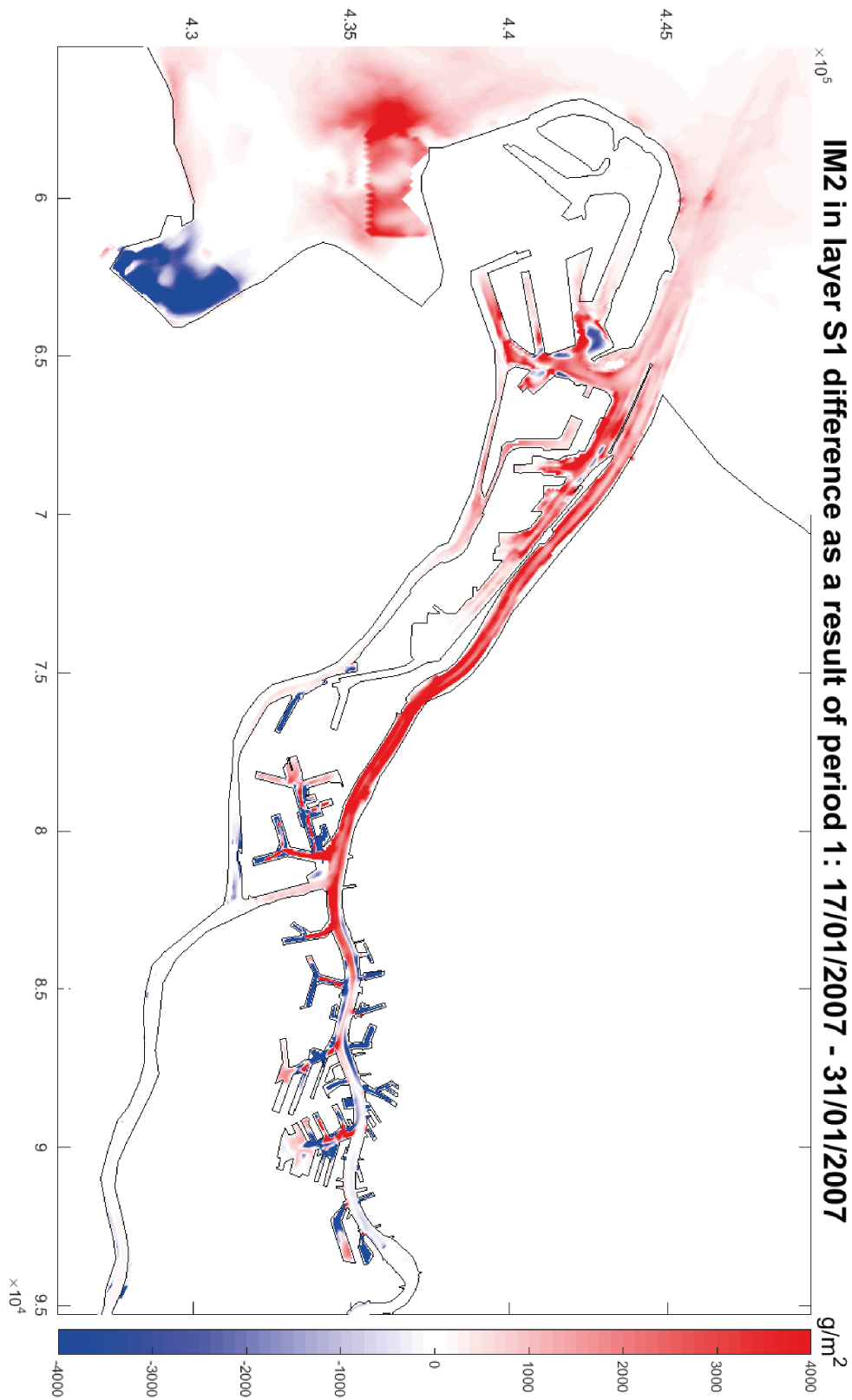


Figure C.2: Difference plot of the concentration of sediment fraction IM2 in bed layer S1 for Period 1. Layer S1 is the most responsive layer of the two, but fraction IM2 has a higher settling velocity than IM1. Sediment is eroded inside the inland harbour basins, and sediment is deposited in the Rotterdam waterway, the basins lining the Maasmond, and at sea. The large amount of deposition in the Rotterdam Waterway contradicts observations. This is a result of the combination of acting and critical shear stresses, and is addressed in sections 6.1 and 6.2.

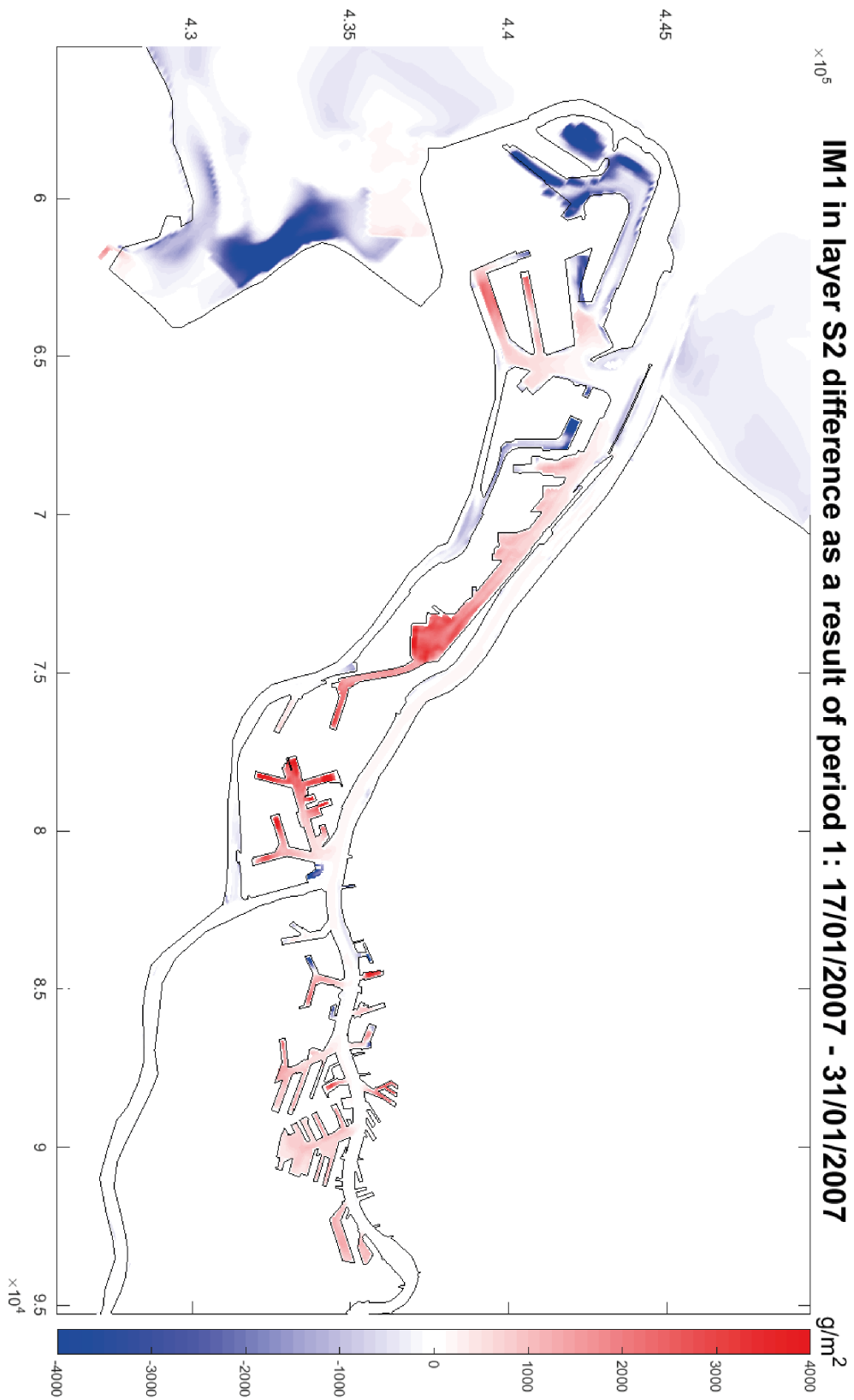


Figure C.3: Difference plot of the concentration of sediment fraction IM1 in bed layer S2 for Period 1. Layer S2 has a higher critical shear stress for resuspension than layer S1, and as a result sediment is deposited rather than eroded. There can be seen to be net erosion at sea and net deposition inside the harbour, which is a desired result of a simulated storm. Maasvlakte 2 forms the exception and shows erosion. This is caused by an error in the wave stress assimilation.

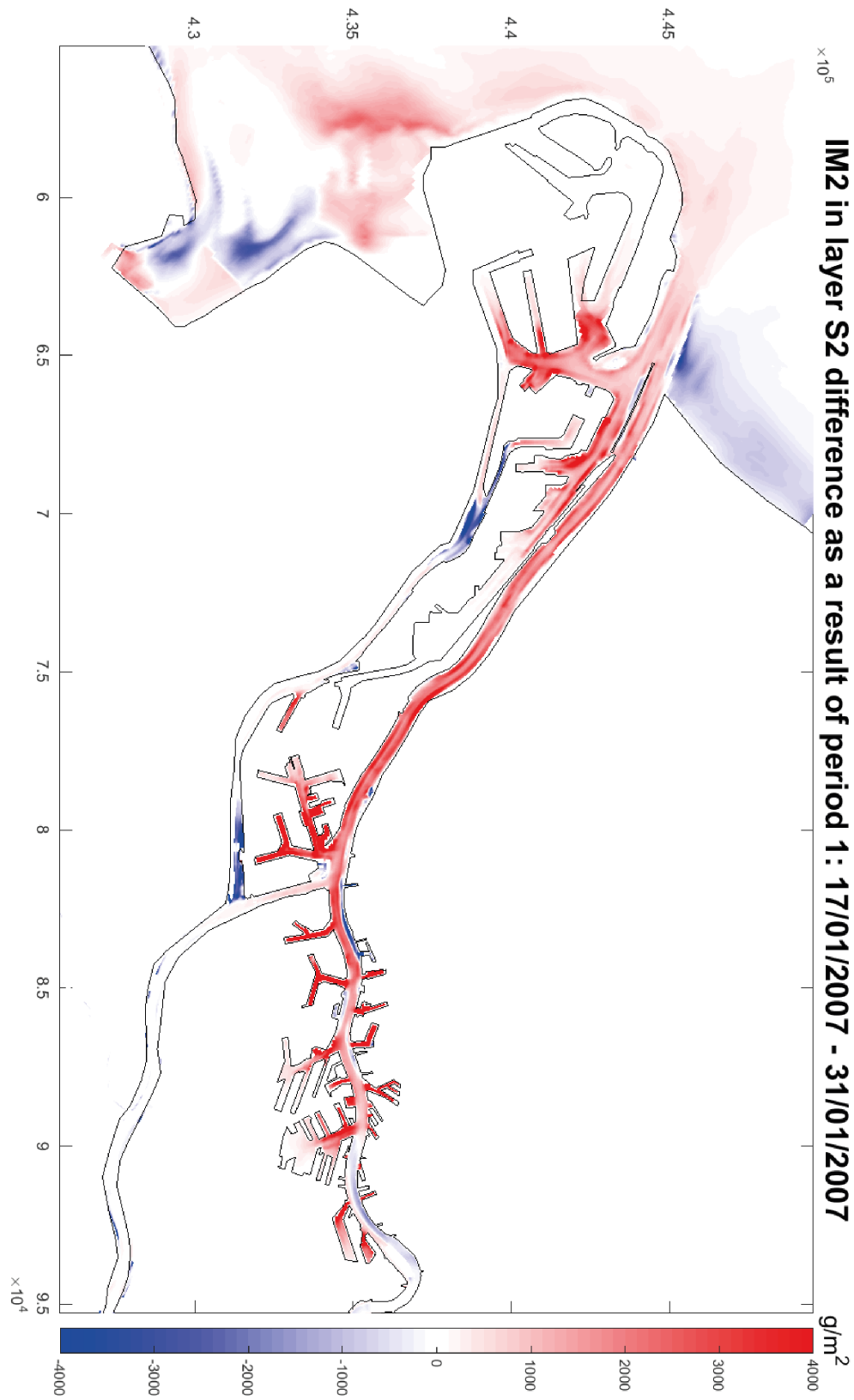


Figure C.4: Difference plot of the concentration of sediment fraction IM2 in bed layer S2 for Period 1. Layer S2 has a higher critical shear stress for resuspension than layer S1, and as a result sediment is deposited rather than eroded. There is a large amount of deposition in the Rotterdam Waterway, which does not correspond to observations. This is a result of the combination of acting and critical shear stresses, and is addressed in sections 6.1 and 6.2.

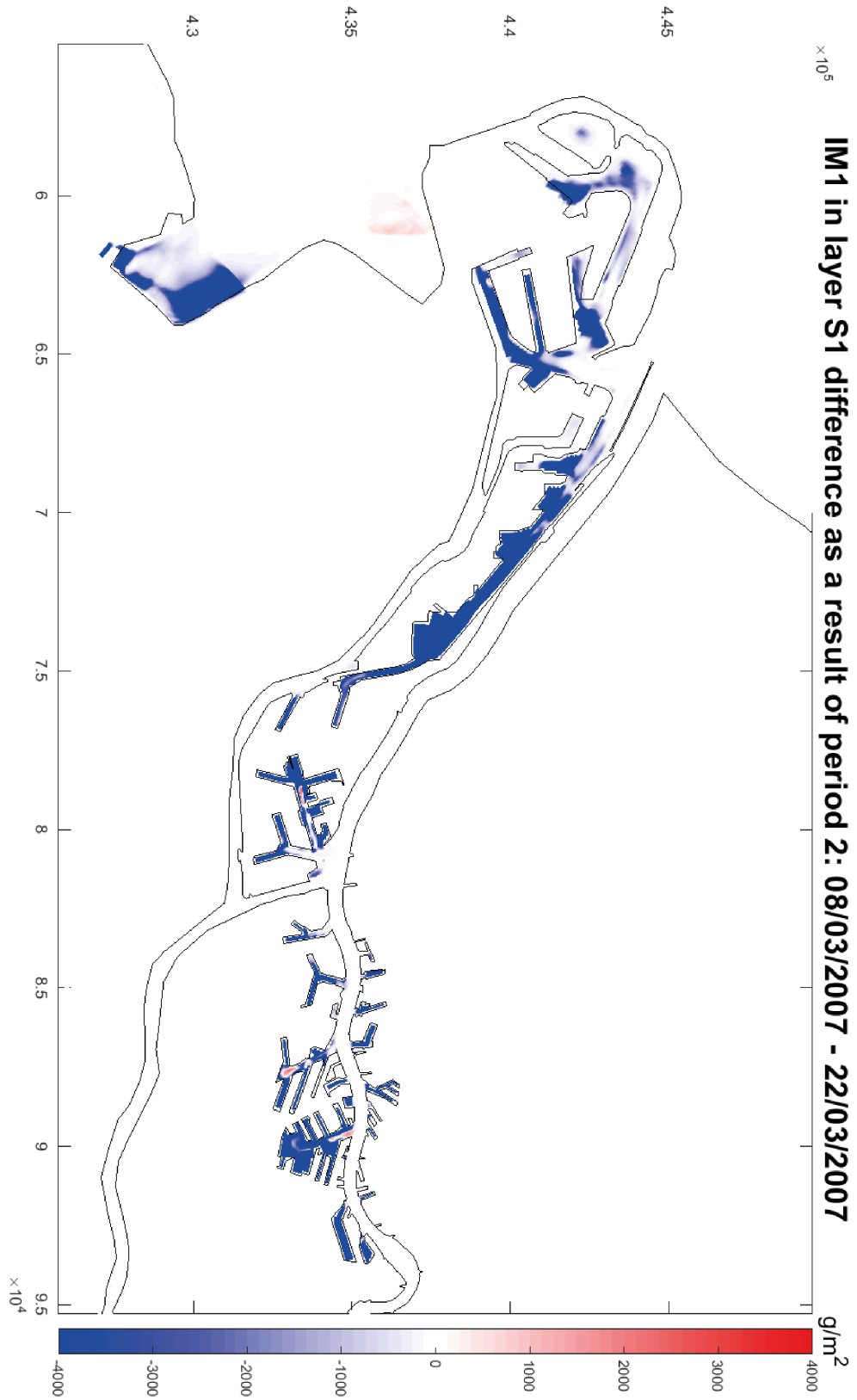


Figure C.5: Difference plot of the concentration of sediment fraction IM1 in bed layer S1 for Period 2. Layer S1 is the most responsive layer of the two, and fraction IM1 is lighter than fraction IM2. As a result, this plot is the most sensitive to bottom shear stresses of this series of plots. There is erosion in virtually all harbour basins. This is an effect of the erroneous wave shear stress assimilation.

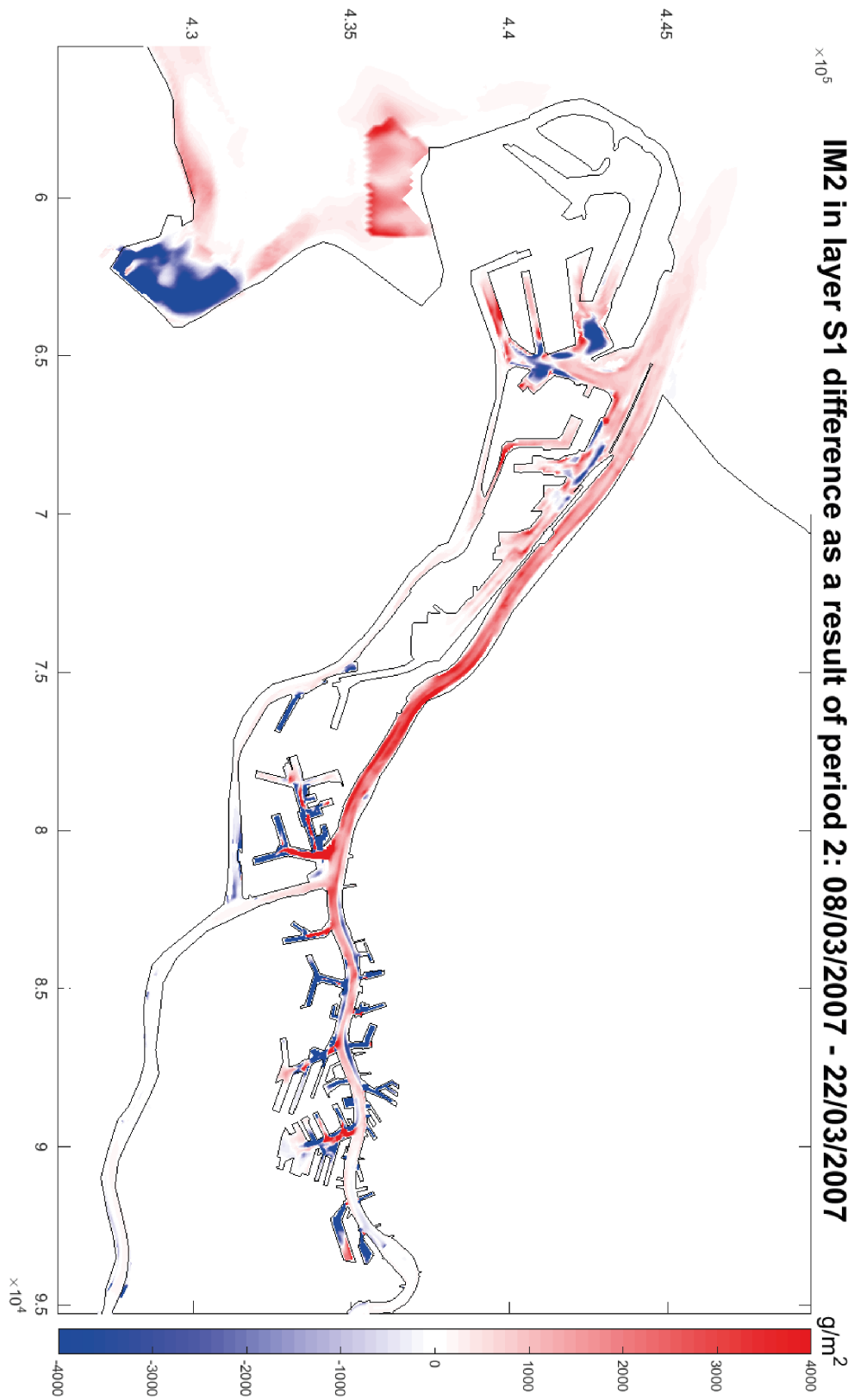


Figure C.6: Difference plot of the concentration of sediment fraction IM2 in bed layer S1 for Period 2. Layer S1 is the most responsive layer of the two, but fraction IM2 has a higher settling velocity than IM1. Sediment is eroded inside the inland harbour basins, and sediment is deposited in the Rotterdam waterway, the basins lining the Maasmond, and at sea. The large amount of deposition in the Rotterdam Waterway contradicts observations. This is a result of the combination of acting and critical shear stresses, and is addressed in sections 6.1 and 6.2.

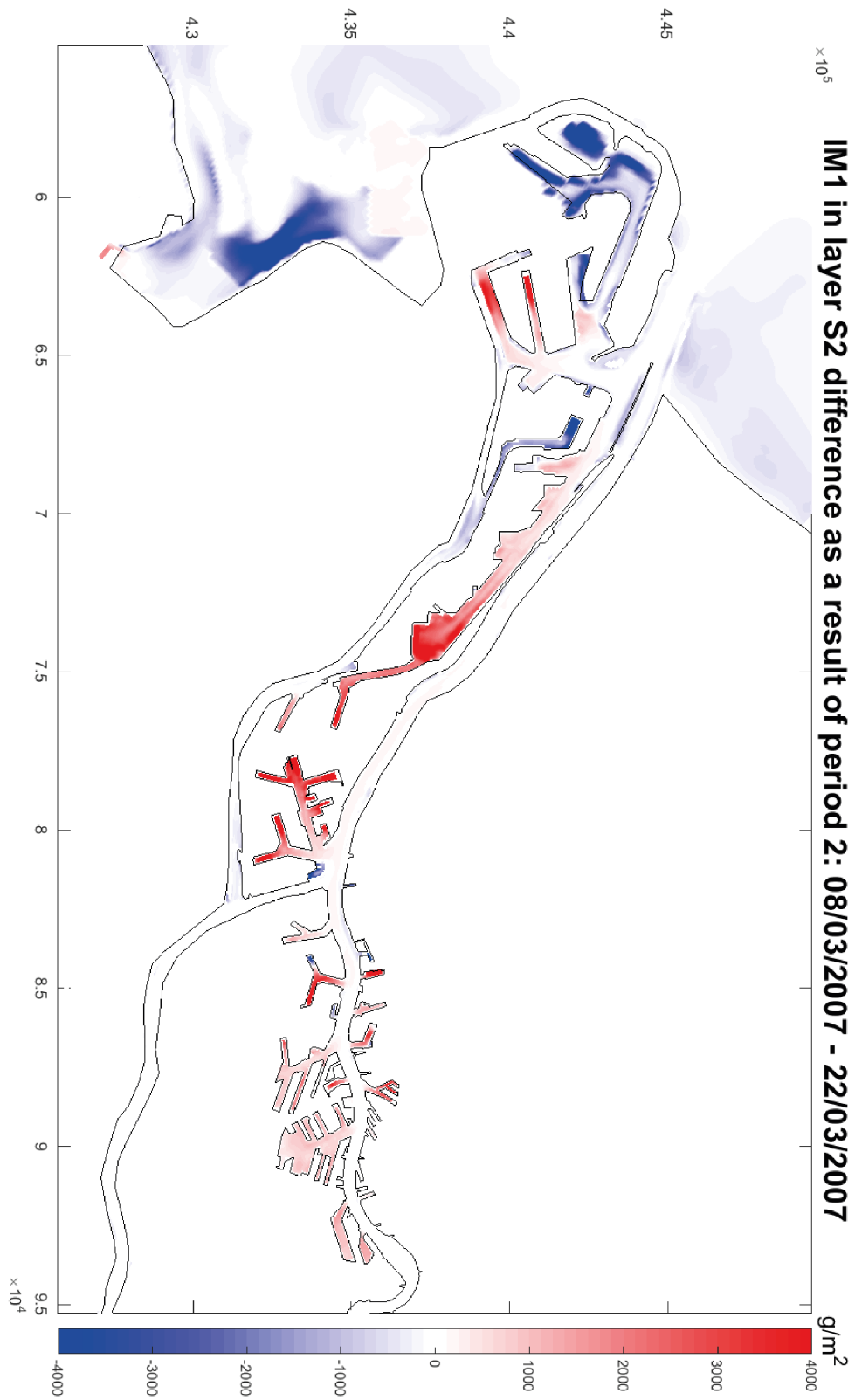


Figure C.7: Difference plot of the concentration of sediment fraction IM1 in bed layer S2 for Period 2. Layer S2 has a higher critical shear stress for resuspension than layer S1, and as a result sediment is deposited rather than eroded. There can be seen to be net erosion at sea and net deposition inside the harbour, which is a consequence of the fact that the modelling scenario includes higher waves than the spin-up period. Maasvlakte 2 forms the exception and shows erosion. This is caused by an error in the wave stress assimilation.

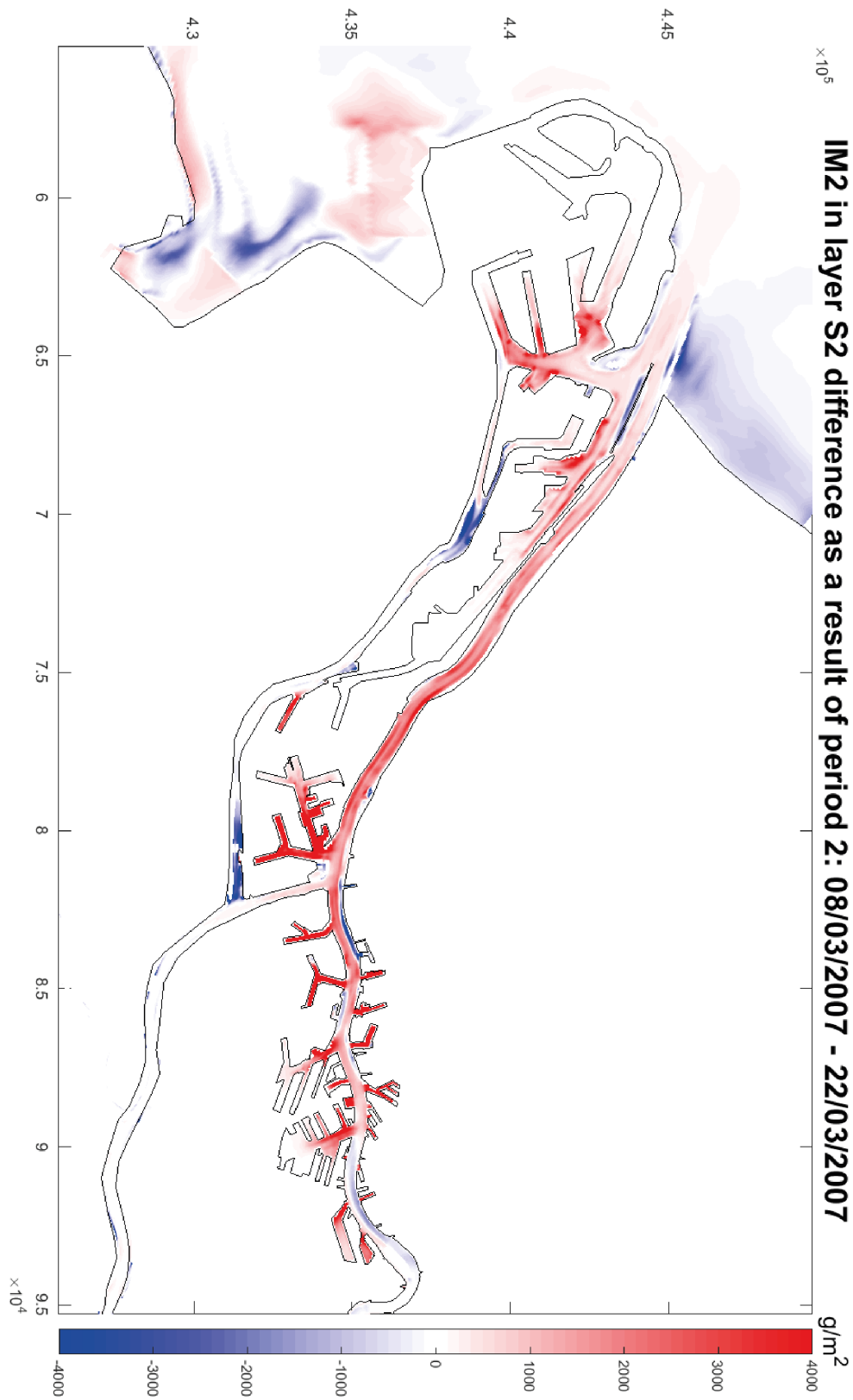


Figure C.8: Difference plot of the concentration of sediment fraction IM2 in bed layer S2 for Period 2. Layer S2 has a higher critical shear stress for resuspension than layer S1, and as a result sediment is deposited rather than eroded. There is a large amount of deposition in the Rotterdam Waterway, which does not correspond to observations. This is a result of the combination of acting and critical shear stresses, and is addressed in sections 6.1 and 6.2.

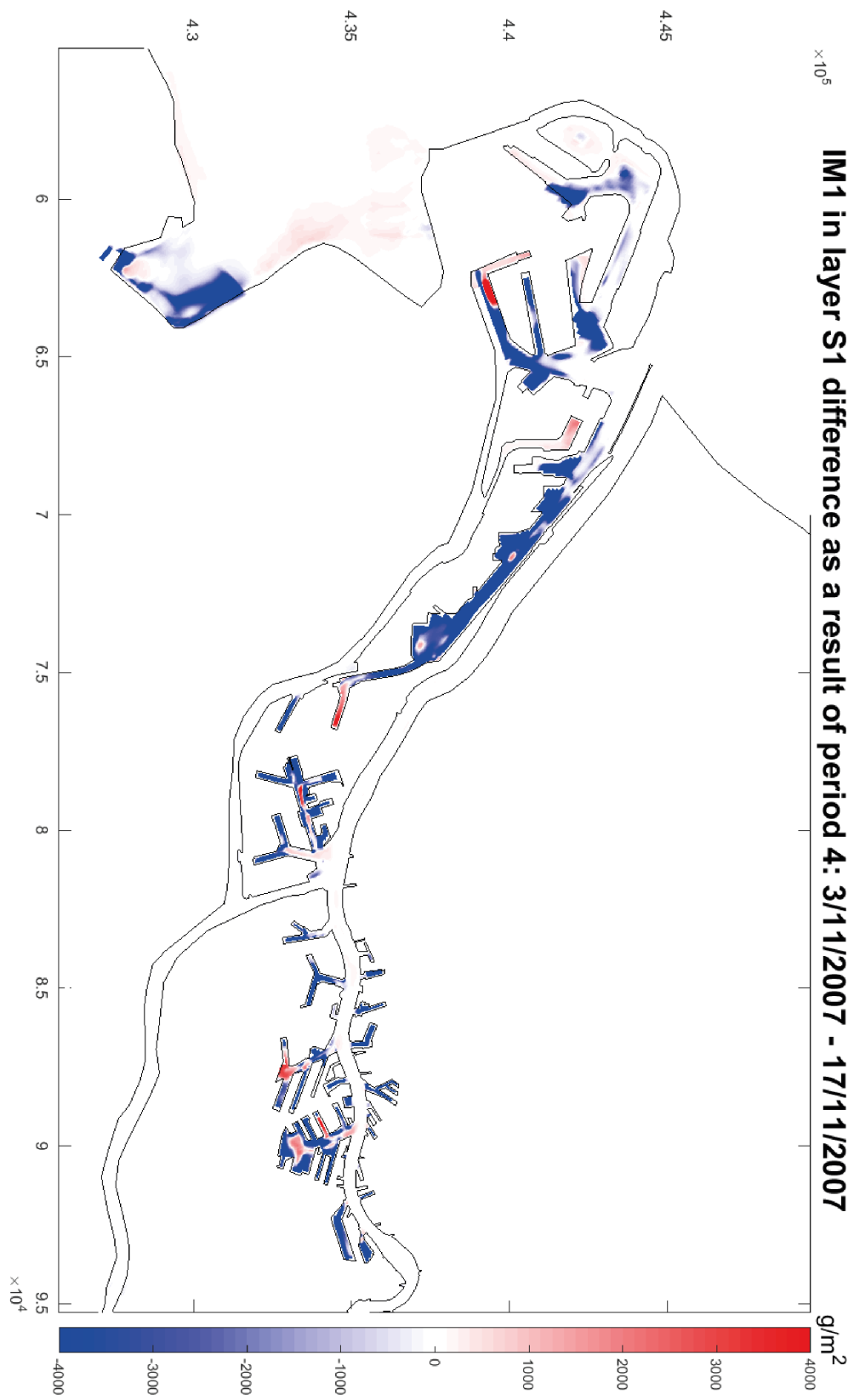


Figure C.9: Difference plot of the concentration of sediment fraction IM1 in bed layer S1 for Period 4. Layer S1 is the most responsive layer of the two, and fraction IM1 is lighter than fraction IM2. As a result, this plot is the most sensitive to bottom shear stresses of this series of plots. Period 4 includes a storm scenario, and as a result there is erosion in virtually all harbour basins. This is an effect of the erroneous wave shear stress assimilation. There is little deposition at sea, which means the sediment remains in suspension or is advected out of the domain.

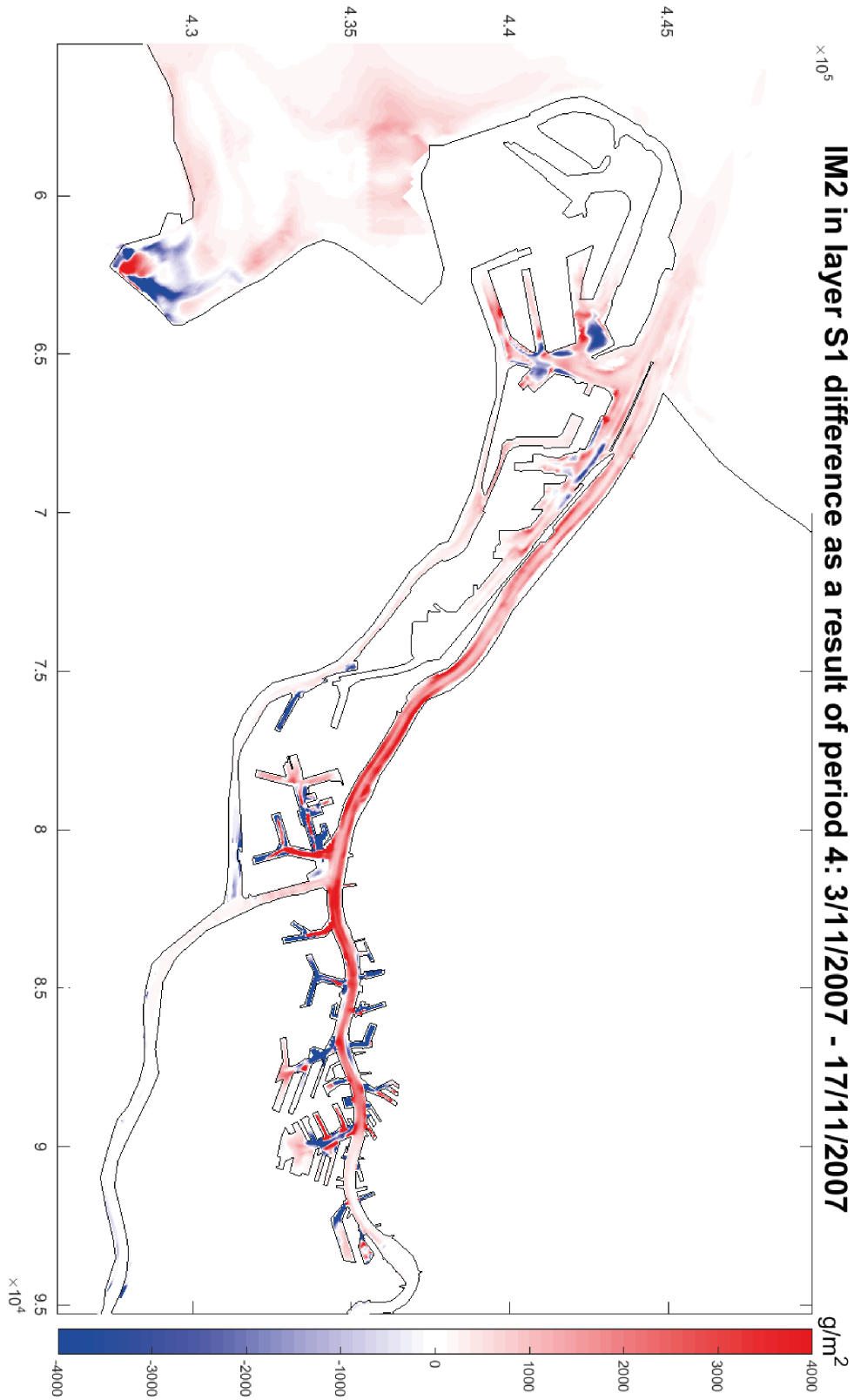


Figure C.10: Difference plot of the concentration of sediment fraction IM2 in bed layer S1 for Period 4. Layer S1 is the most responsive layer of the two, but fraction IM2 has a higher settling velocity than IM1. Sediment is eroded inside the inland harbour basins, and sediment is deposited in the Rotterdam waterway, the basins lining the Maasmond, and at sea. The large amount of deposition in the Rotterdam Waterway contradicts observations. This is a result of the combination of acting and critical shear stresses, and is addressed in sections 6.1 and 6.2.

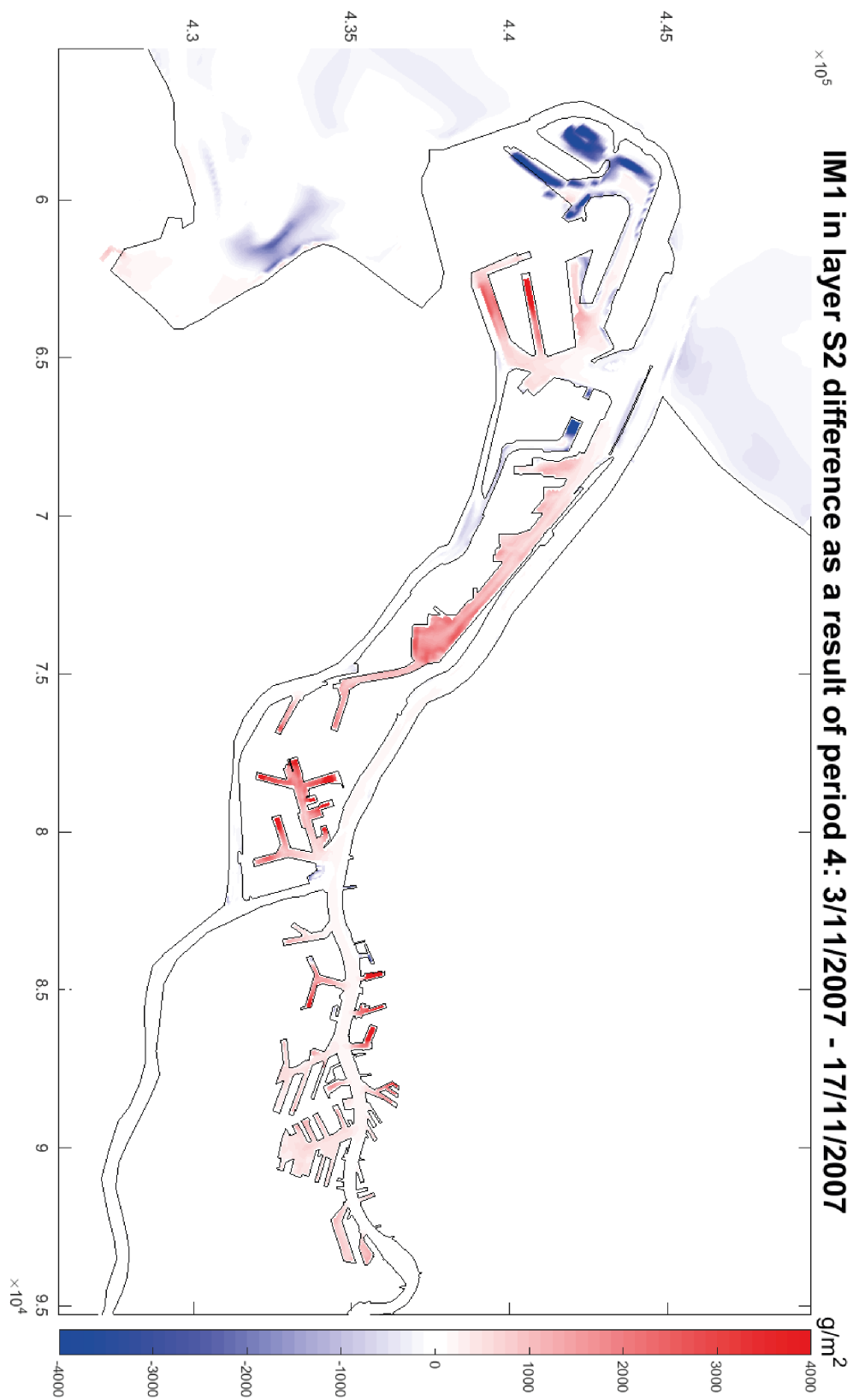


Figure C.11: Difference plot of the concentration of sediment fraction IM1 in bed layer S2 for Period 4. Layer S2 has a higher critical shear stress for resuspension than layer S1, and as a result sediment is deposited rather than eroded. There can be seen to be net erosion at sea and net deposition inside the harbour, which is a consequence of the fact that the modelling scenario includes higher waves than the spin-up period. Maasvlakte 2 forms the exception and shows erosion. This is caused by an error in the wave stress assimilation.

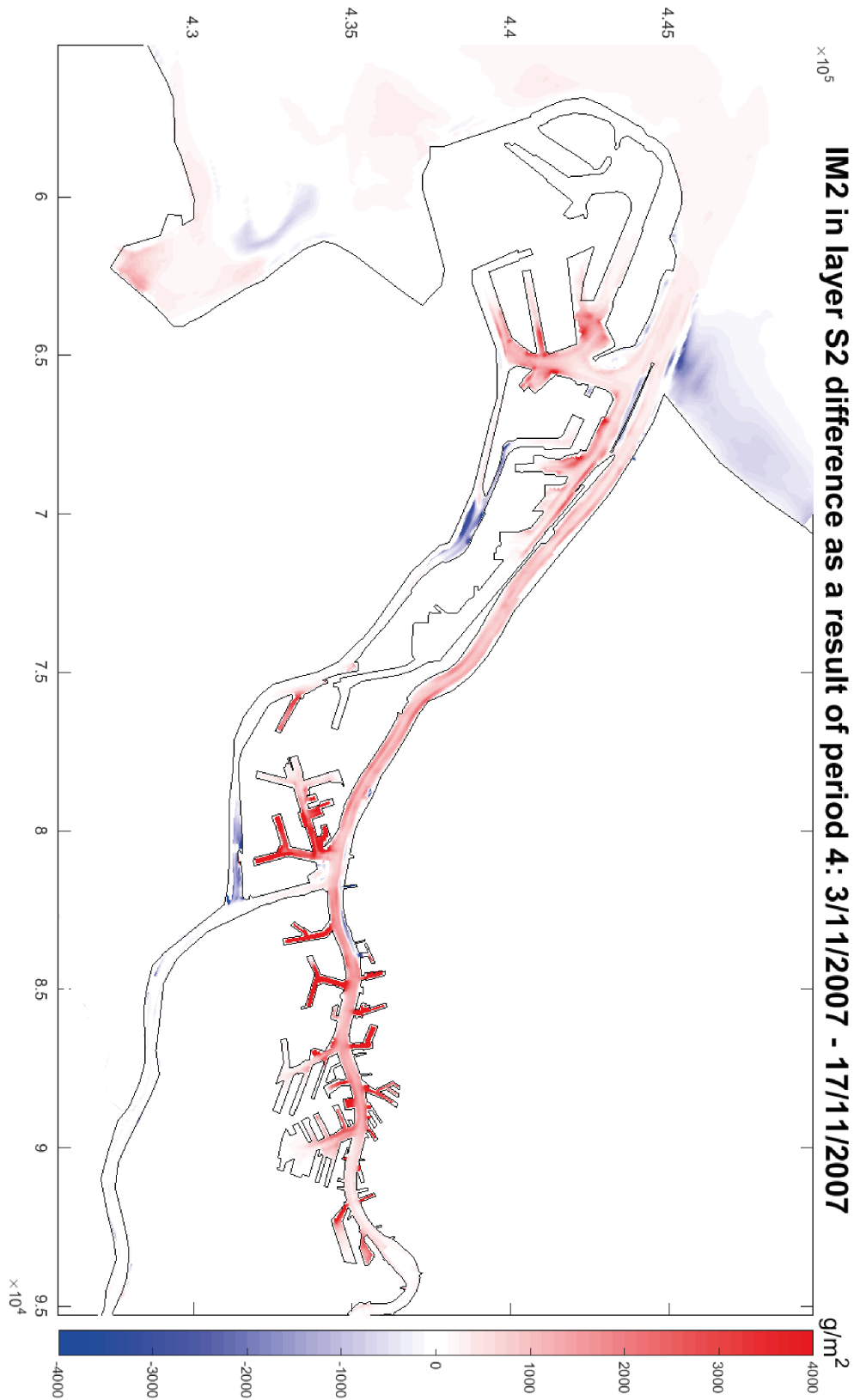


Figure C.12: Difference plot of the concentration of sediment fraction IM2 in bed layer S2 for Period 4. Layer S2 has a higher critical shear stress for resuspension than layer S1, and as a result sediment is deposited rather than eroded. There is a large amount of deposition in the Rotterdam Waterway, which does not correspond to observations. This is a result of the combination of acting and critical shear stresses, and is addressed in sections 6.1 and 6.2.

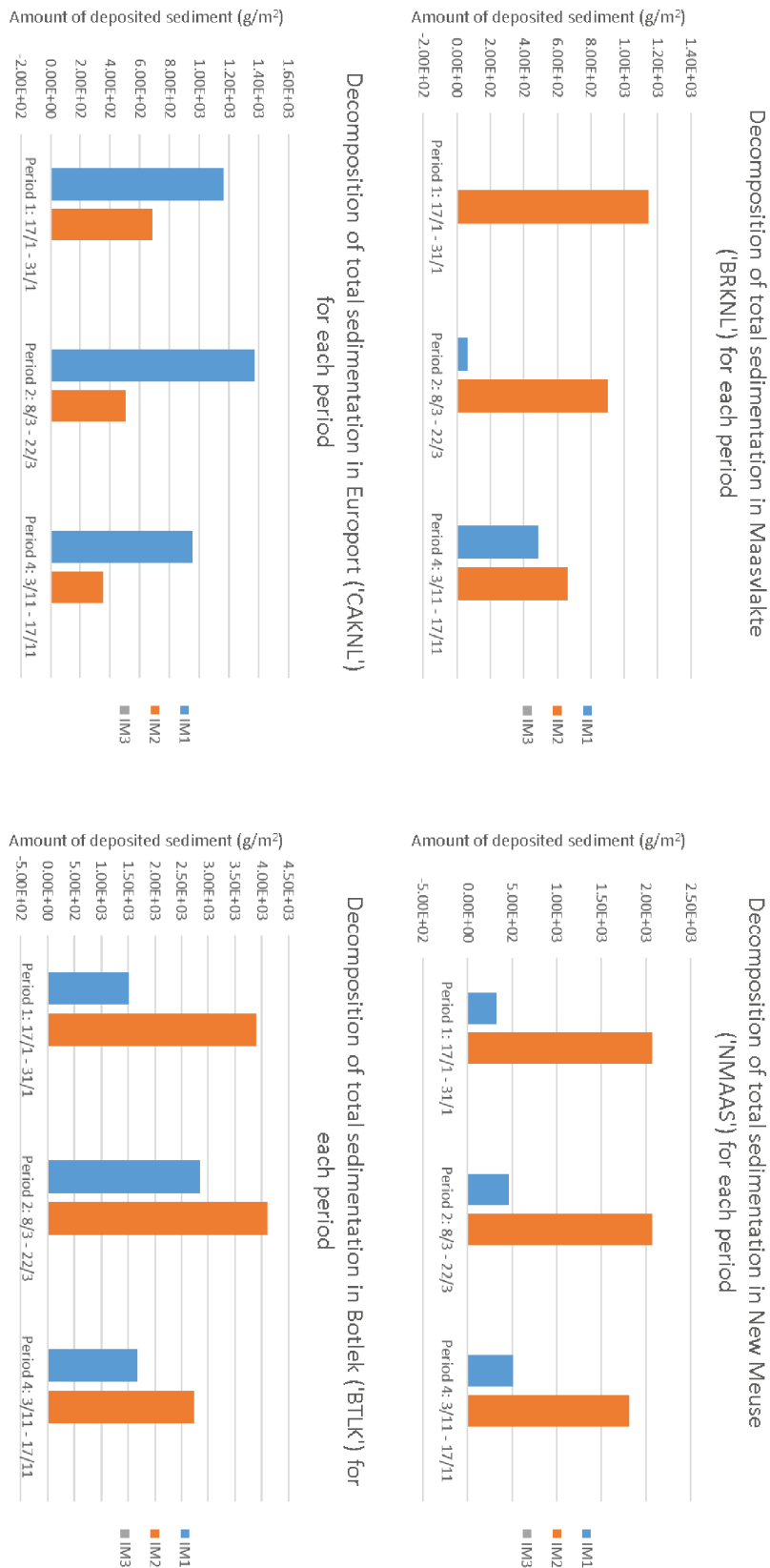


Figure C.13: Decomposition of sedimentation into the different sediment fractions for all periods in the most important harbour basins. In this figure, it can be seen that fraction IM3 plays no role in harbour siltation. Sediment fraction IM2, which has the largest settling velocity, is usually the dominant fraction. The exception is the Caland channel (Europoort), where IM1 dominates.

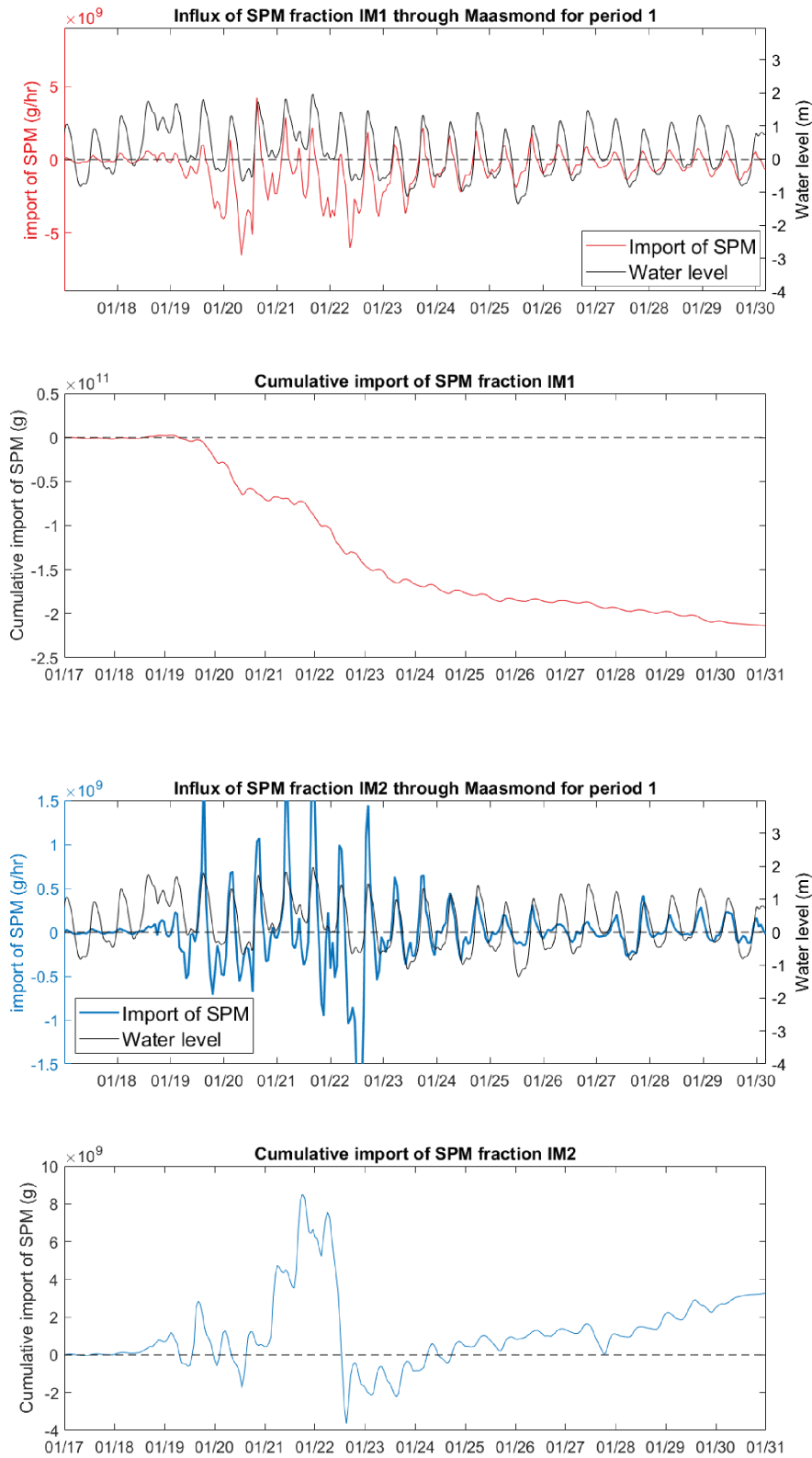


Figure C.14: Import/export of suspended sediment through the Maasmond ('MMD') for period 1, in general, spikes in SPM import correspond to stormy conditions at sea, and IM2 is imported while IM1 is exported.

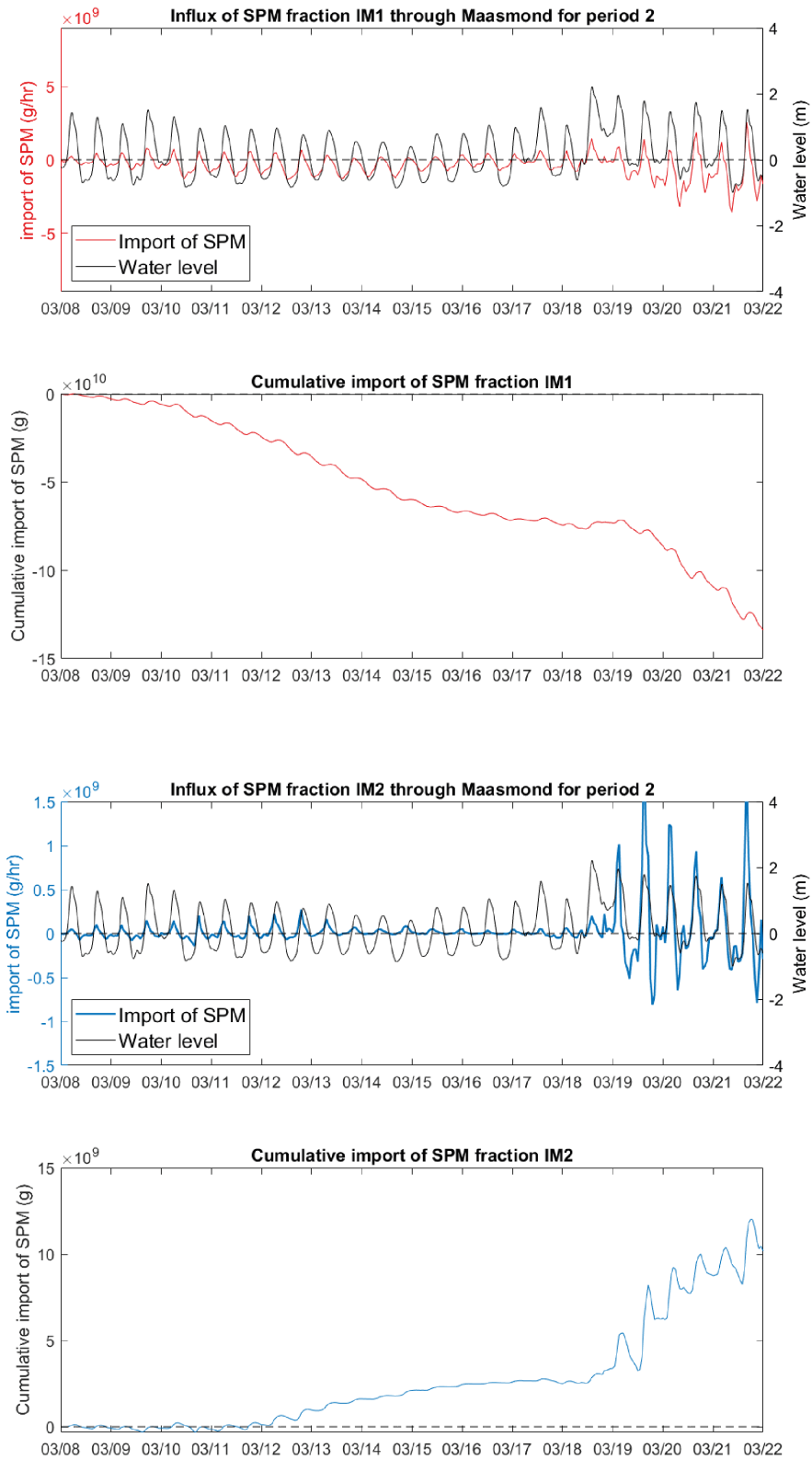


Figure C.15: Import/export of suspended sediment through the Maasmond ('MMD') for period 2, in general, spikes in SPM import correspond to stormy conditions at sea, and IM2 is imported while IM1 is exported.

APPENDIX C. SUPPORTING FIGURES: PLOTS AND CHARTS RELATING TO HARBOUR SEDIMENTATION

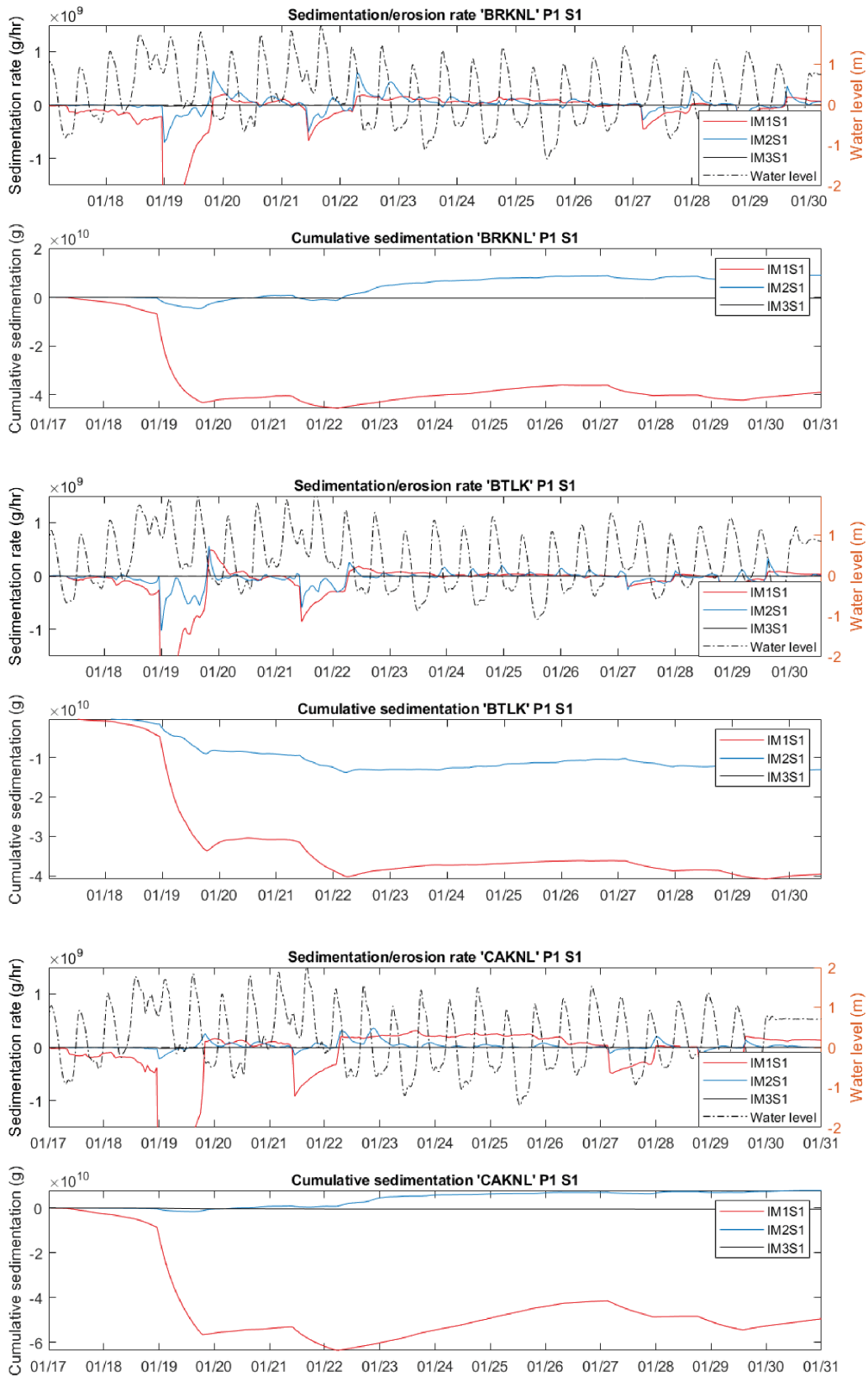


Figure C.16: Time development of sedimentation in layer S1 for three observation areas for Period 1.

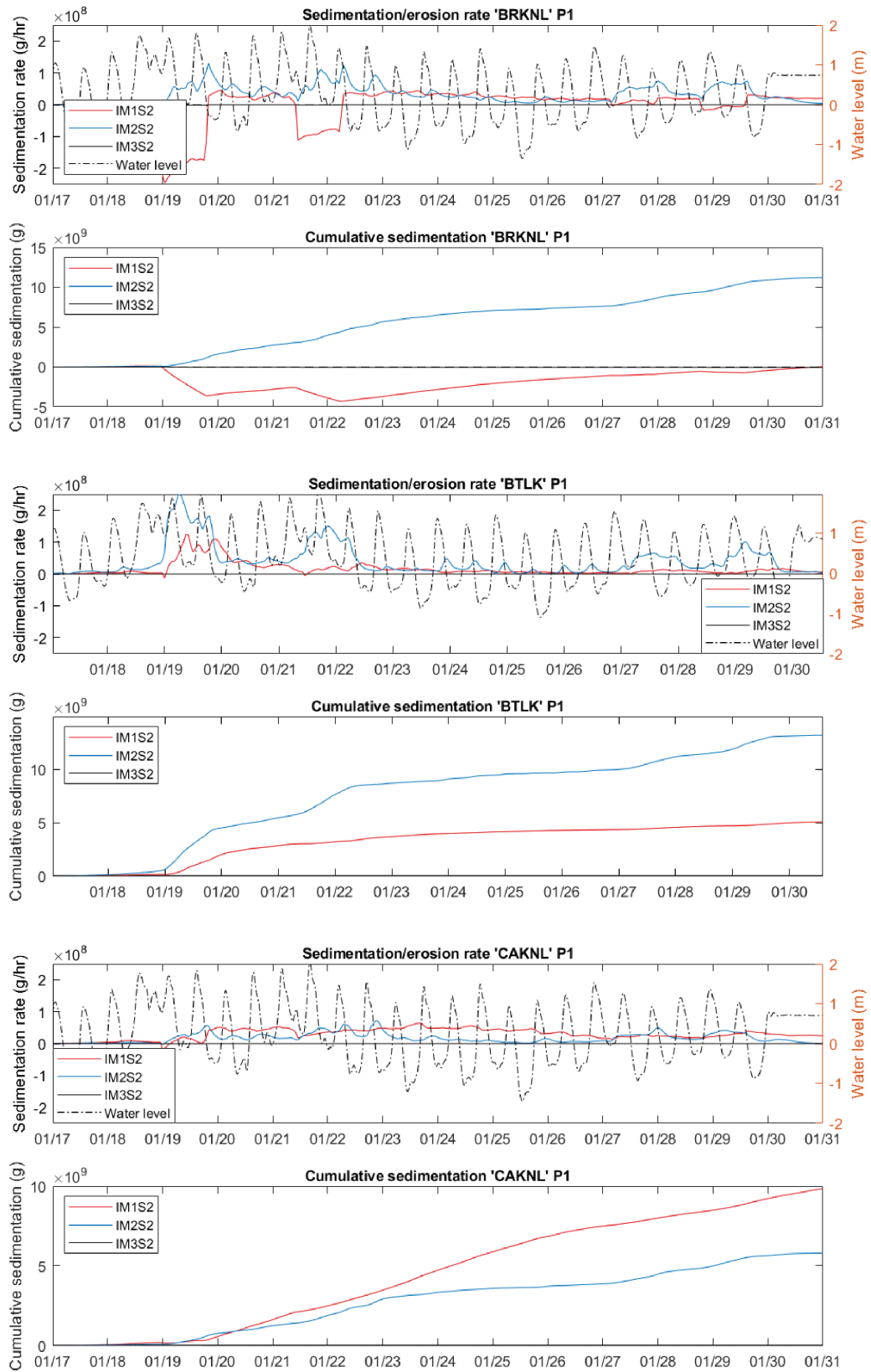


Figure C.17: Time development of sedimentation for three observation areas in layer S2 for Period 1.

APPENDIX C. SUPPORTING FIGURES: PLOTS AND CHARTS RELATING TO HARBOUR SEDIMENTATION

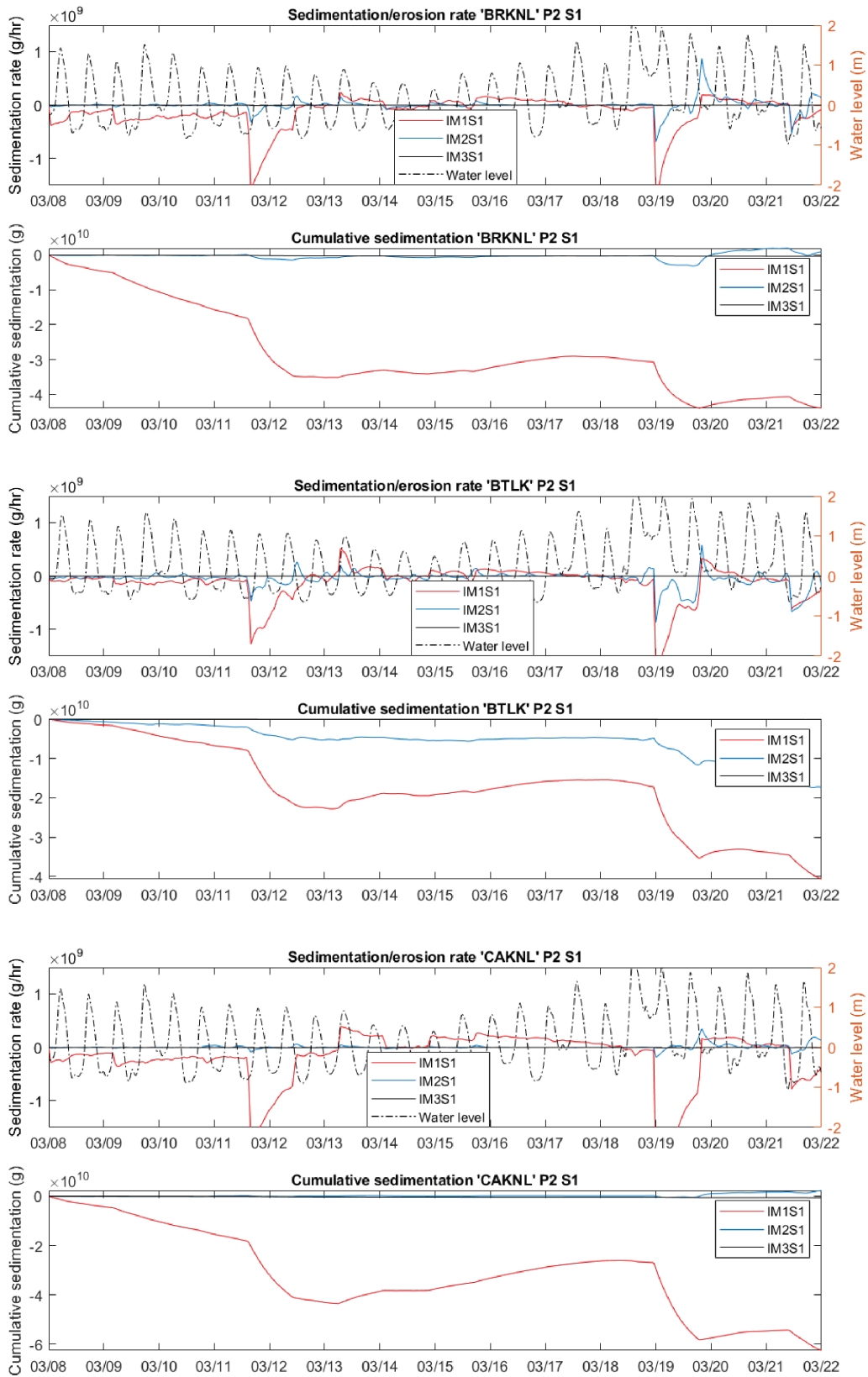


Figure C.18: Time development of sedimentation for three observation areas in layer S1 for Period 2.

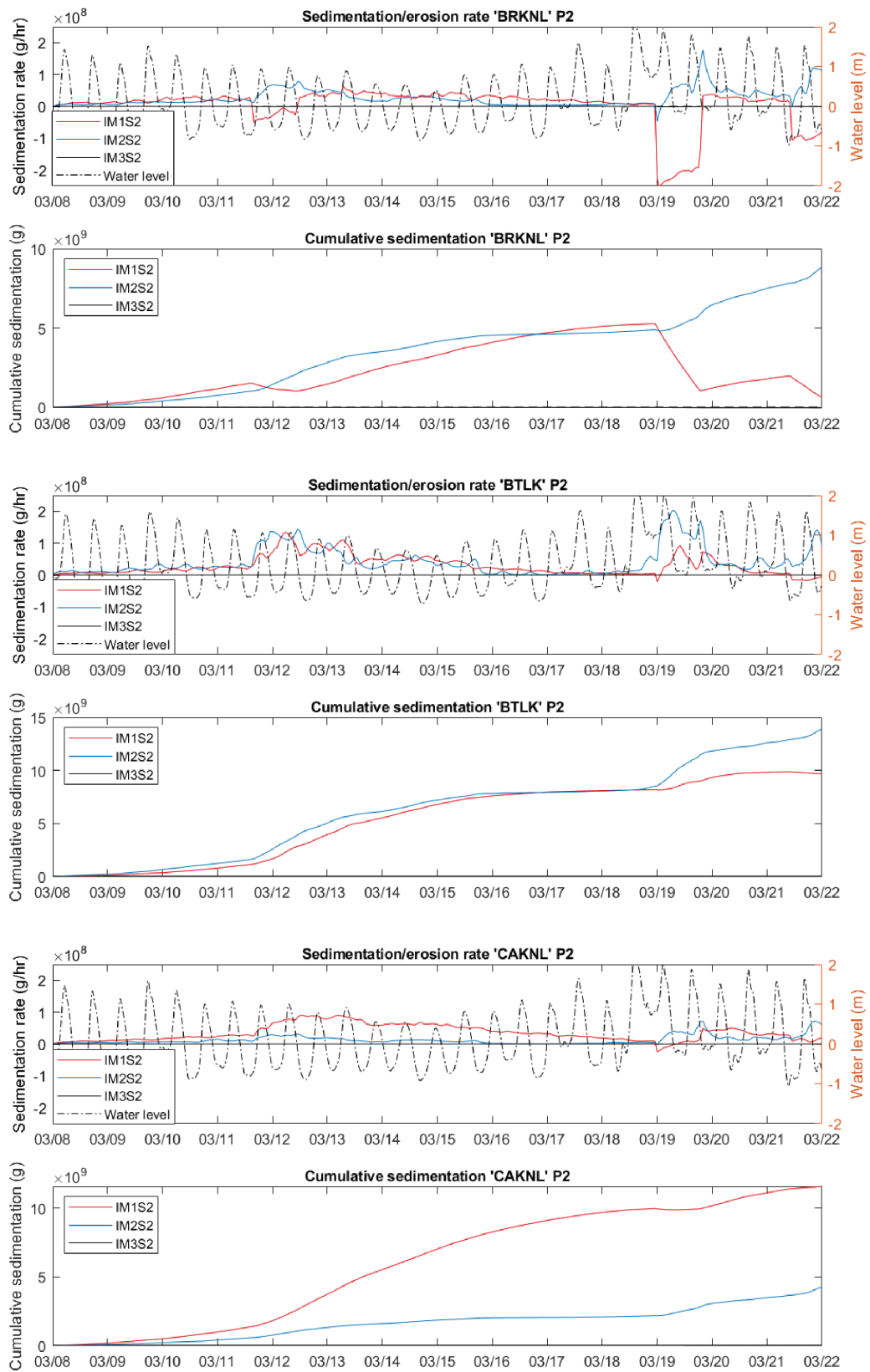


Figure C.19: Time development of sedimentation for three observation areas in layer S2 for Period 2.

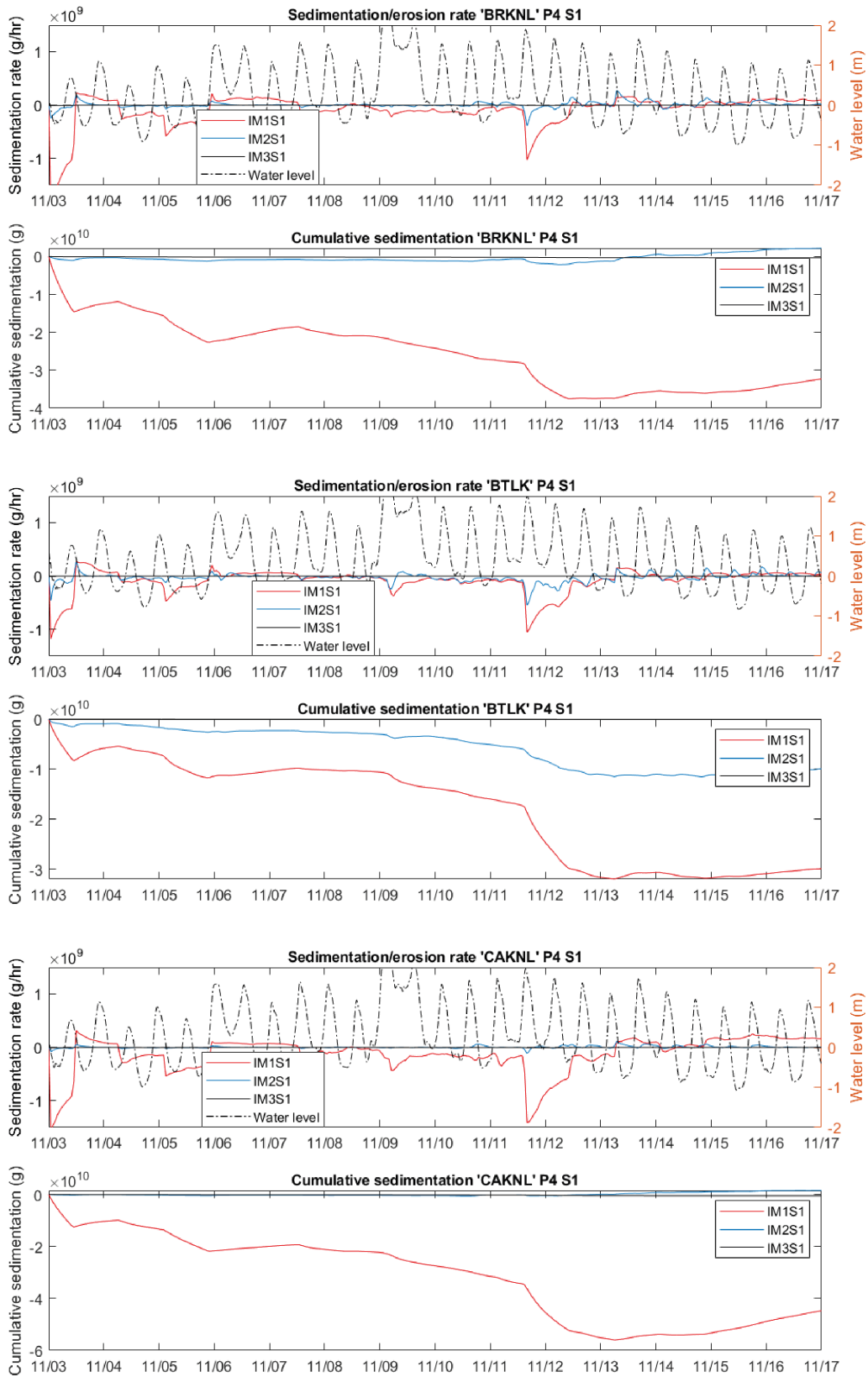


Figure C.20: Time development of sedimentation for three observation areas in layer S1 for Period 4.

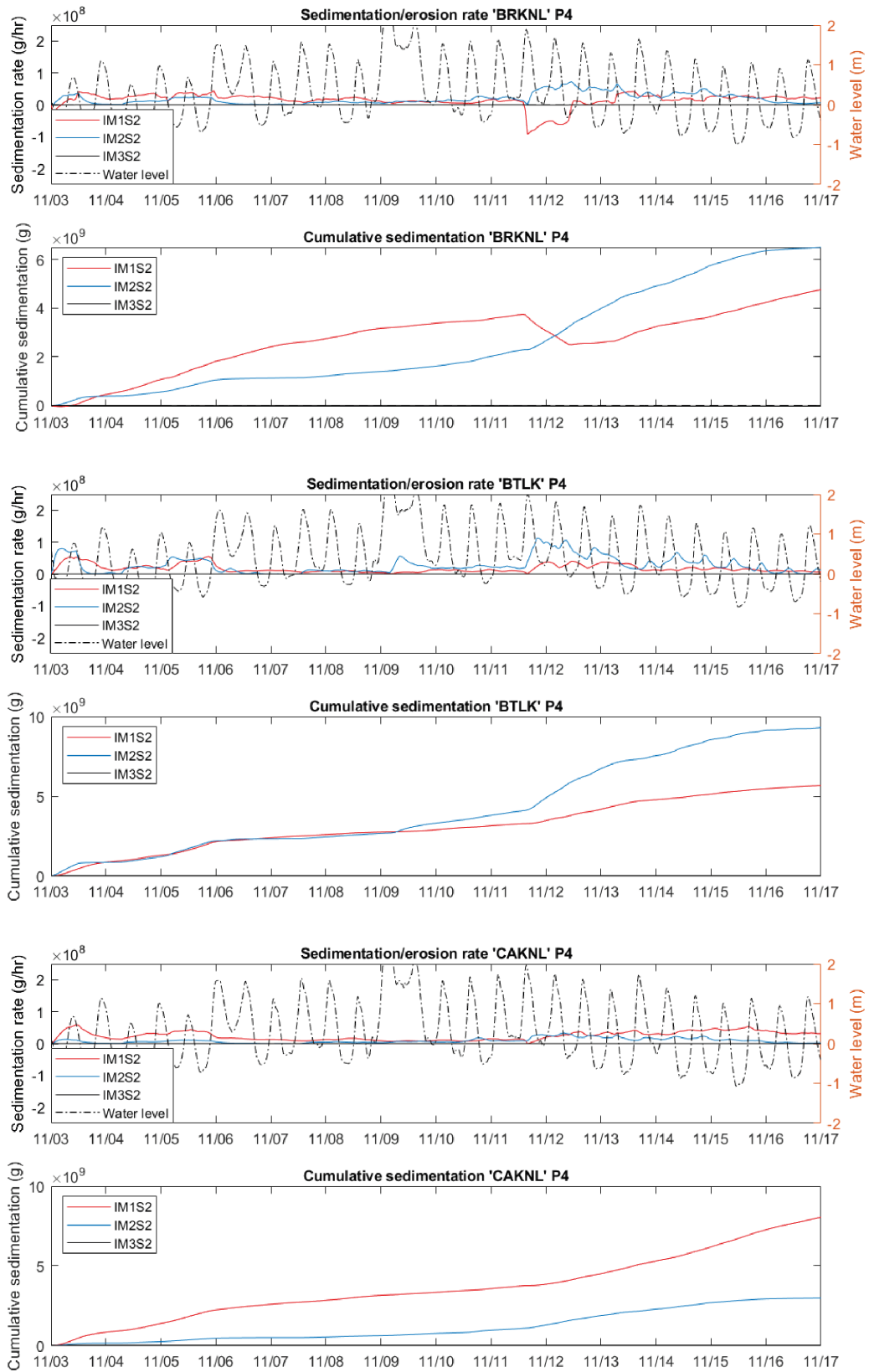


Figure C.21: Time development of sedimentation for three observation areas in layer S2 for Period 4.

# Appendix D

## Mathematical model description

*This appendix provides a mathematical description of the hydrodynamic and sediment models used in this thesis.*

### D.1 Hydrodynamic equations

In this thesis, the hydrodynamics are resolved with Delft3D-FLOW and SIMONA. Both packages resolve the Reynolds Averaged Navier-Stokes (RANS) equations, under a number of assumptions.

- Boussinesq approximation: it is assumed that density differences in the horizontal direction are small with respect to the density itself. This allows for the density terms appearing in the horizontal momentum equations to be replaced by a constant reference density  $\rho_0$ .
- Hydrostatic assumption: it is assumed that the flow is hydrostatic. This allows the vertical momentum equation to be reduced to the hydrostatic balance equation.
- F-plane approximation: the Coriolis parameter is assumed constant for the given latitude.
- Turbulence closure: Turbulence is resolved by computing a turbulent eddy viscosity. This method leans on the Boussinesq hypothesis, which states that turbulent stresses are similar to viscous stresses, but with a turbulent eddy viscosity instead of molecular viscosity. Vertical turbulent eddy viscosities have been resolved with the  $\kappa - \epsilon$  turbulence closure model, while horizontal viscosities are applied by a user defined background diffusivity and viscosity.
- Incompressibility: water is assumed to be incompressible. This removes the water density from the continuity equation.

The derivation of the RANS equations and approximations is not presented here, but may be found in many textbooks on environmental fluid mechanics. For this section, (Deltares, 2018c) has been consulted. The result is presented below for a Cartesian reference frame.

Momentum equations in X,Y, and Z direction:

$$\frac{\partial u}{\partial t} + \frac{\partial u^2}{\partial x} + \frac{\partial uv}{\partial y} + \frac{\partial uw}{\partial z} - fv + \frac{1}{\rho_0} \frac{\partial p}{\partial x} - 2\nu_h \frac{\partial^2 u}{\partial x^2} - \frac{\partial}{\partial z} \left( \nu_t \frac{\partial u}{\partial z} \right) = S_x \quad (\text{D.1})$$

$$\frac{\partial v}{\partial t} + \frac{\partial vu}{\partial x} + \frac{\partial v^2}{\partial y} + \frac{\partial vw}{\partial z} + fu + \frac{1}{\rho_0} \frac{\partial p}{\partial x} - 2\nu_h \frac{\partial^2 v}{\partial y^2} - \frac{\partial}{\partial z} \left( \nu_t \frac{\partial v}{\partial z} \right) = S_y \quad (\text{D.2})$$

$$\frac{\partial p}{\partial z} = -\rho g \quad (\text{D.3})$$

Continuity equation:

$$\frac{\partial u}{\partial x} + \frac{\partial v}{\partial y} + \frac{\partial w}{\partial z} = 0 \quad (\text{D.4})$$

with:

- t: Time
- u: Velocity in X direction
- v: Velocity in Y direction
- w: Velocity in Z direction
- f: Coriolis parameter
- $\rho$ : Water density
- $\rho_0$ : Reference water density
- p: Pressure
- $\nu_t$ : Turbulent eddy viscosity
- $\nu_h$ : Horizontal turbulent viscosity
- g: gravitational constant
- $S_{x,y}$ : Momentum source terms. These include water discharges, wind stress, and bottom friction.

The flow transports the conserves substances salinity and temperature. This transport is described by a convection-diffusion equation:

$$\frac{\partial S}{\partial t} + \frac{\partial uS}{\partial x} + \frac{\partial vS}{\partial y} + \frac{\partial wS}{\partial z} - 2D_h \left( \frac{\partial^2 S}{\partial x^2} + \frac{\partial^2 S}{\partial y^2} \right) - \frac{\partial}{\partial z} \left( D_t \frac{\partial S}{\partial z} \right) = S_{SS} \quad (\text{D.5})$$

$$\frac{\partial T}{\partial t} + \frac{\partial uT}{\partial x} + \frac{\partial vT}{\partial y} + \frac{\partial wT}{\partial z} - 2D_h \left( \frac{\partial^2 T}{\partial x^2} + \frac{\partial^2 T}{\partial y^2} \right) - \frac{\partial}{\partial z} \left( D_t \frac{\partial T}{\partial z} \right) = \frac{1}{\rho} Q_H + T_{SS} \quad (\text{D.6})$$

With:

- S: Salinity
- T: Temperature
- $D_h$ : Horizontal background diffusivity
- $D_t$ : Turbulent diffusivity
- $S_{SS}$ : Salinity source term
- $T_{SS}$ : Temperature source term
- $Q_H$ : Heating flux source term.

The transport of salinity and heat is important because these concentrations impact the water density term in the vertical momentum equation. Water density is related to temperature and salinity through an equation of state (not presented here). Finally, the total water depth and the location of the free surface may be computed with a depth averaged continuity equation:

$$\frac{\partial \eta}{\partial t} + \frac{\partial \bar{U}H}{\partial x} + \frac{\partial \bar{V}H}{\partial y} = 0 \quad (\text{D.7})$$

Where  $\bar{U}, \bar{V}$  are depth averaged horizontal velocities and  $\eta$  and H respectively represent the water level and water depth.

## D.2 Sediment transport equations

### D.2.1 Suspended transport

The hydrodynamics described in section D.1 forms the driving force of suspended sediment transport. Much like salinity and temperature, suspended sediment is a conserved quantity and may be described by a convection diffusion equation. The difference is that this time the mass of the sediment particles is included through a user defined settling velocity.

$$\frac{\partial C}{\partial t} + \frac{\partial uC}{\partial x} + \frac{\partial vC}{\partial y} + \frac{\partial (w - w_s)C}{\partial z} - 2D_h \left( \frac{\partial^2 C}{\partial x^2} + \frac{\partial^2 C}{\partial y^2} \right) - \frac{\partial}{\partial z} \left( D_t \frac{\partial C}{\partial z} \right) = S_{sed} \quad (\text{D.8})$$

with:

- $C$ : Sediment concentration
- $w_s$ : Sediment settling velocity ( $\mathbf{VSed}$ )
- $S_{sed}$ : Sediment source term

Equation D.8 forms the link between the hydrodynamic forcing and the transport of SPM. Source terms of sediment are dredging/dumping and sedimentation/erosion. Dredging and dumping is not modelled in the current model setup, but can be activated in future simulations. Deposition and erosion are very important for this thesis, and this exchange flux is therefore covered in detail.

### D.2.2 Deposition and erosion

In this section, the following symbols are used. Some of the symbols represent user defined model parameters. These are printed in bold. Their values for the current model setup can be found in Table D.1. Information for this section has been obtained from (Deltares, 2018a) and (van Kessel et al., 2010).

- $D_{S1,IM_i}$ : Deposition flux of sediment fraction  $IM_i$  to bed layer S1
- $D_{2,IM_i}$ : Deposition flux of sediment fraction  $IM_i$  to bed layer S2
- $E_{S1,IM_i}$ : Erosion flux of sediment fraction  $IM_i$  to bed layer S1
- $E_{2,IM_i}$ : Erosion flux of sediment fraction  $IM_i$  to bed layer S2
- $\alpha_{IM_i}$ : **FrIM1SedS2**, **FrIM2SedS2**, and **FrIM3SedS2**
- $C_{IM_i}$ : Concentration of sediment fraction  $IM_i$
- $M_{i,1}$ : Mass of sediment fraction  $IM_i$  in layer S1 per surface area
- $M_{i,2}$ : Mass of sediment fraction  $IM_i$  in layer S2 per surface area
- $\tau$ : Acting bottom shear stress
- $\tau_{c,S1}$ : **TaucRS1IM1**, **TaucRS1IM2**, and **TaucRS1IM3**
- $F_{ResPup}$ : van Rijn (1993) pickup factor from layer S2
- $\rho_s$ : **RHOSAND**
- $s$ :  $\frac{\rho_s}{\rho_w}$
- $g$ : **GRAV**
- $D_{50}$ : **GRAIN50**
- $\tau_{shields}$ : **TauShields**
- $\nu$ : **KinViscos**
- $PorS2$ : Volumetric porosity of the (sandy) sediment bed S2
- $\tau_{tot}$ : Total bottom shear stress
- $\tau_{flow}$ : Current induced bottom shear stress
- $\tau_{wave}$ : Wave induced bottom shear stress
- $Flow_{i,j}$ : Discharge through cell face i,j
- $Area_{i,j}$ : Area of cell face i,j
- $Veloc$ : Total horizontal velocity
- $\rho_w$ : **RhoWater**
- $C$ : Chèzy coefficient
- $H$ : Total depth of water column
- $n$ : **Manncoef**

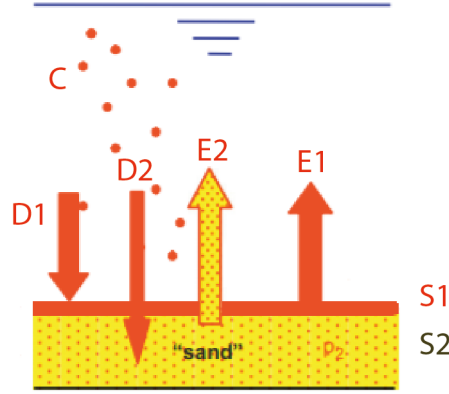


Figure D.1: Overview of the bed schematization used in the sediment model. The sediment bed consists of a transient fluff layer S1 on top of a sandy matrix S2 in which fine sediment is stored. The S1 layer is easily eroded and deposited. The S2 layer responds much slower, and erodes during highly energetic conditions. The release of fines of this layer is governed by the movement of sand from this layer. Image obtained from (van Kessel et al., 2010).

Erosion and deposition are modelled through a schematized sediment bed, and a number of erosion and deposition fluxes between the bed and the sediment concentrations in the lowest sigma layer of the water column (12<sup>th</sup> in this setup). The exchange fluxes are described by an adaptation of (van Kessel et al., 2010) which was obtained through internal communication with Deltares. The sediment bed is modelled as a sandy bed (layer S2) containing fine sediment in its pores, and a thin layer of mud which deposits on top of the sand bed during low energetic conditions (layer S1), and which can easily be eroded. The two bed layers each have their own erosion and deposition fluxes, creating a total of four sediment fluxes for each sediment fraction between the bed and the water column (and 12 fluxes in total for three sediment classes). The two layers and their fluxes have been schematized in Figure D.1.

The exchanges between the short term S1 layer and the bed are described by a modified form of the well known Partheniades and Krone formulations ((Partheniades, 1962) and (Krone, 1962), as cited in (Deltares, 2018b)), which are based on the concept that erosion and deposition of fine sediment scale with the difference between the acting and critical bottom shear stresses. However, no critical shear stress for deposition was applied in this model configuration, such that the critical shear stress for resuspension governs the exchange between the bed and the water column. For the erosion flux, the excess bottom shear stress is multiplied by a first order resuspension rate ( $V_{Res,IM_i}$  until the water column is saturated. The erosion and deposition fluxes from layer S1 are given by Equation D.10 and Equation D.9 respectively:

$$D_{S1,IM_i} = (1 - \alpha_{IM_i}) \mathbf{V}_{Sed,IM_i} C_{IM_i} \quad (D.9)$$

$$E_{S1,IM_i} = \min(\mathbf{Z}_{Res,IM_i}, \mathbf{V}_{Res,IM_i,1} M_i) \left( \frac{\tau_{tot}}{\tau_{c,S1}} - 1 \right) \quad (D.10)$$

The deeper bed layer S2 is schematized as a porous sandy bed into which fines may become trapped. The release of fine sediment from layer S2 is therefore controlled by the mobilization of sand. For that reason, the critical shear stress is set at the mobilization threshold of sand, and a van Rijn type of pickup function for sand is applied to schematize the erosion of fines. The amount of fine sediment that can be stored in layer S2 is controlled by the thickness (ThickS2 in Table D.1), the porosity (PorS2 in Table D.1), and the density (Rhosand in Table D.1) of the layer. The sedimentation and erosion fluxes are given by Equation D.11 and Equation D.12 respectively.

$$D_{2,IM_i} = \alpha_{IM_i} V_{Sed,IM_i} C_{IM_i} \quad (D.11)$$

$$E_{2,IM_i} = f_{IM_iS2} F_{ResPup} \rho_s ((s-1)gD_{50})^{0.5} D_*^{0.3} \left( \frac{\tau_{tot}}{\tau_{shields}} - 1 \right)^{1.5} \quad (D.12)$$

Where  $D_*$  is defined as:

$$D_* = D_{50}((s-1)g/\nu^2)^{1/3} \quad (D.13)$$

$f_{IM_iS1}$  is the fraction of fine sediment present in the bed (which is composed of sand and fines). It is defined as:

$$f_{IM_iS1} = \frac{M_{i,2}}{\mathbf{ThickS2}(1 - \mathbf{PorS2})\rho_{sand}} \quad (D.14)$$

On the North Sea, the storage capacity of fines in the sandy seabed is controlled by a mixing depth over which sandy material can be mobilized by the hydrodynamic conditions and fines can be entrained. This is modelled by a user specified parameter **ThickS2**, which represents the thickness of bed layer S2.

### D.2.3 Calculation of bottom shear stresses

The erosion and deposition of sediment is largely controlled by the acting bottom shear stresses. The total bottom shear stress is computed through a scalar addition of the wave induced bottom shear stresses and the velocity induced bottom shear stresses (Equation D.15).

$$\tau_{tot} = \tau_{flow} + \tau_{wave} \quad (D.15)$$

Here,  $\tau_{wave}$  has been computed independently through a wave buoy assimilation technique.  $\tau_{flow}$  is computed from the hydrodynamics. However, the hydrodynamic input of Delft3D WAQ is in the form of discharges and water volumes instead of velocities and water levels. Therefore, the WAQ module recalculates the horizontal velocity within a cell from the discharges through the cell faces. For each of the two horizontal directions, the average velocity  $VelocAvg$  through the cell is calculated, and the total horizontal velocity  $Veloc$  is calculated by taking the vector sum of the two components.

$$VelocAvg_1 = \frac{\frac{Flow_{1,1}}{Area_{1,1}} + \frac{Flow_{1,2}}{Area_{1,2}}}{2} \quad (D.16)$$

$$VelocAvg_2 = \frac{\frac{Flow_{2,1}}{Area_{2,1}} + \frac{Flow_{2,2}}{Area_{2,2}}}{2} \quad (D.17)$$

$$Veloc = \sqrt{VelocAvg_1^2 + VelocAvg_2^2} \quad (D.18)$$

With the horizontal velocity known, the bed shear stress  $\tau_{flow}$  can be calculated using a roughness formulation. A Chèzy value is calculated using the Manning formula (Equation D.20), and subsequently the current induced bed shear stress is calculated with Equation D.19. This shear stress, combined with the wave shear stresses, controls the suspension of sediment.

$$\tau_{flow} = \frac{\rho_w * g * Veloc^2}{C^2} \quad (D.19)$$

$$C = \frac{\sqrt[6]{H}}{n} \quad (D.20)$$

### D.3 Model parameters

Parameter	Value	Description
Taushields	8.00E-01	Critical shear stress for resuspension S2
GRAIN50	3.00E-04	$D_{50}$ grain size of sand in bed layer S2
GRAV	9.80E+00	Gravitational constant
KinViscos	1.00E-06	Kinematic viscosity
RHOSAND	2.60E+06	Sand density
RhoWater	1.02E+03	Water density
PORS2	4.00E-01	Volumetric porosity of bed layer S2
ThickS2	5.00E-02	Thickness of bed layer S2
MinDepth	1.00E-02	Minimum depth for sedimentation
MaxResPup	3.60E+03	Max resuspension flux from bed layer S2
FactResPup	3.00E-08	van Rijn pickup factor for bed layer S2
VSedIM1	1.08E+01	Settling velocity IM1
TaucSIM1	0.00E+00	Critical shear stress for sedimentation IM1
FrIM1SedS2	1.50E-01	Fraction sedimentation IM1 to bed layer S2
FrTIMS2Max	1.00E+00	Maximum fraction total inorganic matter in bed layer S2
SWResIM1	1.00E+00	Switch resuspension IM1
SWResusp	1.00E+00	Switch resuspension
VResIM1	3.00E-01	First order resuspension rate IM1
ZResIM1	8.64E+03	Zeroth order resuspension rate IM1
TaucRS1IM1	2.00E-01	Critical shear stress for resuspension of IM1 from S1
TaucRS2IM1	1.00E+03	Deactivated. See Taushields
VSedIM2	8.64E+01	Settling velocity IM2
TaucSIM2	0.00E+00	Critical shear stress for sedimentation IM2
SWResIM2	1.00E+00	Switch resuspension IM2
FrIM2SedS2	1.50E-01	Fraction sedimentation IM2 to bed layer S2
VResIM2	1.00E-01	First order resuspension rate IM2
ZResIM2	8.64E+03	Zeroth order resuspension rate IM1
TaucRS1IM2	2.00E-01	Critical shear stress for resuspension of IM2 from S1
TaucRS2IM2	1.00E+03	Deactivated. See Taushields
VSedIM3	1.00E-01	Settling velocity IM3
TaucSIM3	0.00E+00	Critical shear stress for sedimentation IM3
FrIM3SedS2	1.50E-01	Fraction sedimentation IM3 to bed layer S2
SWResIM3	1.00E+00	Switch resuspension IM3
VResIM3	1.00E-01	First order resuspension rate IM3
ZResIM3	8.64E+03	Zeroth order resuspension rate IM1
TaucRS1IM3	2.00E-01	Critical shear stress for resuspension of IM3 from S1
TaucRS2IM3	1.00E+03	Deactivated. See Taushields
TaucRS1DM	1.00E+03	Deactivated. See TaucRS1IMi
TaucRS2DM	0.50E+00	Deactivated through TaucRS2IMi. See Taushields
Rough	1.00E-04	Nikuradse roughness length scale
Manncoef	2.40E-02	Manning coefficient
SwChezy	2.00E+00	Switch to activate Manning roughness formulation
SWTauVeloc	1.00E+00	Switch for calculation of shear stress from velocity
SWTau	2.00E+00	Switch for Swart (1974) formulation. Not used

Table D.1: User defined model parameters



# Bibliography

- [1] M. Baeye et al. “Sediment mobility in response to tidal and wind-driven flows along the Belgian shelf, southern North Sea”. In: *Ocean Dynamics* 61 (May 2011), pp. 611–622.
- [2] G. Böhnecke. *The influence of the tidal stress on the residual circulation*. Tech. rep. University of Berlin, 1922.
- [3] G.J. de Boer. “On the Interaction between Tides and Stratification in the Rhine Region of Freshwater Influence”. PhD thesis. Technische Universiteit Delft, 2009.
- [4] G.J. de Boer, J.D. Pietrzak, and J.C. Winterwerp. “SST observations of upwelling induced by tidal straining”. In: *Continental Shelf Research* (2006).
- [5] L.H. de Bruijn. *Maintainance dredging in the Port of Rotterdam*. MSc thesis. 2018.
- [6] J.M. de Kok. “The Influence Of Freshwater Distribution On SPM Transport In The Dutch Coastal Zone”. In: *Transactions on the Built environment* 58 (2001), pp. 309–323.
- [7] M.A.J. de Nijs and J.D. Pietrzak. “Saltwater intrusion and ETM dynamics in a tidally energetic stratified estuary”. In: *Ocean Modelling* 49.50 (2012), pp. 60–85.
- [8] M.A.J. de Nijs, J.D. Pietrzak, and J.C. Winterwerp. “Advection of the Salt Wedge and Evolution of the Internal Flow Structure in the Rotterdam Waterway”. In: *Journal of Physical Oceanography* 41 (2010), pp. 3–27.
- [9] M.A.J. de Nijs, J.C. Winterwerp, and J.D. Pietrzak. “On Harbour Siltation in the Fresh-Salt Water Mixing Region”. In: *Journal of Physical Oceanography* 29 (2009), pp. 175–193.
- [10] M.A.J. de Nijs, J.C. Winterwerp, and J.D. Pietrzak. “The Effects of the Internal Flow Structure on SPM Entrapment in the Rotterdam Waterway”. In: *Journal of Physical Oceanography* 40 (2011), pp. 2357–2379.
- [11] Deltares. *D-Water Quality Processes Library Description*. Tech. rep. Deltares, 2018.
- [12] Deltares. *D-Water Quality User Manual*. Tech. rep. Deltares, 2018.
- [13] Deltares. “Delft3D-FLOW user manual”. In: *Delft, the Netherlands* (2018).
- [14] G. el Serafy et al., eds. *Data assimilation of satellite data of suspended particulate matter in Delft3D-WAQ for the North Sea*. 2007.
- [15] M.A. Eleveld, R. Pasterkamp, and H.J. van der Woerd, eds. *EARSeL eProceedings 3*. 2004.
- [16] M.A. Eleveld et al. “Remotely sensed seasonality in the spatial distribution of sea-surface suspended particulate matter in the Southern North Sea”. In: *Estuarine, Coastal an Shelf-Science* 80 (2008), pp. 103–113.
- [17] R.P. Flores et al. “The impact of storms and stratification on sediment transport in the Rhine region of freshwater influence”. In: *Journal of Geophysical Research* 122 (2017), pp. 4456–4477.
- [18] W.R. Geyer. “The Importance of Suppression of Turbulence on the Estuarine Turbidity Maximum”. In: *Estuaries and Coasts* 16 (1993), pp. 113–125.
- [19] E. Hendriks and F. Schuurman. *Modellering alternatieve loswal locaties*. Tech. rep. Deltares, 2017.
- [20] L.E. Holmedal and D. Myrhaug. “Wave-induced steady streaming, mass transport and net sediment transport in rough turbulent ocean bottom boundary layers”. In: *Continental Shelf Research* 29.7 (2009), pp. 911–926.

- [21] A.R. Horner-Devine et al. “Cross-shore transport of nearshore sediment by river plume frontal pumping”. In: *Geophysical Research Letters* 44 (2017), pp. 6343–6351.
- [22] J. Joordens, A.J. Souza, and A. Visser. “The influence of tidal straining and wind on suspended matter and phytoplankton distribution in the Rhine outflow region”. In: *Continental Shelf Research* 21 (2001), pp. 301–325.
- [23] W.M. Kranenburg and R. Schueder. *OSR-simulaties voor zoutindringing in de Rijn-Maasmonding zomer 2003*. Tech. rep. Deltares, 2015.
- [24] W.M. Kranenburg, T. van der Kaaij, and A. Nolte. *OSR-simulaties voor zoutindringing in de Rijn-Maasmonding II*. Tech. rep. Deltares, 2015.
- [25] R. Krone. *Flume studies of transport of sediment in estuarial shoaling processes*. Tech. rep. University of California, Berkely, 1962.
- [26] F. Mietta et al. “Influence of shear rate, organic matter content, pH and salinity on mud flocculation”. In: *Ocean Dynamics* 59 (2009), pp. 751–763.
- [27] J.C.J. Nihoul and F.C. Ronday. “The influence of the tidal stress on the residual circulation”. In: *Tellus* 26 (1975), pp. 484–490.
- [28] L. Otto et al. “Review of the Physical Oceanography of the North Sea”. In: *Netherlands journal of sea research* 26 (1990), pp. 161–238.
- [29] E. Partheniades. “A study of erosion and deposition of cohesive soils in salt water”. PhD thesis. University of California, Berkely, 1962.
- [30] J.D. Pietrzak, G.J. de Boer, and M.A. Eleveld. “Mechanisms controlling the intra-annual meso scale variability of SST and SPM in the southern North Sea”. In: *Continental Shelf Research* 31-6 (2011), pp. 594–610.
- [31] R.D. Pingree and D.K. Griffiths. “Currents driven by a steady uniform wind stress on the shelf seas around the British Isles”. In: *Oceanologica Acta* 3 (1980).
- [32] M. Rotsaert. *Afregeling OSR systeem verificatie zout*. Tech. rep. Svasek Hydraulics, 2010.
- [33] J.H. Simpson. “Physical processes in the ROFI regime”. In: *Journal of Marine Systems* 12 (1997), pp. 3–15.
- [34] J.H. Simpson, J.R. Hunter, and K.F. Bowden. “Fronts in the Irish Sea”. In: *Nature* 250 (1974), pp. 404–406.
- [35] J.H. Simpson et al. “Periodic stratification in the Rhine ROFI in the North Sea”. In: *Oceanologica Acta* 16 (1993), pp. 23–32.
- [36] J.H. Simpson et al. “Tidal Straining, Density Currents, and Stirring in the Control of Estuarine Circulation”. In: *Estuaries* (1990).
- [37] A.J. Souza and J.H. Simpson. “Controls on stratification in the Rhine ROFI system”. In: *Journal of Marine Systems* 12 (1996), pp. 311–323.
- [38] A.J. Souza and J.H. Simpson. “The modification of tidal ellipses by stratification in the Rhine ROFI”. In: *Continental Shelf Research* 16 (1995), pp. 997–1007.
- [39] J.M. Suijlen and R.N.M. Duin. *Atlas of near-surface Total Suspended Matter concentrations in the Dutch coastal zone of the North Sea*. Tech. rep. Rijkswaterstaat, 2002.
- [40] J.L.S.J van Alphen. “A mud balance for Belgian-Dutch coastal waters between 1969 and 1986”. In: *Netherlands Journal of Sea Research* 25 (1990), pp. 19–30.
- [41] A. van der Giessen, W.P.M de Ruijter, and J.C. Borst. “Three-dimensional current structure in the Dutch Coastal zone”. In: *Netherlands journal of sea research* 25 (1990), pp. 45–55.
- [42] T. van der Kaaij et al. *Modelondersteuning MER winning suppletie-en ophoogzand Noordzee 2018-2027: Modelvalidatie*. Tech. rep. Deltares, 2017.
- [43] T. van Kessel. “Generation and transport of subaqueous Fluid Mud Layers”. PhD thesis. Technische Universiteit Delft, 1997.
- [44] T. van Kessel, E.D. de Goede, and H.F.P. van den Boogaard. *Year simulations with the ZUNO-DD model on the impact of Maasvlakte-2 on large scale silt transport*. Tech. rep. WL—Delft Hydraulics, 2006.

- 
- [45] T. van Kessel et al. “Modelling the seasonal dynamics of SPM with a simple algorithm for the buffering of fines in a sandy seabed”. In: *Continental Shelf Research* 31 (2010), pp. 124–134.
- [46] S. van Leeuwen et al. “Stratified and nonstratified areas in the North Sea: Long-term variability and biological and policy implications”. In: *Journal of Geophysical Research: Oceans* 120 (2015), pp. 4670–4686.
- [47] P.A.J. Verlaan and R. Spanhoff. “Massive sedimentation effects at the mouth of the Rotterdam Waterway”. In: *Journal of Coastal Research* 16 (2000), pp. 458–469.
- [48] A.W. Visser et al. “The effect of stratification on tidal current profiles in a region of freshwater influence”. In: *Oceanologica Acta* 17.4 (1994), pp. 369–381.
- [49] M. Visser, W.P.M. de Ruijter, and L. Postma. “The distribution of suspended matter in the Dutch coastal zone”. In: *Netherlands Journal of Sea Research* 27.2 (1991), pp. 127–143. ISSN: 0077-7579.
- [50] J. van Wiechen. *Modelling the wind-driven motions in the Rhine ROFI*. MSc thesis. 2011.
- [51] J.C. Winterwerp. *Fluxes of fine sediment along the Dutch coast and the impact of Maasvlakte 2*. Tech. rep. WL—Delft Hydraulics, 2006.
- [52] J.C. Winterwerp. “On the flocculation and settling velocity of estuarine mud.” In: *Estuarine Research* 22 (2002), pp. 1339–1360.
- [53] J.C. Winterwerp. “The Physical Analyses of Muddy Sedimentation Processes”. In: *Treatise on Estuarine and Coastal Science* (2011), pp. 311–360.
- [54] J.C. Winterwerp and T. van Kessel. “Siltation by sediment-induced density currents”. In: *Ocean Dynamics* 53.3 (Sept. 2003), pp. 186–196.